STUDIES IN LOW ENERGY MAGNETIC SPECTROSCOPY USING SOURCES OF RaD, MsTh2 AND ^{233}Pa.

Thesis

submitted by

W. D. Brodie

B.Sc., (St. Andrews)

for the Degree of

Doctor of Philosophy

University of Edinburgh

November, 1952.

CONTENTS.

Chapter V.

THE DISINTEGRATION OF PROTACTINIUM 233.

Explanation of Plates.

Plate 1 (following page 27).

View of the spectrometer tube, the lens, and the rectangular coils for neutralizing the earth's magnetic field. The ionization gauge head and its associated valve voltmeter are also shown.

Plate 2 (following page 27).

View of the accelerating tube and counter filling line. The smaller flask towards the left of the picture is the 250 ml. reservoir for the Geiger counter.

Plate 3 (following page 32).

On the left is the bin housing the scaling unit and the counter power supply. The resistors used for controlling the accelerating potential are on the extreme right and the potentiometer used for measuring the lens current is in the centre of the picture. The main bank of resistors for adjusting the lens current is not shown.

Preface.

The research described in this thesis was carried out in the Department of Natural Philosophy of the University of Edinburgh under the supervision of Professor N. Feather, F.R.S. Part of the work on RaD, namely that described in sections 3.1 to 3.5.5, was carried out in collaboration with Dr. D.K. Butt, who is now in the Research Laboratory, Birkbeck College, London.

Chapter I.

THE MEASUREMENT OF LOW ENERGY ELECTRONS.

In order to measure the energy spectrum of the electrons emitted by a radioactive body it is necessary to disperse the electrons so that those in a small momentum or energy range can be selected, and then to measure the number in that small range. Alternatively, it is possible to use a method in which all the electrons having energies exceeding some selected value are counted. This leads to an integrated spectrum, from which the true momentum or energy distribution is obtained by differentiation.

The simplest method of measuring the electron energies is to measure their absorption in foils of a light material such as aluminium. The absorption curve obtained by plotting the number of electrons penetrating the absorber against its thickness approximates to an integrated spectrum in terms of the range of the electrons in the absorbing material. The shape of the absorption curve is, however, affected by the large amount of straggling in the range of an electron of given energy in the absorber. A beam, initially well collimated and homogeneous in energy, soon loses homogeneity of energy and direction as it passes through matter. Nevertheless, considerable information can be obtained from absorption measurements. For example, the upper

limit of a continuous β-spectrum can be obtained with good accuracy, and conversion lines superimposed on a continuous β-spectrum can sometimes be detected by kinks in the absorption curve. The method can be used down to very low energies by the use of a "windowless" Geiger counter. The counter forms part of a larger vessel in which are placed the source and absorbers, the whole volume being filled with counter gas. Because of the straggling of the electrons in the absorber, the resolving power of the method is low and its only advantages are its simplicity and its high collecting power, which allow the study of sources of low specific activity.

The Wilson cloud chamber is particularly useful for detecting electrons of low energy (say below 50 keV), especially if the radioactive material can be obtained in gaseous form. The energy of the ionizing particle can be deduced from the length of the track, the number of droplets in the track, or its curvature in a magnetic field. Owing to the continual loss of velocity and the small random changes of direction that arise from collisions with gas molecules, measurement of the curvature gives only moderate accuracy. Energy measurements based upon track lengths and droplet counts are subject to large statistical fluctuations so that the resolving power obtainable is fairly low. Useful information on low energy β-ray spectra has, however, been obtained

from cloud chamber experiments. For example, Richardson and Leigh-Smith (1937) showed that 60% of the electrons in the β-spectrum of radium D have energies below 4 keV. Their source was in the form of the gaseous compound lead tetra-methyl.

For accurate and reliable energy measurements, the use of a vacuum β-ray spectroscope is to be preferred whenever possible, and from quite early in its history the magnetic spectroscope has been used for the measurement of low energy electrons. In 1925, Black detected in the spectra of the active deposits of thorium and radium lines with energies as low as 6 keV. He used a semicircular focusing instrument with a photographic plate as detector. This experimental arrangement gives good resolving power at the expense of a low collecting power, and, since the blackening of the photographic plate falls off for low energy electrons, strong sources and long exposures are required. This variation of the blackening "per electron" with energy also makes it difficult to measure the relative intensities of electron lines. The requirement of a strong source means that the semicircular focusing spectrometer, as a low energy instrument, is restricted to the examination of sources which can be obtained with a very high specific activity. In the case of sources of low specific activity the source, to be sufficiently intense, has to

be made so thick that absorption and scattering of electrons in the source itself blur the details of the spectrum at low energies.

In a lens β-ray spectrometer, a considerably larger proportion of the electrons emitted in a given energy range can be focused on the detector. This larger solid angle allows thinner sources to be used with a consequent lowering of the energy at which absorption of electrons in the source becomes serious. While its larger collecting power (at the expense of some loss in resolution) gives the lens spectrometer an advantage over the semicircular type for the study of low energy electron spectra, the problem of detecting and counting the low energy electrons remains. Photographic methods are unsuited to the lens instrument and the standard technique is to use a Geiger counter with a thin window, strengthened, if necessary, by a supporting grid, and to make a correction for the absorption of electrons in their passage through the window.

The apparatus used in the experiments to be described in the following chapters was of this type but also included a post-focusing electron accelerator. This enabled electrons of a given momentum selected by the magnetic lens, to be subsequently given additional energy to enable them to penetrate the counter window. It will be shown that, although there is a limit to the

maximum accelerating potential which can be used with any given thickness of counter window, electron spectra can be conveniently studied with this equipment down to energies of 3 or 4 keV.

Before the apparatus is described in more detail, it is of interest to note two other methods of measuring low energy electron spectra. The first is essentially a refinement of the absorption method, in which the absorbing foil is replaced by an electrical potential barrier. The energy is thus removed from the electrons by a process which is no longer a statistical one, so that a much higher resolving power can be obtained. In the apparatus described by Hamilton and Gross (1950) the electrons move radially outwards from a radioactive source against a spherically symmetrical retarding field, and the current due to electrons having sufficient energy to penetrate the potential barrier is measured. As the retarding potential is varied, an integral spectrum is observed from which the normal spectrum is obtained by differentiation. The use of current detection avoids the difficulties of using thin windowed counters, and the resultant loss in sensitivity is compensated by the use of a very large solid angle. In the instrument of Hamilton and Gross, the solid angle approaches 2π steradians. The apparatus can be used in the range 0 - 30 keV.

The other method, which is closely related to the cloud chamber method, has been described by Curran, Angus and Cockcroft (1949). A proportional counting tube is used in conjunction with a strictly linear amplifier of high gain and low noise level. The size of the output pulse from the counter is proportional to the energy of the particle producing the pulse, so that some method of sorting the pulses as regards amplitude is all that is required to give the energy spectrum. The main advantages of the method are that very weak sources can be used by putting them inside the counter, and that, if the pulses are recorded by photographing a cathode ray oscilloscope trace on a moving film, a record of all the data necessary for analysis may be obtained in a short time. Long term stability requirements are thus relaxed. The resolving power of the method is, however, inherently limited by statistical fluctuation of the number of ion pairs formed in the gas by the incident electrons, and by statistical fluctuation in the gas amplification. Fluctuations due to the noise level of the amplifier also contribute to the observed width of a monochromatic radiation. The proportional counter is sensitive to low energy electromagnetic radiation as well as to electrons, and while this may be advantageous for purposes of calibration, it may lead to difficulties in interpretation of com-

plicated line spectra.

In general, a magnetic spectrometer of high collecting power with a detector specially adapted for counting low energy electrons is the most useful device for the study of low energy electron spectra, but for very low specific activities and possibly also for the very lowest energies (say below 3 keV) cloud chamber and proportional counter techniques are to be preferred.

Chapter II.

DESCRIPTION OF THE APPARATUS.

2.1. General.

The apparatus used in the work to be described was a β-ray lens spectrometer incorporating a post-focusing electron accelerator. The instrument was built by D.K. Butt and has been fully described by him (Butt, 1949a and b; 1950). Only an outline of its construction and operation will therefore be given here. The investigation of the performance of the electron accelerator and the making of thin Geiger counter windows will be described in more detail as much of this work has been the concern of the present writer.

The spectrometer utilizes the principle of focal isolation and is similar in design to that of Deutsch, Elliott and Evans (1944). Figure 2.1 shows a partly schematic diagram of the instrument. Electrons of one particular energy starting from the source S on the axis are focused by the field of the lens coil on to the aperture A. Electrons of other energies, which would be focused at other points, strike the walls of the chamber or the baffles. After passing through the exit aperture A, the electrons traverse the accelerator tube T (to be described later) and enter the counter.

Since the focusing coil is not shielded by iron,

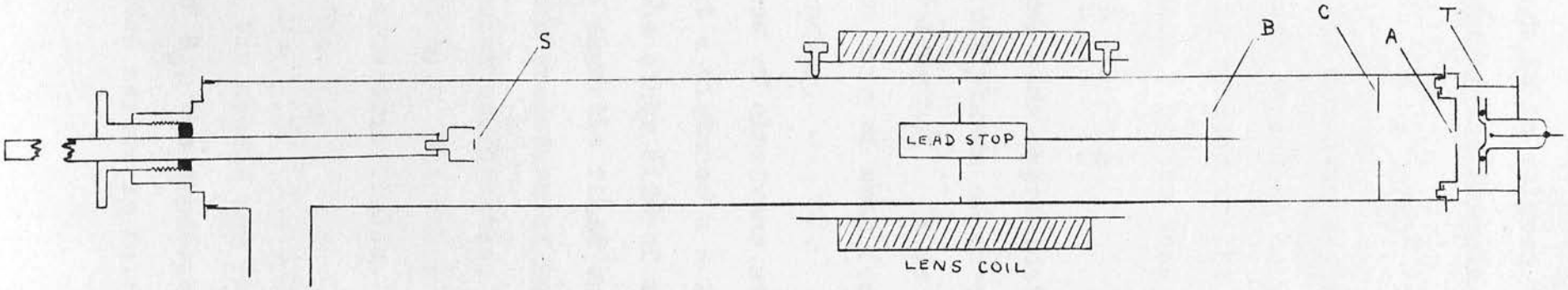

Figure 2.1. Schematic diagram of spectrometer.

the current i through it is related to the momentum of the focused electrons by the formula

$$f = C(\frac{p}{i})^2$$

where $p = (\frac{e}{c})mv$ is the momentum expressed in units of $H\rho$. C is a constant depending only on the lens coil. The focal length f is related to the source distance u and the image distance v by the thin lens formula

$$\frac{1}{u} + \frac{1}{v} = \frac{1}{f}.$$

This formula involves some approximations since, in general, the principal planes of an electron lens change for different focal lengths. It is however, sufficient for an understanding of most features of the operation of the spectrometer.

The trajectories of electrons starting from a point on the axis at a distance u = 2f, and focused at a point v = 2f on the other side of the lens, may be calculated from the magnetic field on the axis of the coil. Following the procedure of Busch (1926), and using cylindrical polar coordinates, we may calculate the vector potential A_θ. The other components of $\underline{A}$ vanish for axially symmetric fields.

$$A_\theta = \frac{r}{2} H_o(z) - \frac{r^3}{2^2.4} H_o''(z) + \frac{r^5}{2^2.4^2.6} H_o^{(iv)}(z) - \cdots \qquad (2.1)$$

H_o'' and $H_o^{(iv)}$ are the second and fourth derivatives with respect to z of H_o, the magnetic field on the axis. The convergence of the series is fairly rapid if r is

small, and with the values used in the spectrometer (r_{max} = R = 4.1 cm.) the first three terms give A and its derivatives with an error of less than 0.2%.

The equations of motion of the electron may be written

$$\left.\begin{aligned} \frac{d}{dt}(m\dot{z}) &= \frac{e^2}{mc^2} A \frac{\delta A}{\delta z} \\ \frac{d}{dt}(m\dot{r}) &= \frac{e^2}{mc^2} A \frac{\delta A}{\delta r} \\ mr\dot{\theta} &= -\frac{e}{c} A \end{aligned}\right\} \qquad (2.2)$$

where m is the relativistic mass of the electron and the dot indicates differentiation with respect to time. When u = v we have the additional relations, in which p_o is the momentum of the focused electron and ϕ the initial angle of its path with the axis,

$$(m\dot{z})_{z=zf} = p_o \cos\phi \,, \quad \dot{r}_{z=0} = 0 \,, \quad r_{z=0} = R \,, \quad \theta_{z=0} = 0 \qquad (2.3)$$

Using these relations the equations (2.2) may be integrated to give

$$\left.\begin{aligned} \frac{(m\dot{z})^2}{2} &= p_o^2 \left(\cos\phi - \int_{zf}^{z} \frac{A}{p_o^2} \frac{\delta A}{\delta z} \, dz \right) \\ r &= R - p_o^2 \int_o^z \frac{dz}{m\dot{z}} \times \int_o^z \frac{A}{p_o^2 m\dot{z}} \frac{\delta A}{\delta r} \, dz \\ \theta &= -\int_o^z \frac{A}{r m\dot{z}} \, dz \end{aligned}\right\} \qquad (2.4)$$

where the momenta are now in $H\rho$ units.

These integrals can be evaluated numerically to give the paths of the electrons. It is found (see Deutsch et al.) that the paths, when expressed in terms of $\frac{r}{R}$, do not vary greatly for different values of R, but, of course, the electrons which cross the axis at z = v have different momenta according to their value of R. This is due to the spherical aberration of the lens. Figure 2.2 shows a typical electron path for the axial magnetic field distribution shown in Figure 2.3. The practical field distribution when the lens was used with a focal length of 20 cm. corresponded fairly closely with that in Figure 2.3. The trajectories calculated in this way are useful in designing the baffles which define the transmitted beam, but final adjustment must be made by experiment.

In principle, it is possible to extend calculations of the above type to the paths of electrons not passing through the exit aperture and to those starting from points off the axis. However, this complicated procedure may be avoided by treating the coil as a thin lens free from all aberrations except spherical aberration. Using this method, Butt (1950) showed that high resolution can be obtained with the focal isolation spectrometer only by using very small sources and counter windows. Under these conditions the

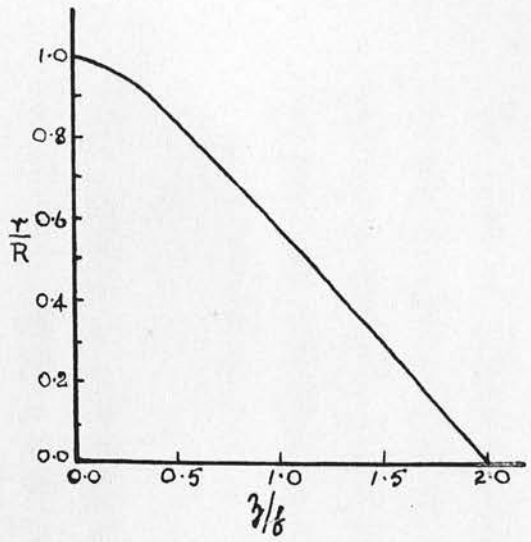

Figure 2.2. Calculated electron path for the axial field distribution shown in Figure 2.3.

Figure 2.3.

collecting power becomes very small. This is due to the fact that, when the source is small, the spherical aberration almost entirely determines the diameter of the disc of least confusion, and, when the counter window is small compared with this, only a low gathering power can be obtained. In practice, sources between 3 and 4.5 mm. in diameter and exit apertures between 3.5 and 5 mm. were used.

2.2. Technical Description.

2.2.1. The Vacuum Chamber.

The vacuum chamber was a cylindrical brass tube 100 cm. long and 10 cm. in internal diameter, mounted horizontally, and connected to the pumps by a vertical pipe 5.5 cm. in diameter soldered near the source end. The end plates, which were removable, were sealed to the tube by means of greased neoprene gaskets. A vacuum of about 10^{-5} mm. of mercury was obtained using a 3-stage "Metrovac" oil diffusion pump and an Edwards 2-stage mechanical rotary pump. Sources were mounted on the end of a rod passing through a vacuum seal in the centre of the end plate of the spectrometer. This allowed the position of the source on the axis to be varied at will.

2.2.2. The Magnetic Lens.

The lens, which had been designed to focus electrons having energies up to 500 keV, consisted of a solenoid

wound on a brass tube. The coil was 20 cm. long, 12.5 cm. in internal diameter and 17 cm. in external diameter. The tube on which it was wound was mounted coaxially with the spectrometer tube by means of two 3-point suspensions. The field on the axis at the centre of the lens was about 100 gauss per ampere.

2.2.3. The Current Supply.

The supply of direct current for the lens coil was obtained from a battery of 50 two volt accumulators, which could be kept on floating charge from the D.C. mains if required. The current was adjusted by a series of rheostats and measured by observing the potential across a standard 1 Ω or 0.5 Ω oil immersed resistance coil, using a Tinsley Ionization Potentiometer. The galvanometer used had a sensitivity of 460 mm. per μA, and the current could be kept constant manually to 1 part in 2,000 or better at all currents.

2.2.4. The Baffle System.

Besides the exit aperture A, an annular slit 0.75 cm. wide and 8.2 cm. in external diameter was placed in the centre of the lens to define the electron beam. A lead cylinder 10 cm. long and 2.5 cm. in diameter prevented the γ-rays emitted by the source from reaching the counter directly, and additional baffles on the counter side of the lens served to stop electrons scattered from the walls of the vacuum chamber. The central lead stop together with the baffles B and C

of Figure 2.1 prevented slow electrons from reaching the counter after performing several spirals in the lens.

2.2.5. The Effect of the Earth's Magnetic Field.

Lens spectrometers are rather sensitive to components of a magnetic field normal to the axis but relatively insensitive to a small longitudinal field. Accordingly the spectrometer was mounted in a North-South direction and the vertical component of the earth's magnetic field was neutralized by a pair of coils. These were rectangular in shape, 150 cm. long by 40 cm. wide, and separated by 40 cm., and each consisted of 90 turns of 27 S.W.G. silk covered copper wire. They were mounted, one above and one below the vacuum chamber as indicated in Figure 2.4. It is clear that the effect of the longitudinal sides of the coils is to produce a vertical field on the axis of the spectrometer (provided they are connected in the proper manner). The disturbing effect of the ends is small, since they are well away from the electron paths.

2.2.6. The Ionization Gauge.

The pressure in the vacuum chamber was measured by means of an ionization gauge connected to the spectrometer at the accelerating tube. The gauge consisted of a double diode with a heated filament placed between the two anodes. A constant source of ionization was applied to the gas by a current of electrons flowing to

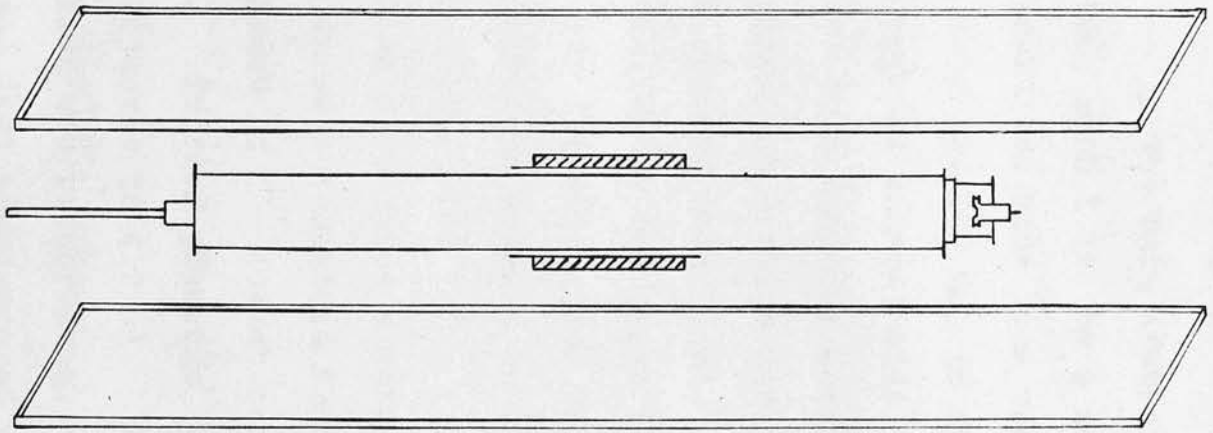

Figure 2.4. Showing the positions of the neutralizing coils.

one anode, while the other anode, connected to a stabilized potential of — 60V, collected the positive ions produced. The ion current was measured by a valve voltmeter.

The gauge was in the form of two parallel anode plates of tantalum, each 1 in. by $\frac{5}{8}$ in., separated by $\frac{3}{8}$ in. The filament was made from two pieces of tungsten wire 12 cm. long and 0.2 mm. in diameter, wound in the form of two spirals mounted side by side and connected in parallel. This filament carried a heating current of about 6 amps. at 8 volts and yielded a maximum electron current of more than 50 mA.

A circuit diagram of the gauge is shown in Figure 2.5. In operation the electrodes were outgassed by passing a 50 mA electron current to the two anodes connected in parallel. The valve voltmeter was then set up by adjusting R3 to give a meter reading of 100 μA when a 10 μA current (obtained from the 120V stabilized supply) flowed in the lowest section R of the grid resistance. To read pressure, the electron current to D1 was adjusted to 4.0 mA. The reading on the microammeter, which was proportional to the ion current flowing to D2, was then a measure of pressure. When set up in this way, full scale deflection (250 μA) on the three ranges corresponded to pressures of 2.5×10^{-4}, 2.5×10^{-5} and 1.25×10^{-5} mm. of mercury.

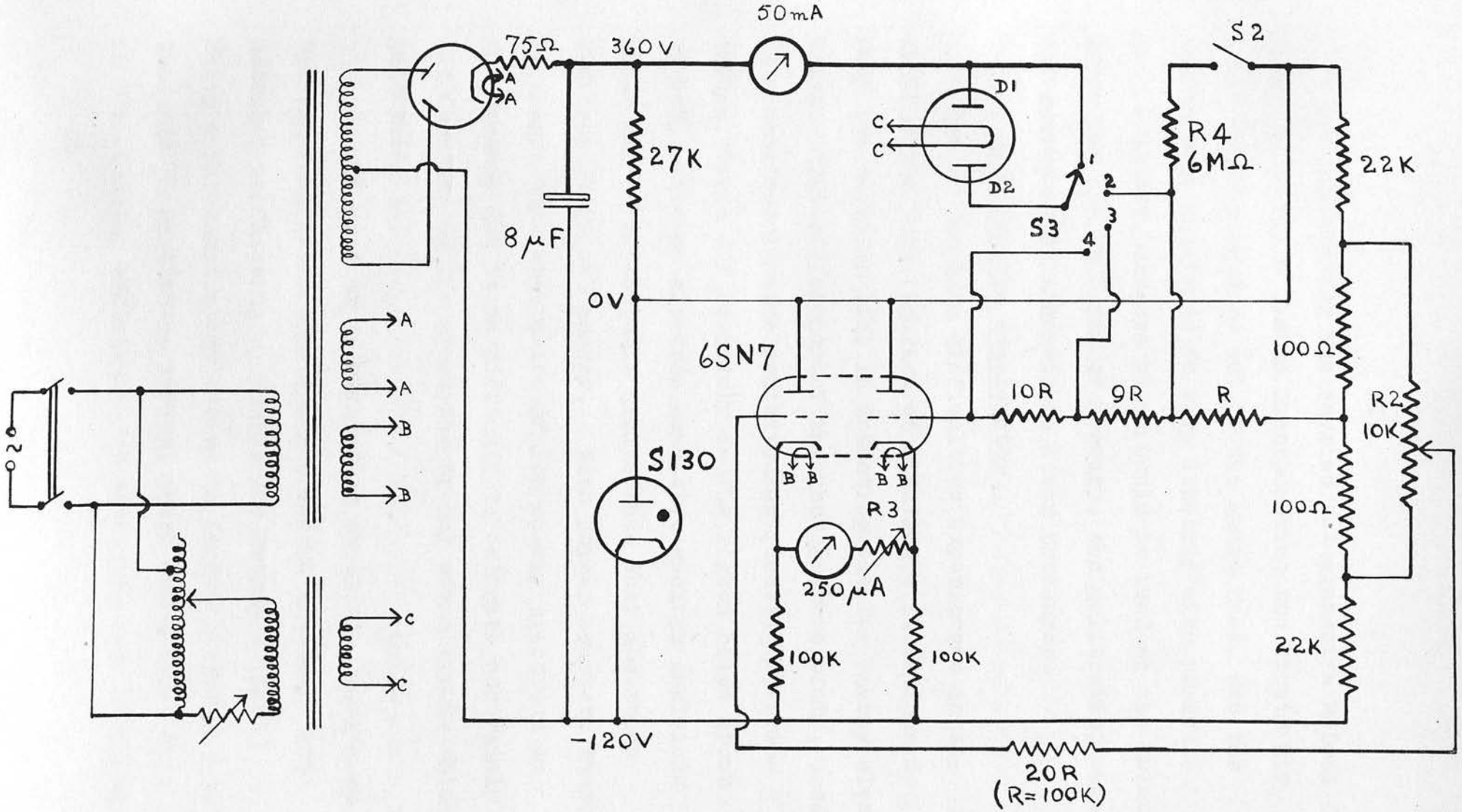

Figure 2.5. Circuit diagram of ionization gauge.

The calibration was carried out against a McLeod gauge in a vacuum system incorporating two liquid air traps to keep vapours out of the gauge head, and the ion current was found to vary linearly with pressure. As the lowest pressure which could be read on the McLeod gauge was 5×10^{-5} mm. of mercury, the calibration curve was extrapolated linearly to lower pressures.

2.2.7. The Electron Accelerator.

One of the main difficulties experienced in extending the investigation of electronic radiations to very low energies lies in detecting the low energy electrons. The efficiency of the photographic plate, used as a detector in some semicircular focusing spectrometers, falls off seriously in the region below about 25 keV, and even electron sensitive nuclear emulsions yield only 3 developable grains when they absorb an electron of 10 keV energy. With Geiger counters there is always some absorption of low energy electrons in the window, and it is difficult to estimate accurately the fraction of the electrons of any given energy which penetrate it.

In the case of scintillation counters, reports on the counting efficiency for low energy electrons are somewhat conflicting. Ramler and Freedman (1950), using a photomultiplier cooled in liquid nitrogen, found that for an anthracene crystal there was a rapid fall in the counting efficiency for electrons with energies

below 15 keV, but West, Meyerhof and Hofstadter (1951) suggested that this may have been due to inefficient light collection. West et al. observed an efficiency of greater than 50% for x-rays of 2 keV using a sodium iodide crystal.

There is some indication that the performance of photomultipliers is seriously affected by the presence of magnetic fields, so that in most designs of magnetic spectrometers a light guide would be required to enable the multiplier to be mounted in a field-free region. This would reduce the efficiency at low energies.

It is also possible to use an electron multiplier directly as a detector of β-particles (Allen, 1947). Its efficiency is about 100% for electrons of very low energies (~500 eV), but falls off rapidly above 1 keV. Allen estimates it to be only 40% at 6 keV and 10% at 150 keV.

The difficulty of detecting low energy electrons can clearly be overcome by accelerating them before they enter the counter. This can be done conveniently in the present instrument after electrons of one energy have been selected by the focusing coil. Either a Geiger counter or a scintillation counter could be used in conjunction with an accelerator - an electron multiplier, on the other hand, would require the electrons to be slowed down before reaching it if a high counting efficiency was to be maintained. In practice an end-

window Geiger counter proved quite satisfactory.

The details of the accelerator are shown in Figure 2.6. The Geiger counter is insulated from the rest of the spectrometer by the Pyrex glass accelerating tube T, and the counter can be raised to any desired electrical potential in a manner to be described. The electrons are focused through the exit aperture A, the diameter of which mainly determines the resolution of the spectrometer. After passing through A, the electrons are accelerated by the electric field towards the Geiger counter window W, consisting of a thin nylon foil supported on a brass grid. Electrons which would otherwise be absorbed in the counter window thus pick up enough energy to enable them to penetrate it. As will be explained later, there is an upper limit to the accelerating potential which can be used, depending on the thickness of the counter window.

Since the Geiger counter is, of necessity, at this high positive potential, it was found most convenient to raise the counter scaling circuit and power pack to the same potential. The general layout of the apparatus is shown in Figure 2.7. The scaler, a Dynatron Radio Type 200, and the stabilized power supply for the counter (a circuit designed by Evans (1934)), were housed in a bin lying horizontally on four insulators. The purpose of the bin was to present a smooth high

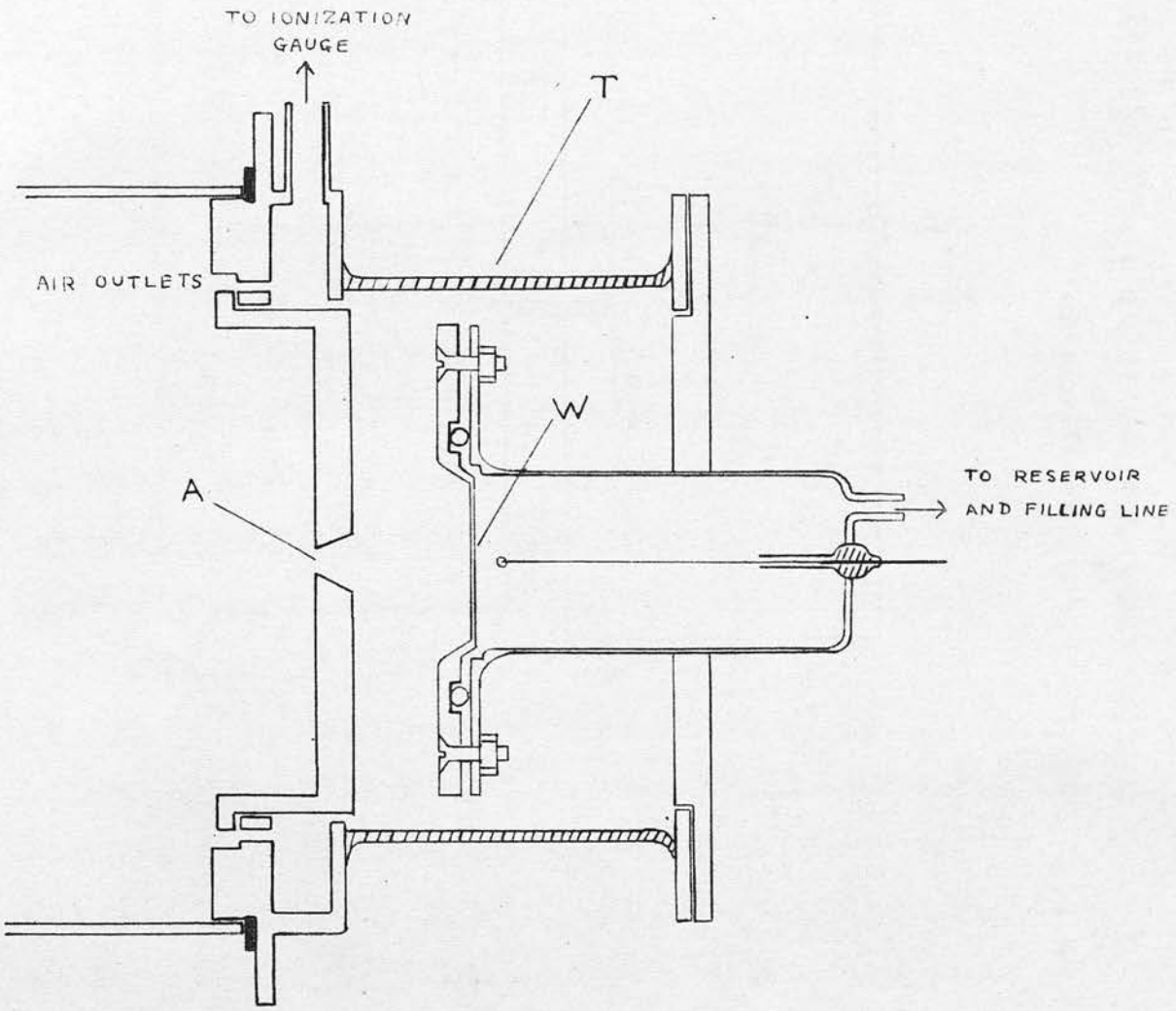

Figure 2.6. The electron accelerator and Geiger counter.

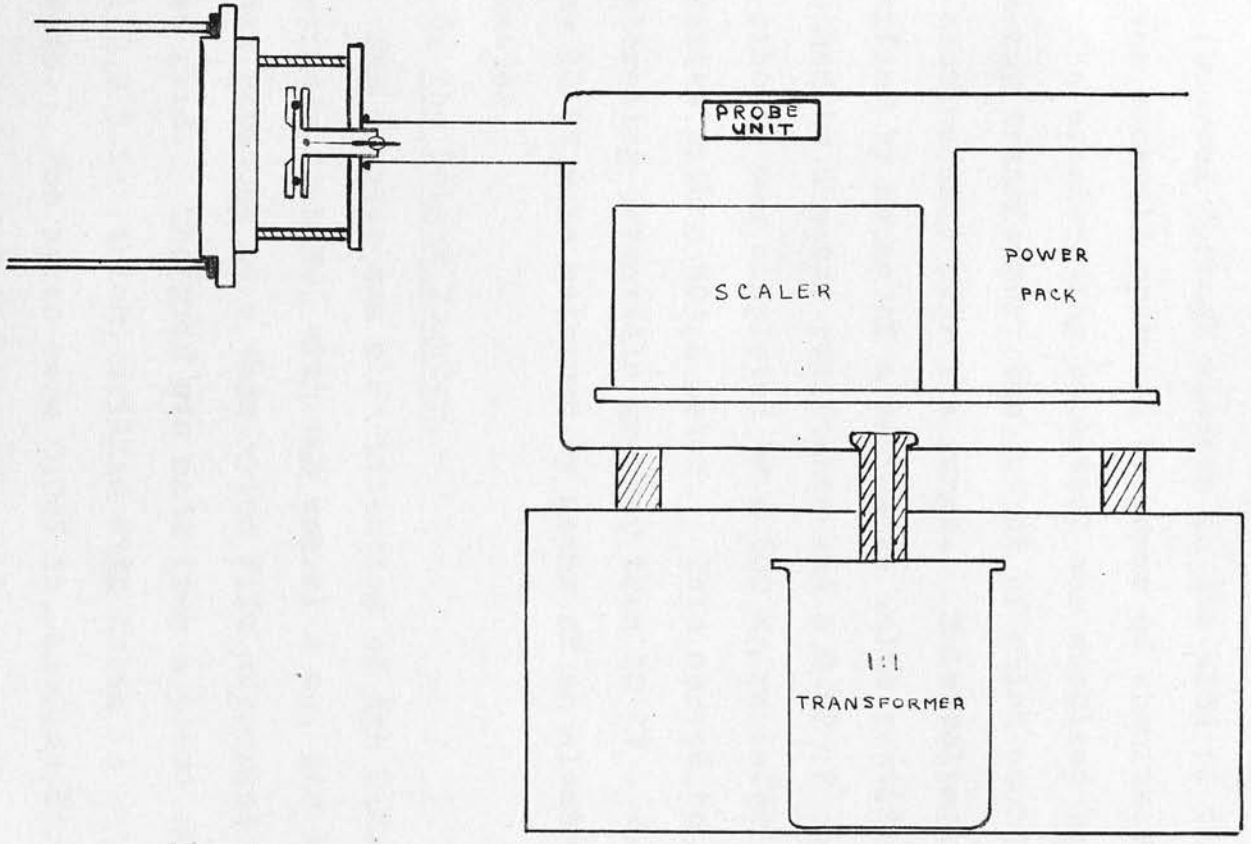

Figure 2.7. Layout of counting apparatus.

The bin and contents are at a high positive potential.

potential surface, thus preventing any corona or point discharges. The A.C. supply to these units was insulated from the A.C. mains by a 1:1 ratio transformer, the primary of which was insulated from the secondary to a potential of 100 KV. The dials of the scaler were observed through windows in the side of the bin, and the controls operated by means of ebonite rods.

The accelerating potential was supplied by a 100 KV x-ray transformer, the output of which could be varied continuously over its range. This voltage was rectified by means of a half-wave valve rectifier and smoothed by a water resistance and a 0.02 μF condenser. The circuit was completed by a 500 MΩ resistor chain in series with a 50 μA meter. This served to measure accelerating potentials greater than 10 KV - voltages below 10 KV were measured by means of an electrostatic voltmeter.

2.2.8. The Geiger Counter.

The counter was a modification of the G.E.C. G.M.4 end-window counter, with the normal 4 mg. per cm.^{2} window replaced by a thin nylon film supported on a brass grid. The grid was made from a piece of brass foil 0.015 in. thick, drilled with holes in a honeycomb pattern. The holes were 0.025 in. in diameter and were spaced 0.027 in. between centres. After the drilling, which was carried out on a vertical milling machine to ensure correct spacing of the holes, the grid was

polished to make the surface perfectly smooth. The network of holes was roughly circular, 0.9 in. in diameter, and transmitted 60% of the incident electrons. As can be seen from Figure 2.6 the grid was soldered to a flange which was bolted to a second flange soldered to the counter body. A neoprene "O" ring fitting in a suitable groove ensured a vacuum seal.

2.2.9. The making of thin nylon counter windows.

The counter windows were made from nylon film, and were fixed round the circumference of the supporting grid with "Durofix" cement. At first pieces cut from a nylon sheet supplied by A.E.R.E., Harwell, were used. These windows, which were about 0.35 mg. per $cm.^2$ in thickness, were not entirely satisfactory, because the nylon sheet was somewhat creased and tended to leak slightly. It was sometimes necessary to fit several windows before one was obtained which would withstand the pressure of the counter gas without leaking. It was afterwards found that much thinner nylon films could be made and used as counter windows, provided they were not folded or stretched in any way. To avoid straining the films, they were transferred directly from the wire frame on which they were made to the brass supporting grid, and the excess nylon was cut away, after the cement was quite dry, using a hot wire.

The nylon films were made by allowing a suitable nylon solution to evaporate on water. Of the many varieties of nylon, one type, manufactured in the United States, is soluble in iso-butyl alcohol at 100°C. The resulting solution, if allowed to stand for some hours, forms a thick, milky gel, and must be reheated each time films are to be made. To make a film about 20 μgm. per cm.^{2} in thickness, two or three drops of this solution were allowed to evaporate on ordinary tap water for three minutes, and the film was then lifted up on a rectangular wire frame previously immersed in the water. The plane of the rectangle was kept vertical, so that the nylon draped over both sides of the frame, forming a double film.

The time allowed before the films were picked off the water was found to be quite critical. It is probably dependent on the concentration of the nylon solution, but it was found that with several solutions three minutes was about the optimum time. Films left much longer than this tended to contract and to become creased, while shorter times usually gave a film which disintegrated soon after it was picked up.

Counter windows were made from four or five of these films stuck together. It was found that this could be successfully achieved either by re-immersing the original film on its frame in the water and forming

a new film on top of it, or by transferring each film immediately it was made to another frame. The films were found to adhere together perfectly, forming effectively one film, provided the process was carried out while they were wet and provided care was taken to prevent air inclusions. The nylon films were allowed to dry thoroughly before they were mounted as counter windows.

Windows made in this way were about 0.1 mg. per $cm.^2$ in thickness and, when supported by the brass grid, easily withstood the pressure of the gas filling the counter - about seven cm. of mercury. They would not, of course, withstand any appreciable pressure inwards towards the counter, so the vacuum chamber of the spectrometer and the counter were evacuated simultaneously. The counter was then filled with 1 cm. of alcohol and 6 cm. of argon, giving a plateau ~250 volts long and with a slope of ~0.03% per volt. Figure 2.8 shows a typical plateau. The counter was permanently connected to a 250 ml. reservoir so that slight leakage through the window would not appreciably affect the pressure inside the counter.

2.3. Performance of the Accelerator.

As Butt (1950) discovered, the maximum accelerating potential which can be used is limited by the onset of spurious counts. It was found that as the

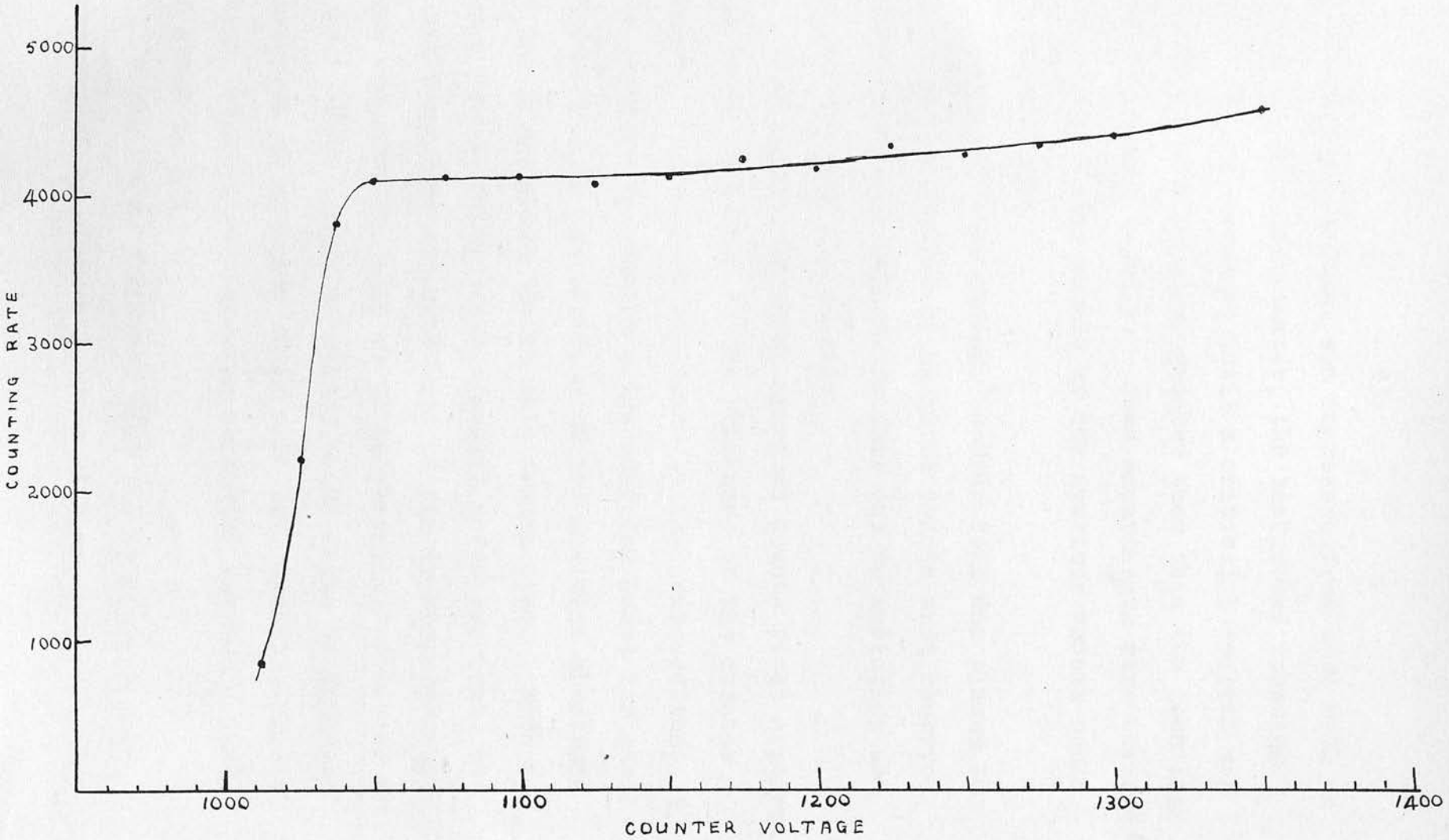

Figure 2.8. Geiger counter plateau.

accelerating potential was increased from zero with no source in the spectrometer, the background counting rate remained constant until a critical potential was reached. For voltages greater than this the counting rate increased rapidly. Some experiments were carried out to see if the nature of the spurious counts could be ascertained.

When a 20 mg. per cm.^{2} copper foil was placed in front of the counter no spurious counts were observed. This proved that the counts were due to radiation actually entering the counter.

The voltage at which spurious counts first appeared was found to depend on the thickness of the counter window. As will be explained in the next section, it was possible to measure a transmission curve for each window showing the fraction of the incident electrons of any given energy which were transmitted. With a nylon window which would transmit a few per cent. of 8 keV electrons incident upon it the spurious counts were observed to begin at an accelerating potential of 8 KV. With a thicker window which began to transmit electrons at energies of 13 - 14 keV, spurious counts began when the accelerating potential reached a value of about 14 KV.

These facts indicated that the spurious counts were caused by electrons, some at least of which origin-

ated at the cathode of the accelerator and so picked up enough energy from the accelerating field to allow a fraction of them to be transmitted through the counter window.

To verify this, the background counting rate was observed as a function of accelerating voltage with a magnetic field applied across the accelerating tube, perpendicular to the electric field. Under these conditions electrons originating at the cathode would traverse cycloidal paths as indicated in Figure 2.9, the distance d being given by

$$d = \frac{2X}{H^2} \cdot \frac{m}{e} \qquad (2.5)$$

where X is the electric field in e.m.u. per cm.

H is the magnetic field in e.m.u.

and e/m is the ratio of the electron charge to the electron mass in e.m.u. per gm.

In the accelerating tube the spacing between the cathode and the counter was 1.3 cm. and the mean magnetic field (obtained from a permanent magnet) was 280 gauss. Putting these figures in the above equation gives the value 11.6 KV for the accelerating potential at which electrons will just reach the counter window.

The experimental results are given in Figure 2.10 which shows the background counting rate as a function of accelerating voltage with and without a transverse

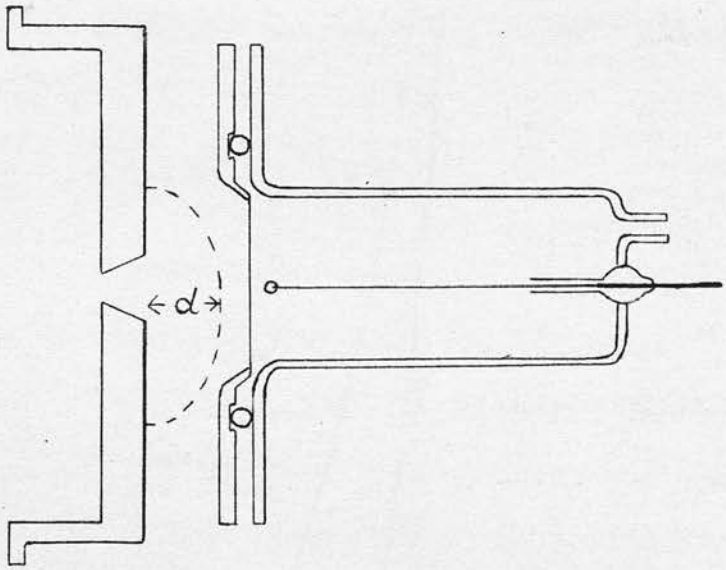

Figure 2.9. Cycloidal path traversed by an electron in the accelerator when a transverse magnetic field is applied.

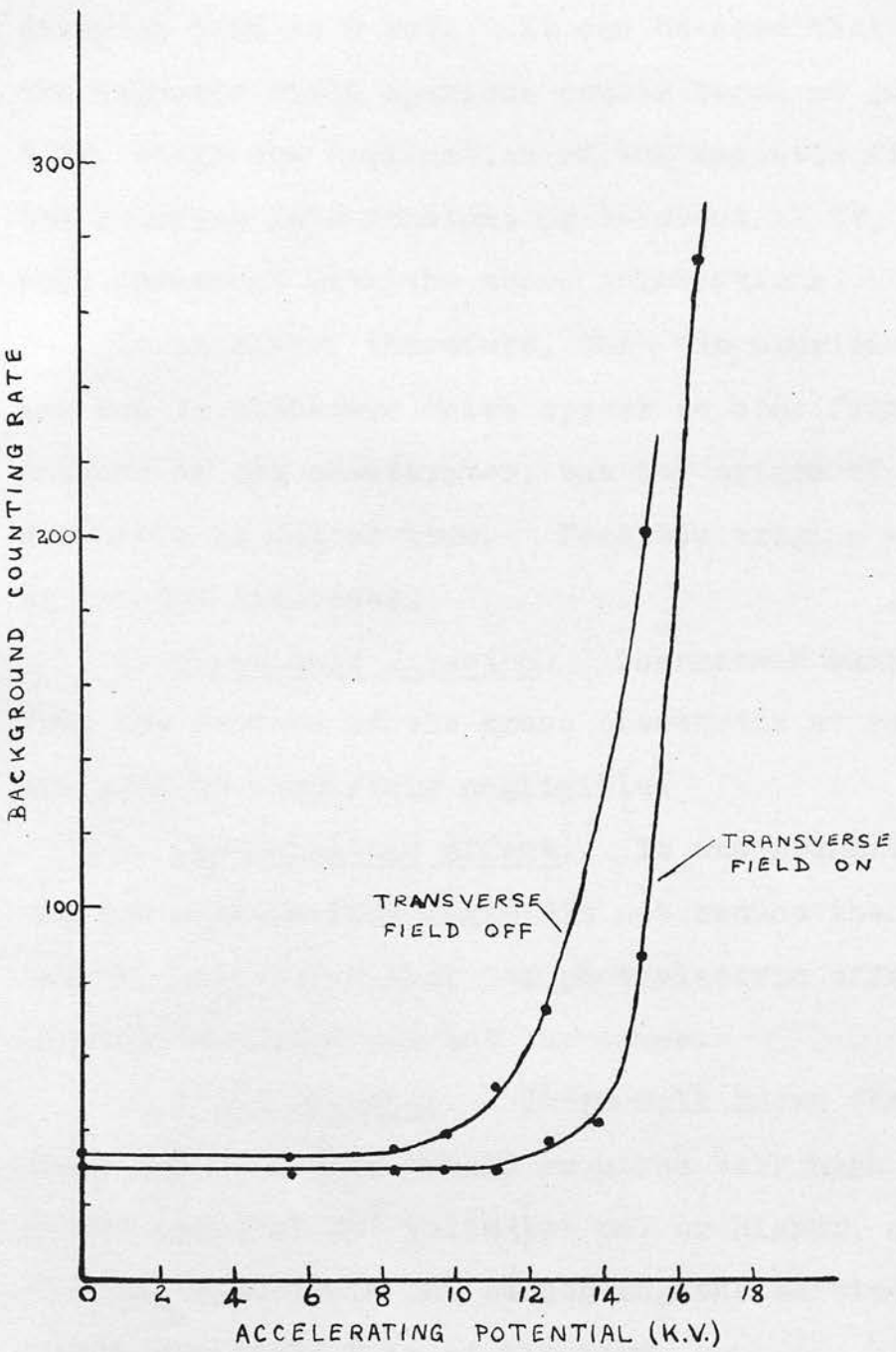

Figure 2.10. Influence of a transverse magnetic field on the spurious counts.

magnetic field. The counter window was about 0.1 mg. per cm.^{2} in thickness and transmitted electrons with energies down to 8 keV. It can be seen that without the magnetic field spurious counts began at just over 8 KV, while the application of the magnetic field kept the counting rate constant up to about 12 KV, in reasonable agreement with the above calculations.

It is clear, therefore, that the spurious counts are due to electrons which appear to come from the cathode of the accelerator, but the origin of these electrons is not obvious. Possible origins will now be briefly discussed.

1. Thermionic Emission. Thermionic emission from the surface of the brass electrodes at room temperatures is completely negligible.

2. Photoelectric effect. It was found that shielding the cathode from light did not reduce the spurious counts, indicating that the photoelectric effect of incident sunlight was not the cause.

3. Field Emission. It is well known that normal field emission from metals requires very high fields, of the order of 10^7 volts per cm. or higher, and since the Fowler-Nordheim law connecting the emitted current i with the field F is of the form

$$i = CF^2 e^{-B/F} \qquad (2.6)$$

where C and B are constants for a given metal, a

reduction in F by a factor of 10^3 would reduce the current effectively to zero. However, several writers have reported enhanced field emission effects at fields considerably lower than 10^7 volts per cm. For example, Jones and de la Perrelle (1951) have reported currents of the order of 10^4 electrons per second at fields of 10^5 volts per cm. in air. These workers found that the effective work function in the presence of a field was about 0.1 volt instead of the normal value of 4 or 5 volts, and deduced that the electrons were emitted from a very thin, even monomolecular, surface oxide layer rather than from the metal itself.

4. Ion effects. Although the pressure in the accelerating chamber was low, it is possible that ions formed in the residual gas play a part in the process. Positive ions, on being accelerated towards the cathode of the accelerator, would give electrons by secondary emission. Mühelpfordt (1938) in experiments using a specially prepared cathode similar to that described by Malter (1936) has reported that even at pressures of 10^{-5} mm. of mercury the contribution of positive ions is not negligible. The effect he was studying was, however, somewhat different from the one discussed here. Mühelpfordt concluded that the ions maintained a surface charge on the thin insulating layer with which his cathode was covered, so that Malter emission took place.

Conclusions. It seems likely that the electrons which give the spurious counts are produced either by a form of field emission, perhaps from a very thin oxide layer on the cathode, or by secondary emission caused by positive ion bombardment, the ions being produced by the electrons themselves. Both of these processes may well take place together.

Although a complete investigation of the effect has not been made, since it was too far away from the main research, it appears that the use of a Geiger counter as one electrode in a discharge tube would be useful in investigating field emission, secondary emission and similar phenomena at extremely low emission currents.

2.4. Measurement of Counter Window Transmission Curves.

Because of the effect just discussed, the slowest electrons cannot be given enough energy to allow them to be transmitted through the counter window with 100% efficiency. However, this is not a serious disadvantage because the transmission curve for any window can be quickly and accurately determined. The method used was as follows. With a suitable source in the spectrometer, thorium active deposit, for example, the lens was made to select electrons of one momentum and the counting rate observed. The accelerating potential was then applied and increased in steps, counting being

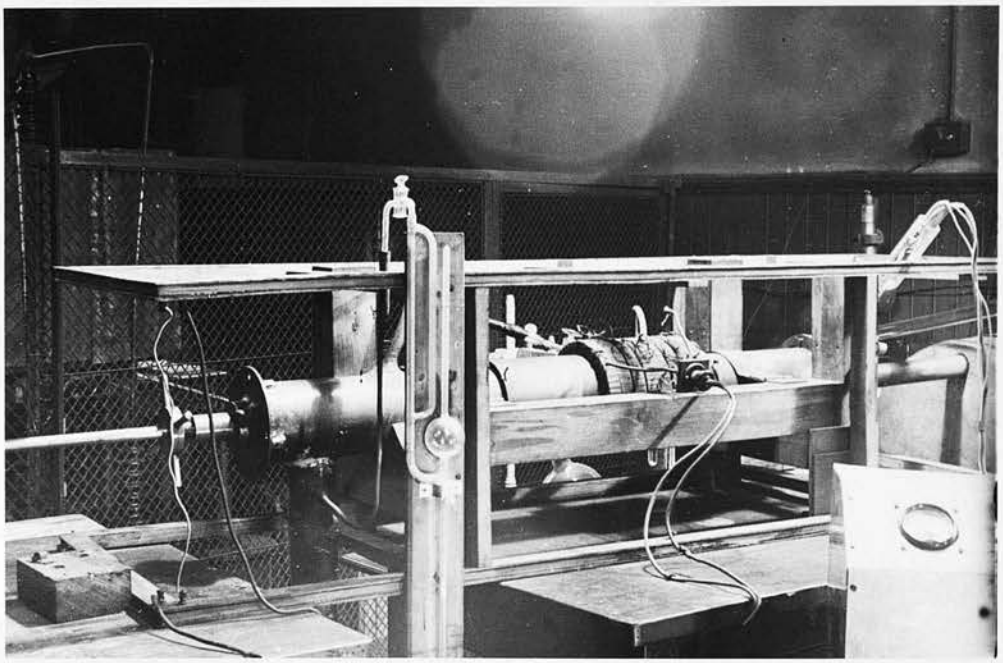

Plate 1. Spectrometer tube, lens and neutralizing coils.

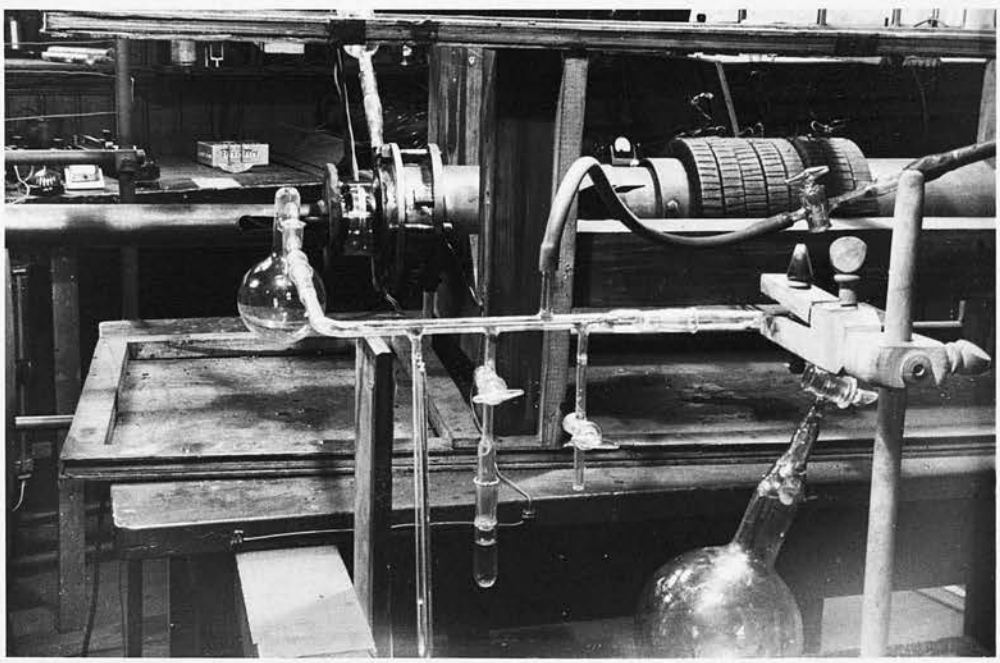

Plate 2. Accelerating tube and counter filling line.

continued until a saturation rate was reached. It was usually necessary to measure the transmission curves in two or more sections because of the limit imposed on the accelerating potential by the onset of the spurious counts. A typical curve obtained in this way, for a counter window 0.1 mg. per $cm.^2$ in thickness, is shown in Figure 2.11 from which it can be seen that, with an accelerating voltage of 7 KV, electrons of 3 keV energy are transmitted with nearly 20% efficiency. This is regarded as the practical limit of the instrument.

2.5. Normalization of Spectra.

As is the case in all magnetic spectrometers, the observed distribution of counting rate against field setting does not give a true picture of the momentum spectrum of the electrons emitted by the source. The corrections to be applied, apart from those for the decay of the source and for absorption by the counter window, will now be discussed.

The curve usually termed the line shape given by any particular spectrometer can be interpreted in two ways. As its name suggests, it represents the transmission factor for electrons of one velocity as the magnetic field is varied, but it also represents the relative transmission factors of the spectrometer for various velocities.

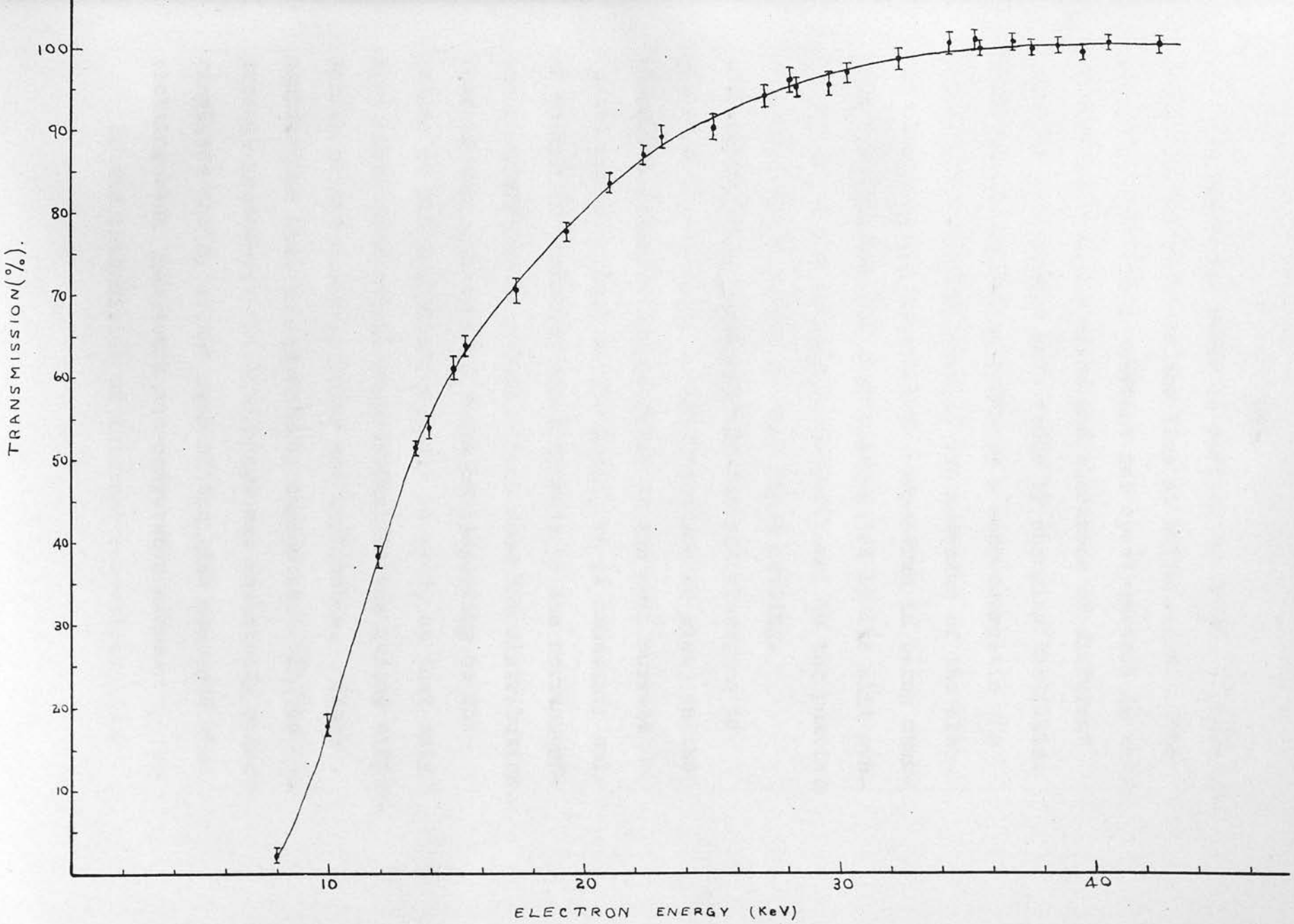

Figure 2.11. Counter window transmission curve.

The resolving power is defined by $\frac{\Delta(H\rho)}{H\rho}$, where $\Delta(H\rho)$ is the width of the line at half-height. The fraction $\frac{\Delta(H\rho)}{H\rho}$ is a constant for spectrometers in which the counter remains fixed and electrons of different energies are brought into focus by changing the field. Thus the observed line width of a mono-energetic β-radiation is proportional to the momentum of the electrons, and when a continuous β-spectrum is being measured the momentum interval transmitted by the slit system at any field setting is proportional to the particle momentum corresponding to that field setting.

Since the momentum of the focused electrons is directly proportional to the field and so also, in the present instrument proportional to the coil current (there being no iron in the lens), it is necessary only to divide the observed counting rate by the corresponding lens current to obtain a true momentum distribution. This assumes that the $H\rho$ value corresponding to the median of the transmission curve is used, so that only line shape corrections proportional to the second differential of the spectral shape are applicable. These corrections can, in general, be neglected. In the present instrument the line shape was reasonably symmetrical, so the $H\rho$ of the peak of the line was used when plotting both β-spectra and conversion lines.

If the intensities of internal conversion lines

are to be compared with each other, this may be done by comparing the observed counting rates on the peaks of the lines, or by comparing the areas under the line profiles. Since, as has been explained, the observed widths of the lines are proportional to their $H\rho$ values, the lines must be normalized in the same way as the continuous spectrum if the latter method is to be used. The result of this is clearly the same as reducing all the lines to the same width; this assumes, of course, that each is a truly mono-energetic radiation, not broadened by scattering in the source or its backing.

The measurement of line intensities in terms of the areas under the line profiles has the added advantage that the absolute intensity of a line can be found by comparison with the area under the continuous β-spectrum which, of course, represents one electron per disintegration, provided no branching takes place in the decay. That such a comparison is valid is easily seen from the following argument.

Let the shape of the continuous spectrum by represented by $F(p)$.

Let the shape of the line profile be $f(p)$, extending over the range p_1 to p_2

Let the number of electrons in the continuous spectrum be N_o

Let the number of electrons in a particular line be N_L.

We may disregard the constant solid angle for collection of the spectrometer.

Area under a line profile $= \int_{p_1}^{p_2} f(p)dp.$

The width of f(p) is proportional to p_o, the momentum of the peak of the line, lying between p_1 and p_2.

∴ by dividing by p_o we normalize the integral so that, if the maximum of f(p) is set equal to unity, the integral $\int_{p_1}^{p_2} \frac{f(p)}{p_o}\, dp$ is a constant, k.

∴ number of electrons observed in the line is

$$N_L \int_{p_1}^{p_2} \frac{f(p)}{p_o}\, dp = N_L k.$$

Observed number of electrons in the continuous spectrum is

$$\int_o^{p_{max.}} F(p_o) \left\{ \int_{p_1}^{p_2} \frac{f(p)}{p_o}\, dp \right\} dp_o$$

$$= k \int_o^{p_{max.}} F(p_o)\, dp_o$$

$$= k N_o$$

∴ The ratio of the area under the normalized line to the area under the normalized continuum is N_L/N_o.

∴ putting N_o equal to unity gives the number of times the line is emitted per disintegration.

2.6. Performance of the spectrometer at low energies.

There are two possible effects which might lead to distortion of line energies at the lowest energies measured in the spectrometer. These were pointed out and tested experimentally by Butt (1950). The first is the possible leakage of the accelerating field through the exit aperture A (Figure 2.6) into the spectrometer chamber. This would distort the paths of the focused electrons. Butt checked that this effect did not take place, and his result was verified by examining the internal conversion lines of RaD with and without an accelerating potential of 12.5 KV. No change in the position or shape of the lines was detectable.

The other effect arises from the horizontal component of the earth's magnetic field, which is not compensated. The axial field is, therefore, not strictly proportional to the focusing current. To check whether this was affecting the measured energies of low energy lines the spectrum of the active deposit of thorium was examined in the energy range 6 to 12 keV with the current in the focusing coils passing first in one direction and then in the other. The observed energies agreed within the limit of accuracy ($\sim 1\%$) with which the energies could be determined.

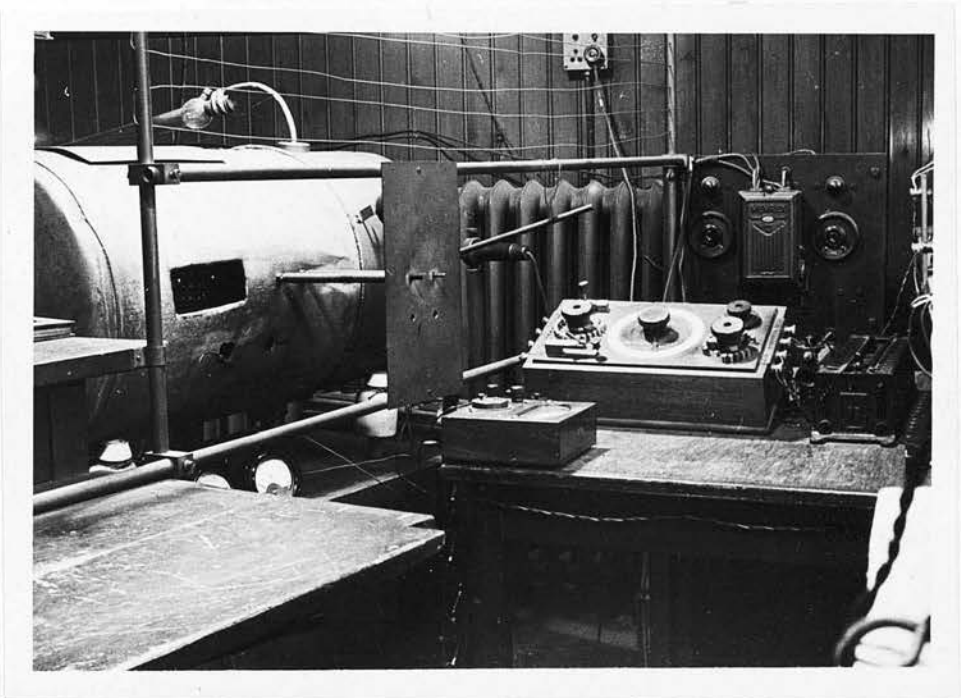

Plate 3. Bin housing the counting apparatus; and controls of the spectrometer.

Chapter III.

THE DISINTEGRATION OF RADIUM D.

3.1. Historical.

RaD has been the subject of many investigations, but, because of the softness of its radiations doubt still remains regarding its mode of disintegration. For many years it was believed that a single mode of β- disintegration (maximum β-particle energy ~15 keV) leaves the RaE nucleus in a state of 46.7 keV excitation. However, the energy of the γ-ray, observed in emission and internal conversion was the only well established evidence on which this belief was based.

In 1939, difficulties concerning intensities began to appear serious. The unconverted γ-radiation had been shown to have an intensity of about 3 or 4 quanta per hundred disintegrations (Bramson, 1930; Gray, 1932; von Droste, 1933; Stahel, 1935) but the values given by various workers for the intensity of the internal conversion electrons ranged from 15 to over 80 per hundred disintegrations. Stahel (1931), using a counter method, obtained 0.83 electrons per disintegration and, in 1935, he deduced from a measurement of the L x-radiation emitted from a source of RaD that the internal conversion electrons were emitted 0.97 times per disintegration. Kinsey (1948b) pointed out that the

second result was certainly too high since the relative intensities of the L, M and N internal conversion lines given by Curtiss (1926), on which it was based, were not corrected for the rapidly changing sensitivity of the photographic detector. Further, the fluorescence yield used by Stahel was inappropriate. Even Stahel's first result should be regarded as an upper limit since the effects of scattering and reflection would tend to increase it.

Very much lower figures were given for the number of internal conversion electrons by Lee and Libby (1939) and by Ouang, Surugue and Tsien (1943). In these experiments the effect of absorption is not clear so it is difficult to assess the value of the results.

While the work to be described in this chapter was in progress, Cranberg (1950), using a semicircular focusing β-ray spectrometer, found 74 $\pm$ 5 conversion electrons per hundred disintegrations.

Also in 1939, the presence of a second, weaker γ-radiation was reported by Amaldi and Rasetti (1939), and subsequent work by Tsien and his collaborators using selective absorption techniques and crystalline diffraction, indicated the presence of 4 γ-rays. A study of the photo-electrons projected by the γ-rays in a Wilson cloud chamber by Tsien and Tsien and Marty revealed two more γ-rays with energies of 23.2 and 7.3 keV respectively. These results by the Paris workers

have been summarized in a letter to "Physical Review" by Tsien (1946).

Curran, Angus and Cockcroft (1949) have also observed the two last mentioned γ-rays using proportional counter techniques. They give their energies as 25.8 and 7.8 keV respectively.

Feather (1949), in a review article, has listed the seven γ-rays which appear, with their estimated intensities in Table 3.1, and he pointed out that five of the seven might arise from the unique excitation of the 46.7 keV level, since within the limits of experimental error 16.1 + 31.3 = 46.7 and 16.1 + 7.3 + 23.2 = 46.7.

Table 3.1.

Quantum Energy (keV)	46.7	42.6	37 ± 0.5	31.3 ± 0.8	23.2 ± 0.6	16.1 ± 0.4	7.3 ± 0.7
Emission Intensity (%)	3.5 ± 0.4	0.2 ± 0.1	0.2 ± 0.1	0.4 ± 0.2	~1	~0	~10

Many attempts have been made to detect the primary β-radiation of RaD, but the problem is a difficult one since the end point is believed to be in the 15 keV region. Richardson and Leigh-Smith (1937) succeeded in introducing RaD into a Wilson cloud chamber in the form of the gaseous compound lead tetra-methyl, and showed that 60% of the β-rays have energies less than 4 keV. Assuming a Fermi allowed shape for the spectrum, this means that the end point is about 16 keV. Some

very recent papers on the RaD β-continuum confirming this result will be discussed at the end of this chapter.

3.2. Present Objectives.

The objects of the present work were:-

(1) to search for the L-Auger electrons emitted during the rearrangement of the ionized RaE atom and, if possible, make an estimate of their intensity,

(2) to measure the total number of the conversion electrons of the 46.7 keV transition emitted per disintegration of RaD,

(3) to see if there was any evidence for conversion electrons of the various lower energy γ-rays listed in Table 1, and

(4) to search for the very low energy continuous β-spectrum of RaD.

With regard to the measurement of the intensity of the internal conversion electrons of the 46.7 keV γ-ray, there are several possible approaches, direct and indirect. If the number of disintegrations taking place per second in the source is known, for example by watching the growth of RaE or polonium, and if the solid angle of the spectrometer and efficiency of the counter are also known, a direct estimate of the number of conversion electrons can be made. Another direct method is to compare, in the observed spectrum, the intensity

of the conversion lines with the continuous spectrum of RaE, in equilibrium with the RaD. This method is valid because, for all practical purposes, the only mode of disintegration of RaE is to the ground state of RaF by β-emission.

A possible indirect method involves a knowledge of the number of L x-ray photons emitted per disintegration by the ionized RaE atom, and the total fluorescence yield of the L shells. From these, the total number of ionizations in the L shells is obtained. This is, of course, the total number of L conversion electrons emitted per disintegration; since there is no γ-ray of sufficient energy to be converted in the K shell, no L shell ionization can be caused by the emission of K x-rays or Auger electrons. If it is now assumed that the L shell ionization is entirely due to internal conversion of the 46.7 keV γ-ray, a measurement of the relative intensities of its internal conversion electrons in the L, M and N shells is all that is required to give the total number of conversion electrons emitted per disintegration. The second and third of the methods just described were used in the present work.

3.3. Source Preparation.

If the self-absorption of electrons of very low energies is to be minimized, care must be taken in the

preparation of the sources to keep them thin and uniform. The second of these requirements is as important as the first since, as has been shown by Langer, Motz and Price (1950), variations in thickness of up to 100 times are possible when sources are deposited by evaporation from solutions, unless special precautions are taken. In the case of RaD, two methods of source preparation are available which should yield thin uniform sources. These are the electrolysis of carrier-free RaD solution, and deposition of RaD from radon gas. The latter method is practicable since all of the elements in the radioactive series from radon to RaD have fairly short half-lives. Both methods were tried.

Source no. 1 was prepared from radon. A piece of nylon sheet 0.7 mg. per cm.^{2} thick was mounted on a thin aluminium ring 0.5 cm. in diameter, and placed nylon side down, on the flat bottom of the small chamber shown in Figure 3.1. The chamber was then evacuated, and 500 mC of radon gas pumped in through the capillary tube. The chamber was sealed off for one month, after which the remaining radon was pumped out. These processes were carried out by the staff of the Radiochemical Centre, Amersham.

From the decay constants of radon, RaA, RaB, RaC and RaD it is easy to show that after 28 days the radon will have deposited 235μC of RaD. If only one tenth of this is deposited on the nylon foil, a RaD source of

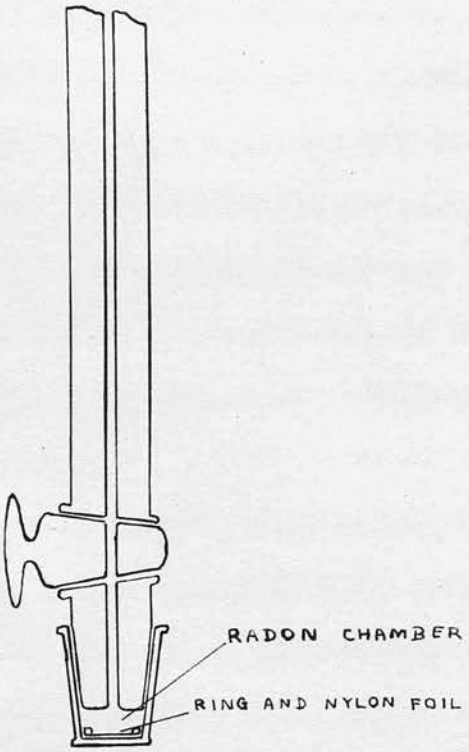

Figure 3.1. Radon activation chamber.

about 24 μC will have been produced. The actual strength of the source was estimated as approximately 40 μC.

When the nylon foil was removed from the chamber after exposure to the radon, it was brown in colour, and rather brittle, and it had partly torn away from the ring on which it was mounted. This was doubtless due to the intense α-particle bombardment. It was therefore removed from the ring and supported on a thin collodion film which in turn was mounted on the end of a brass source holder. This consisted essentially of a short brass tube 1.5 cm. in diameter and 3 cm. long fitting into the end of the source rod of the spectrometer. The experiments carried out with this source will be described later.

Source no. 2 was prepared from a supply of old glass radon needles. The needles were boiled in chromic acid, rinsed in distilled water and finely crushed under about 10 ml. of concentrated nitric acid. This solution was boiled and centrifuged, and the acid, containing the RaD, was decanted. The solution was then evaporated to dryness and taken up again with about 2 ml. of 0.1 N HNO_3. The RaD was collected on a platinum foil 0.3 $cm.^2$ in area and about 0.075 mm. thick, by an electrolysis in which the platinum foil was positive with respect to the platinum crucible containing the

solution. One side only of the platinum foil was activated by lowering it on to the surface of the solution, and then raising it about 1 mm. so that contact was maintained only by surface tension. A current of 10^{-4} amp. was passed for 10 hours. By this means only RaD was collected on the anode since it alone of the elements present forms a complex negative ion. In particular, this method of collection has the advantage of rejecting any traces of mercury which might have been present in the radon tubes. The foil was carefully washed in distilled water, the surplus liquid being removed with filter paper. The foil was then mounted in the spectrometer for a preliminary study of the spectrum.

Since this initial run showed up the well-known internal conversion lines of the 46.7 keV γ-ray and also indicated the presence of lines in the energy range between about 8 and 15 keV it was decided to transfer the RaD to a thinner backing material. Since this was to be accomplished electrolytically it was necessary to choose a conducting foil which would not dissolve too rapidly in the dilute acid, when it was made the anode of an electrolytic cell. On carrying out a test experiment, aluminium leaf was found to be unsatisfactory but gold leaf was much more resistant. The RaD was therefore transferred electrolytically to a piece of

gold leaf 0.22 mg. per $cm.^2$ in thickness and 0.6 cm. in diameter, backed for extra strength by a collodion film of weight negligible compared with that of the gold. The platinum disc was mounted horizontally and a drop of 0.1 N HNO_3 spread over its upper surface. The gold leaf, mounted on a tubular source holder, was then lowered until contact with the acid was made. A current of 10^{-4} amp. was passed for one hour through the cell so formed, the gold leaf being the anode. The gold was washed with distilled water and the surplus liquid removed, as before, with the edge of a piece of filter paper. The source so formed was a disc of about 4.5 mm. in diameter and was a practically invisible deposit on the gold leaf. In fact, when viewed by transmitted light, the area of the gold covered by the source appeared distinctly thinner than the remainder. The strength of the source was measured by observing the growth of the polonium α-activity using a spark counter kindly loaned by Dr. R.D. Connor. It was found to be 10 μC.

3.4. Results obtained with source no. 1.

3.4.1. Experimental Arrangement.

As the diameter of the source prepared by radon activation was about 3.5 mm., an exit aperture 4 mm. in diameter was used, with a source - counter distance of

80 cm. This arrangement gave a resolving power of about 4.5%.

3.4.2. Internal Conversion Electrons of the 46.7 keV transition.

The internal conversion electrons due to the 46.7 keV transition were examined using this source, and Figure 3.2 shows the spectrum obtained. Line a corresponds to conversion in the L shells of RaE and b to conversion in the M and N shells. In addition there is a line at about 544 gauss cm., on the low energy side of the main line. If this were due to L conversion electrons it would correspond to a γ-ray of about 42 keV, and a γ-ray of about this energy has, in fact, been reported by Amaldi and Rasetti (1939) and later by Tsien and his collaborators (see Tsien, 1946). However, no previous worker has reported internal conversion electrons of this transition and it seems clear that a line as intense as that appearing in Figure 3.2 would have been detected. Accordingly, an alternative explanation for its presence was sought.

The most obvious explanation is that the extra line is due to the presence of some RaD on the back of the nylon foil supporting the source. The conversion electrons emitted from this deposit would lose energy in traversing the film, and the spectral line would be broadened, particularly on the low energy side.

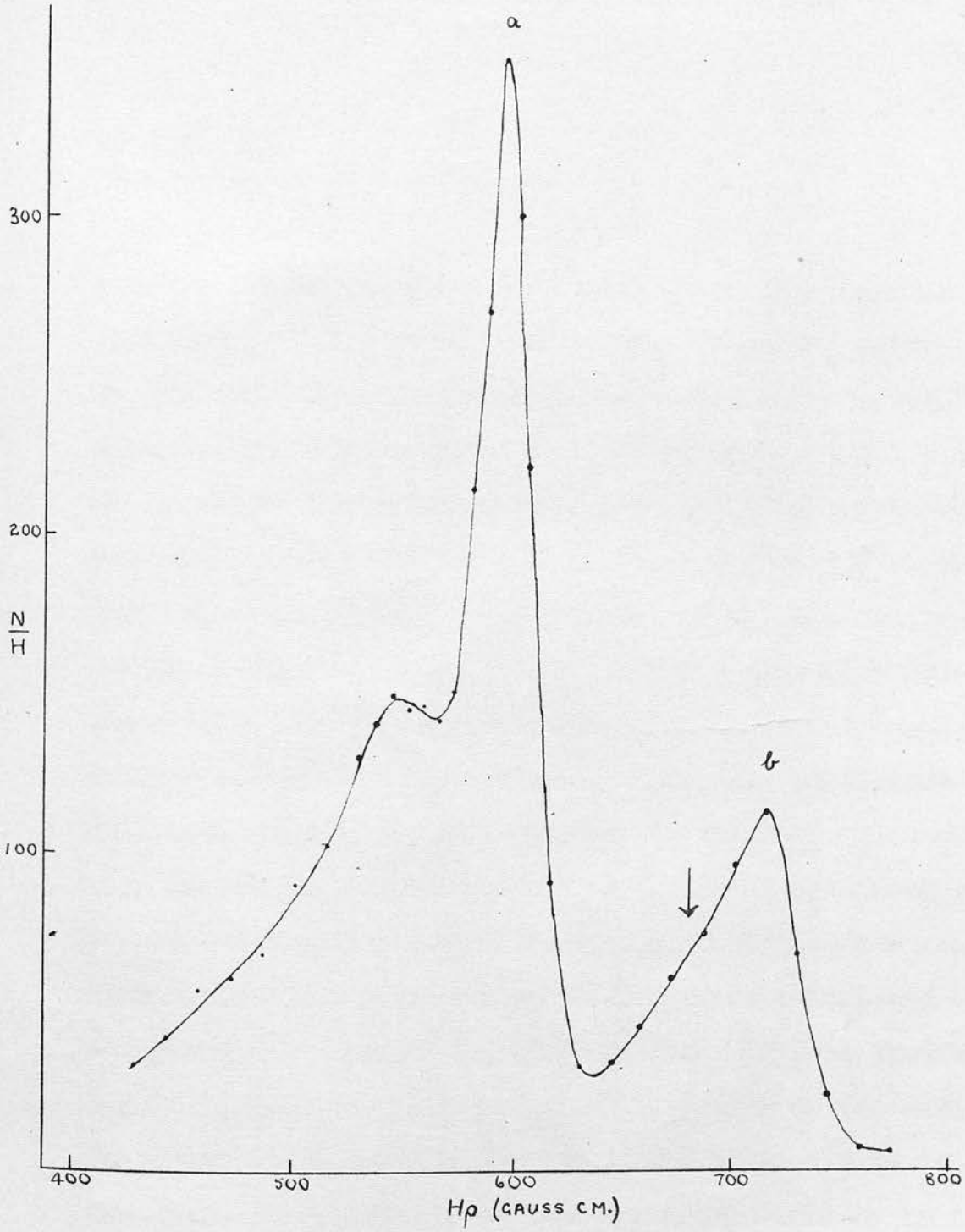

Figure 3.2. Conversion electrons of RaD as observed with source no. 1.

Several workers have dealt with the problem of the passage of electrons through matter and White and Millington (1928) have shown that the broadening of the curves is everywhere roughly proportional to the peak displacement m, which is itself given in gauss cm. by the relation

$$\frac{m\beta^3}{\sigma} = m_o$$

where β is the ratio of the velocity of the incident electrons to the velocity of light, σ is the thickness of the foil in centigrams per square centimetre, and m_o is a constant. These workers found the value of m_o to be 29. When this relation is applied to the present case it is found that the peak of the L conversion line (594 gauss cm.) would be displaced by 57 gauss cm. to 537 gauss cm. This is in reasonable agreement with the observed value, in view of the fact that White and Millington tested their relation only for thicknesses of 2 mgm. per sq. cm. and greater.

If this explanation is correct, there should be a similar effect on the low energy side of the M conversion line. Its position, calculated from White and Millington's relation, is shown by the arrow in Figure 3.2. In this case the change in momentum is too small for it to be resolved from the main M line. However, the shape of the M line on the low energy side is in general agreement with this theory.

In view of the presence of activity on the back of the source support, it was decided that no quantitative results could be obtained from this source, so it was discarded.

3.5. Results obtained with source no. 2.

3.5.1. Experimental arrangement.

As source no. 2 was considerably weaker than source no. 1, it was found necessary to increase the collecting power of the spectrometer. This was done by reducing the source - counter distance to 55 cm. The source size was 0.45 cm. and the exit aperture slightly larger, giving a resolution, $\frac{\Delta(H\rho)}{H\rho}$, of about 1/20.

3.5.2. Observations.

Figures 3.3 and 3.4 show the spectrum obtained with source no. 2 after equilibrium between the RaD and its product RaE had been established. The two most prominent lines in Figure 3.3 are formed by internal conversion electrons due to the 46.7 keV transition. Line e corresponds to conversion in the L shells of the RaE atom, and f to conversion in the M and N shells. The low energy group a, b, c, d will be discussed in section 3.5.5.

3.5.3. Intensity of the Internal Conversion Electrons of the 46.7 keV transition.

As has been explained in section 3.2 of this chapter, a comparison of the areas of lines e and f with

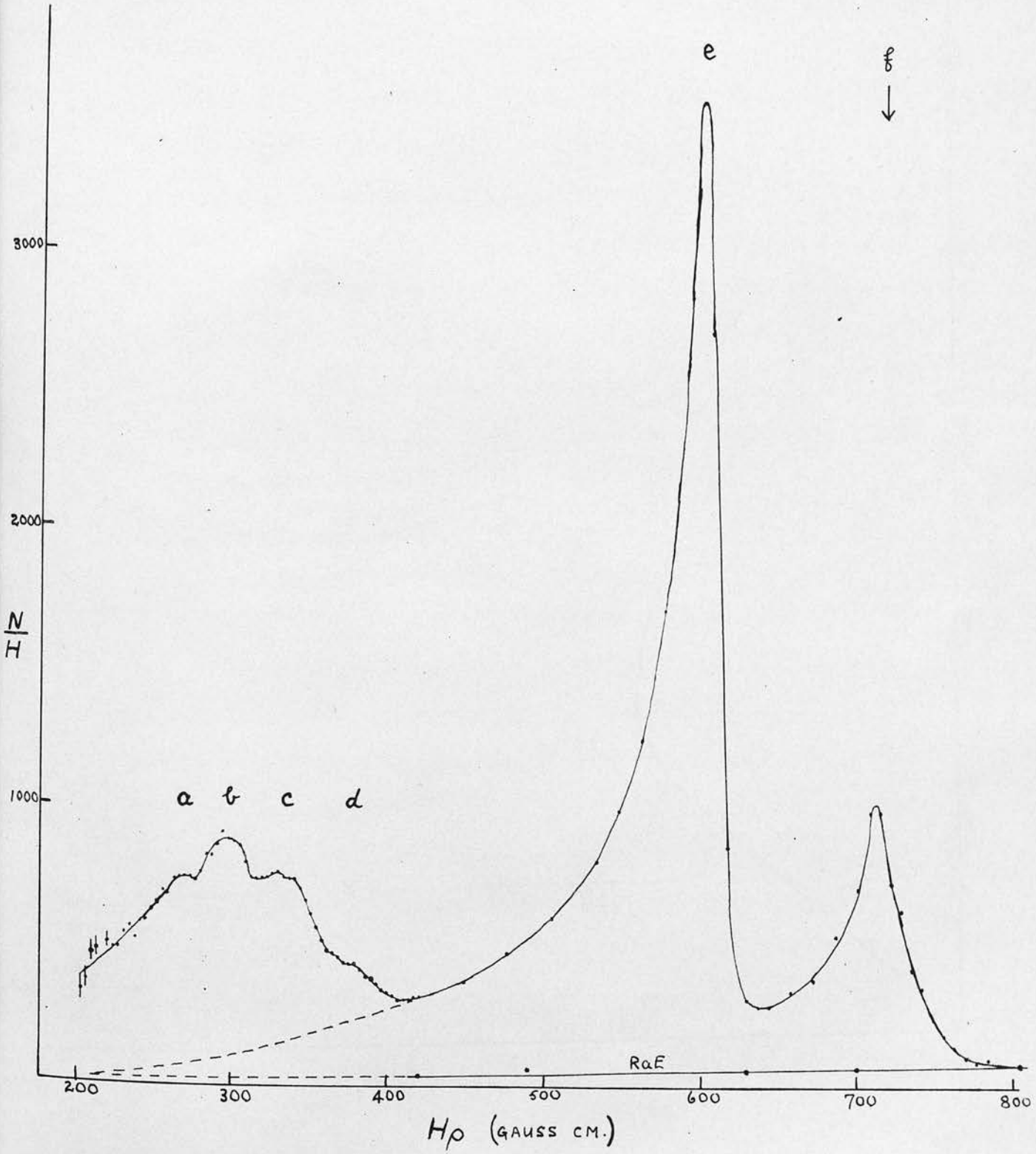

Figure 3.3. Conversion and Auger electrons of RaD.

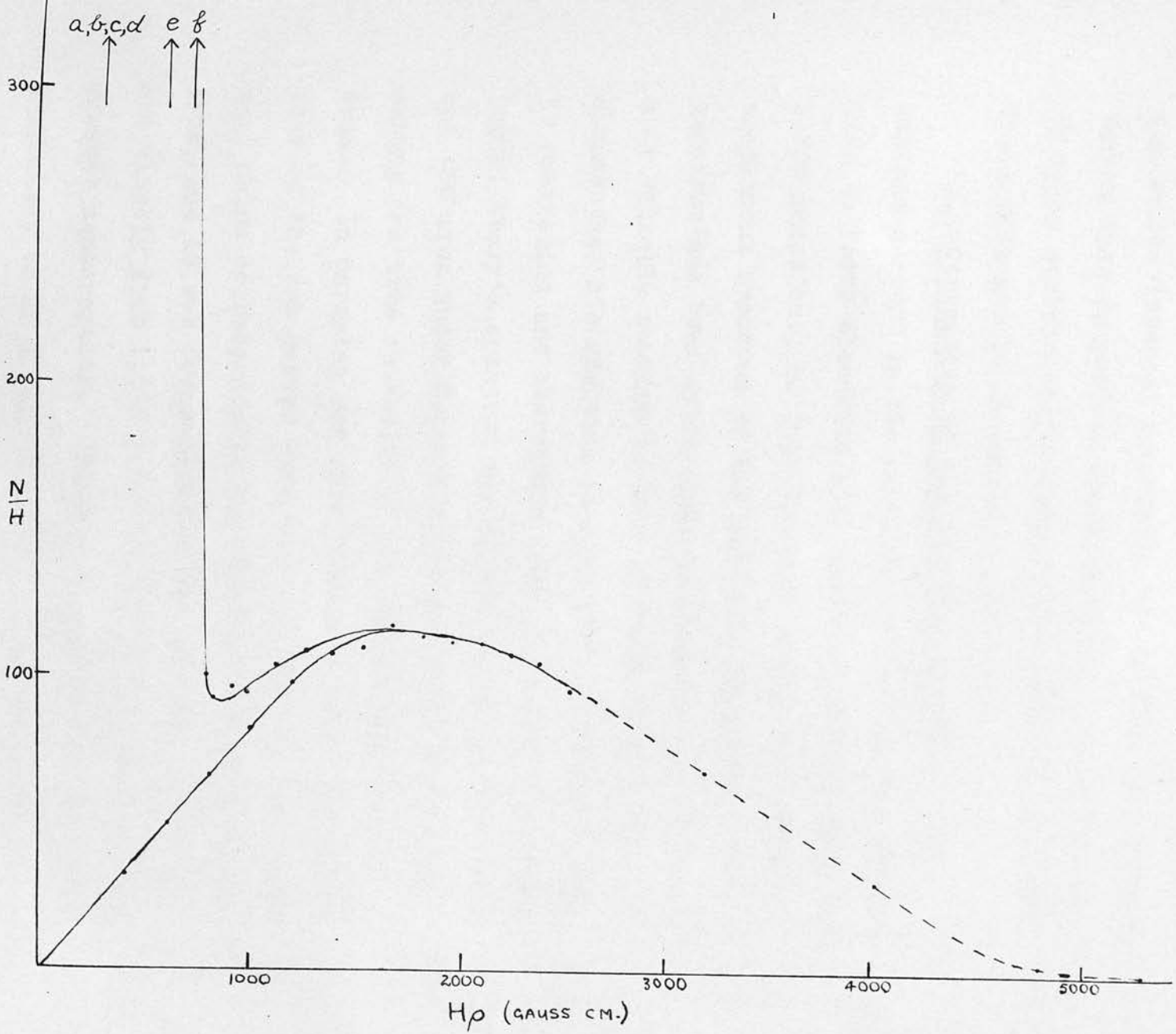

Figure 3.4. RaE continuous spectrum.

that of the RaE β-spectrum gives the fraction of the decays involving excited atomic levels of the RaE atom due to the internal conversion of the 46.7 keV γ-ray. Before this comparison could be made it was necessary to apply certain corrections to the observed spectrum. These will now be discussed.

1. Correction of the RaE β-spectrum. With maximum current in the spectrometer coil it was impossible to focus electrons with momenta greater than about 2,500 gauss cm., so that the high energy part of the continuous spectrum of RaE had to be estimated. This spectrum has been extensively studied and one of the most reliable results is that of Neary (1940), who claims that his spectrum is free from distortions due to scattering and absorption down to 13 keV. Accordingly, Neary's spectrum was fitted to the present one, and the area under Neary's curve was taken as representing the true intensity of the RaE continuous spectrum. In carrying out this fitting process the ordinates of the two curves were made the same at 1,800 gauss cm., which corresponds to the maximum of Neary's spectrum, and it was found that the two spectra corresponded closely from 1,550 gauss cm. up to the limit of the present measurements. Below 1,550 gauss cm., which is equivalent to an energy of 180 keV, our RaE spectrum lies above that of Neary. This deviation was assumed

to be due to back-scattering, and it will be shown later (section 3.5.4) that there are good grounds for this assumption.

2. Corrections to be applied to lines e and f.

The intensity due to RaE in the region of the internal conversion lines was found by examining in the spectrometer the β-radiation from a source of pure RaE deposited electrolytically on a gold foil similar to that used for the RaD. This source was prepared from a solution containing Ra(D + E + F), together with some milligrams of inactive lead, by the following method described by Broda and Feather (1947).

Most of the polonium was removed from the solution on two copper foils, and thereafter the RaE was extracted on two nickel foils which were immersed in the solution for 45 minutes each, the acidity being kept at 0.1 N HCl. The RaE was dissolved off the nickel foils in nitric acid, about 200 mgm. didymium nitrate was added, and didymium and RaE precipitated as hydroxides with ammonia. The precipitate was washed with ammonia to remove all traces of nickel and was dissolved in trichloracetic acid. The solution was electrolysed overnight using a small platinum vessel as anode and a platinum electrode about 0.5 cm. square as cathode. The RaE was then transferred from the platinum to a gold leaf by the same method as was used for the RaD,

except, of course, that the gold leaf was now the cathode. Currents of 0.03 mA were used in these electrolyses. The final source of RaE was about 50 μC in strength and was an invisible deposit on the gold leaf. The RaE spectrum obtained with this source was fitted to the original spectrum of Ra(D + E) to give the line marked 'RaE' in Figure 3.3. This line was used as a base line when the intensity of the conversion electrons was being considered. To correct the area of the conversion lines for back-scattering use was made of the formula given by Hamilton and Gross (1950). These authors state that the back-scattering ratio (the number of scattered electrons per primary) reaches an asymptotic value called the back-scattering constant S for a thickness t_o of scattering material at an energy V_c given by $V_c = 800\left[(Z^2/A)t_o\right]^{\frac{1}{2}}$, where V_c is in keV, Z and A are the atomic number and mass number of the scatterer and t_o its thickness in gm./cm.^{2}. The value of S has little energy dependence. Applying this equation to the source support used in the present investigation we obtain V_c = 67 keV. This value appears to be a reasonable one for saturation back-scattering since our RaE spectrum begins to depart from that of Neary at about 180 keV. It is nevertheless possible that the source backing was actually thinner than 0.22 mg./cm.^{2} owing to the solution of some of the gold in the 0.1 N HNO_3 during the electrolysis of the RaD.

However this may be, we assume that back-scattering has reached saturation over the whole range of energy (45 keV and less) with which we are at present concerned.

To find the value of S the following experiment was carried out. Thorium B was deposited by recoil on 0.2 mg./cm.^{2} aluminium leaf and the spectrum in the neighbourhood of the F line (148 keV) was plotted. A fairly reliable estimate of the area of the ThB F line free from back-scattering was obtained from this curve. A platinum tipped brass rod was then placed immediately behind and in contact with the aluminium leaf and the spectrum plotted again. This gave the area of the F line of ThB under conditions of saturation back-scattering. Finally, the experiment was repeated under the original conditions to make sure that, after correction for the decay of the source, the third set of counts corresponded with the first set. A comparison of the areas of the F line of ThB in the two cases gave the value 0.55 ± 0.05 for the number of back-scattered electrons per primary under the solid angle conditions obtaining in our spectrometer. We regard this as an upper limit for our Ra^D correction since, as indicated above, the source mount was probably thinner than 0.22 mg./cm.^{2}.

Applying the appropriate corrections to the areas of the RaE spectrum and of lines e and f, the number of

conversion electrons due to the 46.7 keV γ-ray was calculated as 59.2 $\pm$ 5 per hundred disintegrations, of which 46.7 $\pm$ 4 (i.e. 79%) were found to be due to conversions in the L shells. Since we have probably over-corrected for back scattering these values should be regarded as lower limits.

Taking the intensity of the unconverted 46.7 keV γ-ray as 3.5 per hundred disintegrations, the ratio of the number of L-conversion electrons to the number of unconverted γ-rays is 13.5.

As has been explained in 3.2 of this chapter, the number of conversion electrons of the 46.7 keV γ-ray can be deduced from (i) the number of L x-rays produced as a result of internal conversion in the L shells, (ii) the fluorescence yield of the L shells and (iii) the fraction of the internal conversion electrons which originate in the L shells. Stahel's (1935) result for (i) is 25.1 per hundred disintegrations, and Kinsey (1948b) has obtained 0.47 for the fluorescence yield. These figures, with the present result of 79% for (iii), give 67.5 conversion electrons per hundred disintegrations. This method eliminates the fitting of our incomplete RaE spectrum to Neary's, but ignores any ionization of the L shells which may be produced by conversion of the recently discovered low energy γ-rays.

3.5.4. Conversion Electrons of γ-rays other than the 46.7 keV radiation.

A search was made for internal conversion electrons of the other γ-rays listed in Table 3.1. In many cases the energies of the internal conversion electrons of these transitions would fall in the same energy region as the L-Auger electrons, which make up the group a, b, c, d in Figure 3.3, so the conversion lines would be masked. However, L conversion electrons of the 31.3 and 37 keV γ-rays would have energies of about 15 and 20 keV respectively which are above the Auger range, so the search was restricted to these transitions.

No convincing evidence was found for the conversion electrons and it is estimated that, if present, their intensities are certainly less than 1 per 100 disintegrations in each case. The L conversion electrons of the 23.2 keV γ-ray, which is reported to have an intensity in emission of $\sim$1 per 100 disintegrations, would appear very close to line a in Figure 3.3 so it is possible that internal conversion electrons of this transition may be present among the Auger electrons.

3.5.5. The L-Auger lines of RaE.

With the proviso just mentioned, the group of lines marked a, b, c, d in Figure 3.3 are considered to be L-Auger lines associated with the ionization of the L shells of the RaE product atom. Although the lines are not clearly resolved, at least four are easily distinguishable and the peaks marked b, c and d may each

consist of two or more unresolved lines. In table 3.2 six lines have been suggested. Their momenta have been computed by using, for calibration purposes, the value of 594.3 gauss cm. given by Curtiss (1926) for the L_I internal conversion line of the 46.7 keV γ-ray.

Table 3.2.

RaD source		Thorium active deposit
Identification letter	$H\rho$ (gauss cm.)	$H\rho$ (gauss cm.)
a	269 ± 2	270.6
	-	282.5
	-	289.5
b	297 ± 3	300.4
c	329 ± 4	329
	339 ± 2	340
d	(364 ± 3)	369
	377 ± 2	377

The table also shows the momenta of the low energy lines in the spectrum of thorium active deposit obtained by Butt (1950). Butt has shown that his spectrum should contain L-Auger lines from elements 83 and 81 and, since ThC (element 83) is an isotope of RaE, the L-Auger spectra obtained from sources of thorium active deposit and of RaD should contain some lines common to both. In Butt's determination, Flammersfeld's (1939) energy

for the A line of ThC-C" was used for calibration purposes but a very recent determination by Craig (1952) has shown that Flammersfeld's value is about 0.5% high. Table 3.2 shows Butt's momenta recalculated on the basis of Craig's value for the A line. The agreement is good except for the rather doubtful 364 gauss cm. line suggested in the RaE spectrum. The lines which appear only in the spectrum of thorium active deposit may be due to element 81, but no attempt has been made to re-analyse Butt's observations.

3.5.6. Interpretation of the low energy lines.

Before the transitions which lead to the observed Auger lines can be deduced it is necessary to estimate the distribution of the L shell ionization amongst L_I, L_{II} and L_{III}. This calculation is relatively simple, as the L shell ionization can be assumed to be due to conversion of the 46.7 keV γ-ray only, no strong conversion electrons of any of the other γ-rays listed in table 3.1 having been reported.

Cranberg (1950) has shown that the relative intensities of the L_I, L_{II} and L_{III} conversion electrons are in the ratio 90.1: 8.1: 1.8. These ratios do not give the relative intensities of ionization in the three L shells because they are modified by Auger transitions of the type first identified by Coster and Kr"onig (1935). Coster and Kr"onig explained anomalies

in the intensity distribution of x-ray emission lines and their satellites on the basis of the high probabilities of the two transitions $L_I \rightarrow L_{III}\ M_{IV}$ and $L_I \rightarrow L_{III}\ M_V$. Such a process is energetically possible for atoms having atomic numbers less than 50 or greater than 73. The exact fraction of the initial L_I ionization which is transferred to L_{III} by these transitions is difficult to estimate, but Coster and Krönig calculate that it can be as high as 0.80. Kinsey (1948a) has given the value 0.70 for element 83.

The transition $L_I \rightarrow L_{II}\ N$ is energetically possible for element 83, and there is some evidence to indicate that it does take place in this element. Kinsey (1948b) by comparing the observed and calculated fluorescence yields for the L shells in ThC deduced that 12% of the ionization initially in the L_I shell is transferred to L_{II}. If Kinsey's figures for the fractions of the L_I ionization transferred are accepted we find that the final distribution of ionization in L_I, L_{II} and L_{III} is 16.2:18.9:64.9. While these figures may not be highly accurate, they indicate that the most probable L-Auger transitions will be those involving the L_{III} shell.

Using this conclusion as a guide an attempt may now be made to fit the observed L-Auger lines into a scheme. For this purpose the values of the L and M

shell ionization energies given by Slack (1952) were used. As Slack did not include N shell ionization energies in his table, these were calculated from the x-ray term values given in the Landolt-Bornstein tables (1950).

As first indicated by Ellis (1933) the energies of the Auger lines cannot be obtained accurately from such x-ray data, since the atom left by an Auger electron is ionized doubly, not singly as in the case of x-ray ionization. For K-Auger lines of ThB Ellis estimated that the additional binding energy for a second L-ionization was between 100 and 300 eV. For L-Auger electrons, the two ionizations will be in M or N levels, so the additional binding energy will be much less. In the present case, however, the atom may already be doubly ionized (e.g. in L_{III} and M_{IV}) after a Coster-Krönig transition, and becomes triply ionized (e.g. in M_{IV}, M_V and N) after the Auger transition which is observed. In these disintegrations obviously slightly greater binding energy will apply.

Table 3.3 shows possible transitions on the basis of the conclusions reached in the above paragraphs. The notation is the one now generally used - for instance $L_{III} \rightarrow M_V\ M_{III}$ indicates a transition in which the atom was initially ionized in the L_{III} shell, while after the emission of the Auger electron, the ionization

is in the M_V and M_{III} shells. It will be noticed that in table 3.3 more than one possible origin has been indicated for some of the lines, and that some of the theoretical values are bracketed, the differences being too small to show up as distinct lines. It is satisfactory, however, that the most prominent Auger lines are associated with the L_{III} shell, and in fact the strong lines 2 and 4 in table 3.3 are due to "conversion" of the intense $L\alpha_1$ x-ray ($L_{III} \rightarrow M_V$).

Table 3.3.

Observed Line		Suggested Transition	
$H\rho$ (gauss cm.)	Energy (keV)		(keV)
269 ± 2	6.33 ± 0.10	$L_{III} \rightarrow M_{III}\, M_I$ $L_{III} \rightarrow M_{III}\, M_{II}$	6.26 6.55
297 ± 3	7.70 ± 0.13	$L_{III} \rightarrow M_V\, M_{III}$ $L_{III} \rightarrow M_V\, M_{IV}$	7.65 8.13
329 ± 4	9.40 ± 0.20	$L_{II} \rightarrow M_{IV}\, M_I$ $L_{II} \rightarrow M_{IV}\, M_{II}$ or $L_{III} \rightarrow M_{III}\, N_I$ $L_{III} \rightarrow M_{III}\, N_{II}$ or $L_I \rightarrow M_{III}\, M_I$ $L_I \rightarrow M_{III}\, M_{II}$	9.03 9.32 9.3 9.43 9.21 9.50
339 ± 2	10.0 ± 0.10	$L_{III} \rightarrow M_V\, N_I$ $L_{III} \rightarrow M_V\, N_{II}$	9.89 10.04
(364 ± 3)	(11.45 ± 0.20)	$L_{II} \rightarrow N_{IV}\, M_I$ $L_{II} \rightarrow N_{IV}\, M_{II}$ or $L_I \rightarrow M_I\, N_I$	11.26 11.55 11.44
337 ± 2	12.35 ± 0.15	$L_{II} \rightarrow M_{IV}\, N_I$ $L_{II} \rightarrow M_{IV}\, N_{II}$ or $L_I \rightarrow M_{III}\, N_{II}$	12.1 12.2 12.38

3.5.7. Intensity of the Auger Lines.

The expected number of L-Auger electrons can be calculated from the observed number of L conversion electrons and the total L shell fluorescence yield. Kinsey (1948b) has calculated the yield for element 83 on the basis of conversion in L_I, L_{II} and L_{III} in the ratio 0.90: 0.09: 0.01, which is almost exactly the ratio observed by Cranberg (1950) for the lines of RaD. The value given by Kinsey is 0.47. Assuming that the Auger lines are produced by ionization of the L shells as represented by line e only (Figure 3.3), and using Kinsey's value of 0.47 for the fluorescence yield, the Auger lines should have a combined intensity of 0.53 x 46.7 = 25 per hundred disintegrations. The combined intensity of the group of lines a, b, c, d is roughly 24 per hundred disintegrations. This value was obtained by comparison with line e - as back-scattering has reached a constant saturation value for all of these lines, a direct comparison gives the result. The agreement between the calculated and measured values is probably accidental, for an appreciable fraction of the area under the low energy lines may well be due to the β-radiation of RaD together with any conversion electrons of the 23.2 keV γ-ray. In view of these considerations it is probable that some source self-absorption was taking place at these energies and that this has at

least partially annulled the expected rapid rise of the RaD continuous β-spectrum.

3.6. Discussion.

3.6.1. The L-Auger electrons.

The momenta of the Auger electrons of RaE have been found to agree reasonably well with some of the lines present in the spectrum of thorium active deposit, one constituent of which is an isotope of RaE. The interpretation of the observed Auger lines in terms of electronic transitions suggested in table 3.3 is in agreement with the Coster-Krönig theory of transfer of L_I ionization to the L_{III} shell with the emission of an electron from M_{IV} or M_V. A very high resolving power would be required to decide between the alternative transitions suggested in table 3.3.

The transfer of ionization from L_I to L_{II} with the expulsion of an N electron is energetically possible in element 83 but it was not possible with the present apparatus to decide whether it takes place. Such a transfer would affect the relative intensities of the L_I and L_{II} Auger lines.

Evidence for this process has, however, been obtained by Ewan (1952) from measurements of the relative intensities of the L x-rays emitted from a source of RaD. On the other hand, Cohen and Jaffe (1952), using

a proportional counter and pulse analyser to study the L x-radiation, concluded that such a transfer is a relatively improbable process. The results of Cohen and Jaffe, however, appear to be suspect, since they have assumed that one of the x-ray lines they observed was entirely due to $L\gamma_1$ radiation, whereas it has been shown by Frilley, Gokhale and Valadares (1951) that in RaE $L\gamma_1$, $L\gamma_2$ and $L\gamma_3$ are all of comparable intensity, contrasting with the fluorescence spectrum of bismuth in which the intensity of $L\gamma_1$ is very much greater than that of $L\gamma_2$ and $L\gamma_3$. The apparatus of Cohen and Jaffe would not resolve these three closely spaced lines, so the intensity which they attributed to $L\gamma_1$ should have been divided among all three x-rays. This would invalidate their subsequent calculations.

3.6.2. The continuous spectrum of RaD.

No convincing evidence was found regarding the very low energy RaD continuum, presumably because of absorption in the source, and this in turn led to uncertainty in estimating the total intensity of the L-Auger lines. Very recently, however, Bannerman and Curran (1952) and Insch, Balfour and Curran (1952), using scintillation and proportional counter techniques, have given the end point of the Ra^D continuous spectrum as 18 ± 2.5 keV, in agreement with the value of 16 keV deduced by Richardson and Leigh-Smith (1937) from their

cloud chamber measurements. This result may not be incompatible with the findings of Teillac, Falk-Vairant and Victor (1952) who, from a coincidence experiment using windowless Geiger counters, claim that 90% of the RaD β-rays have energies less than 5 keV.

3.6.3. Internal conversion electrons.

No internal conversion electrons of any of the recently discovered γ-rays have been detected, with the possible exception of the L conversion electrons of the 23.2 keV transition, which may be present in the L-Auger spectrum.

The present measurements of the intensity of the conversion electrons of the 46.7 keV transition have shown that decay by this route can at most account for only about 70% of the disintegrations of RaD. Cranberg (1950) gives a figure of 74%. The presence of the softer γ-rays allows an alternative mode of de-excitation of the 46.7 keV level, as indicated in Figure 3.5. However, the present work, in agreement with Cranberg (1950) and Cork et al. (1951) indicates that the intensities of the internal conversion electrons of these γ-rays are very low, and table 3.1 shows that, with the exception of the 7.8 keV γ-ray, they are weak in emission also. It seems doubtful, therefore, whether a cascade process of the type shown in Figure 3.5 can account for the remaining 30% of the disintegrations.

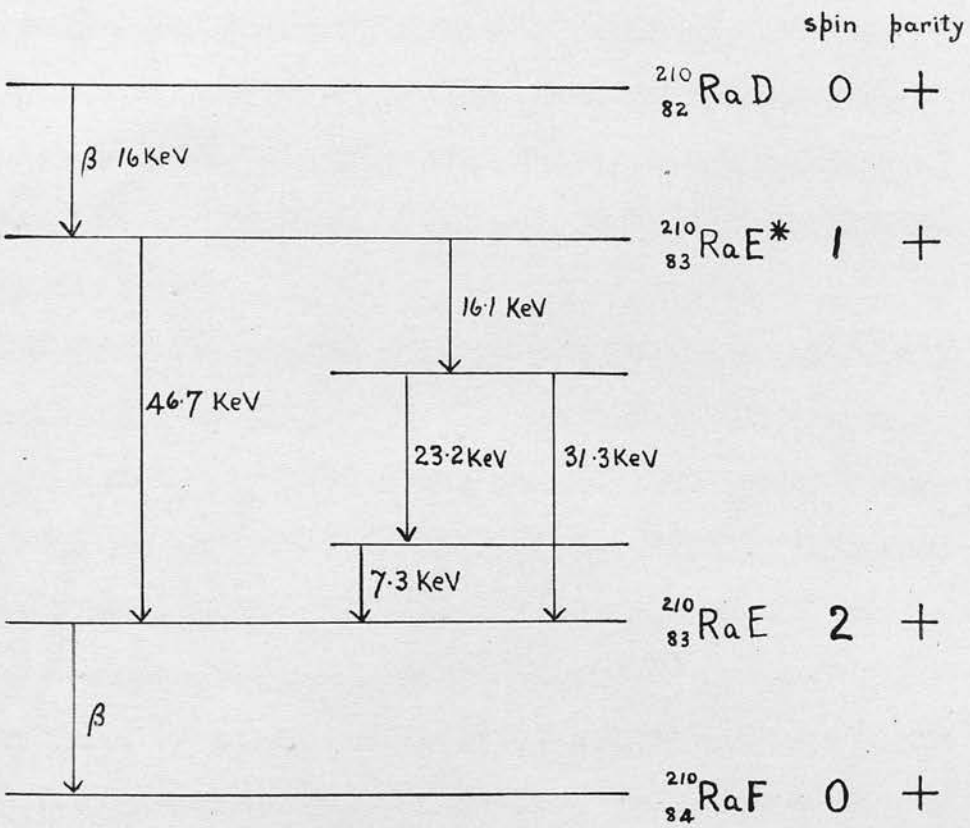

Figure 3.5. Possible level scheme for the RaE nucleus after β-decay of RaD.

3.6.4. Spin and parity relations.

Assuming that the even-even nuclei RaD and RaF have zero spin and even parity and accepting an end point of the RaD spectrum at about 18 keV so that the transition is an allowed one, the 46.7 keV excited state in the RaE nucleus has spin 1 and even parity. If the RaE spectrum is regarded as second forbidden (Feather and Richardson, 1948) the ground state of RaE has spin 2 and even parity on the basis of the Gamow-Teller selection rules. Moreover, according to Konopinski (1943) a suitable combination of vector and tensor interaction can explain the somewhat unusual shape of the RaE spectrum on the basis of a spin change of 2 with no parity change. We therefore conclude that the 46.7 keV radiation carries off one unit of angular momentum and that, since there is no parity change, the radiation will be magnetic dipole with possible admixture of electric quadrupole. Gellman, Griffith and Stanley (1952) have recently published calculated values of the L shell internal conversion coefficients and the value measured in the present work (13.5) agrees with the value calculated for magnetic dipole radiation. The ratios of the L_I, L_{II} and L_{III} conversion lines observed by Cranberg (1950) are also in good agreement with the calculations for magnetic dipole radiation.

The predictions of the shell model are not, however,

in agreement with the above conclusions, since shell theory suggests that the ground state of RaE has odd parity and that the RaE β-spectrum is first forbidden. Pestchek and Marshak (1952) have shown that the shell theory requirements can be satisfied on the basis of a $0 \rightarrow 0$ transition with parity change if a mixture of tensor and pseudo-scaler interaction is assumed. This would require a spin change of unity with parity change for the 46.7 keV transition, indicating electric dipole radiation. The observed internal conversion coefficient is not in agreement with this.

Chapter IV.

THE ELECTRON SPECTRUM OF MESOTHORIUM 2.

4.1. Historical Introduction.

Mesothorium 2 has been less thoroughly studied than most of the other "classical" radioactive bodies. It grows from the long-lived mesothorium 1 and decays by β-emission to radiothorium with a half-value period of 6.13 hours. The internal conversion electrons emitted by MsTh2 were photographed by Black (1924) using a semicircular magnetic spectrometer, and by Yovanovitch and d'Espine (1927) using the direct deviation method. These experiments showed the existence of a large number of internal conversion lines, the most intense having energies below 350 keV. From the conversion lines which he observed, Black deduced the presence of 8 γ-rays. Some of the γ-rays of MsTh2 were also detected by Thibaud (1926), who studied the spectrum of photoelectrons which they produced in a lead radiator. Yovanovitch and Proca (1926) attempted to extend the investigation of the MsTh2 spectrum into the very low energy region, and reported the presence of lines down to about 3 keV.

Cloud chamber studies by Lecoin, Perey and Teillac (1949) showed that the total number of electrons emitted per disintegration of MsTh2 was approximately 2. Half

of the electrons were found to have energies below about 60 keV, and Lecoin et al. also deduced that there was a time delay greater than 0.01 sec. between the emission of a nuclear electron and a low energy conversion electron.

Using the method of selective absorption Lecoin, Perey and Riou (1949) observed the L x-rays emitted by a source of MsTh2 and found that their total intensity was 0.30 ± 0.06 per disintegration.

The primary β-spectrum has been shown by several workers to extend to high energies, but their conclusions as to the ultimate end point show considerable disagreement. (Lecoin, 1935 and 1938; Libby and Lee, 1939; and Feather, 1930 and 1938).

4.2. Objects of present investigation.

A study of the β-spectrum of mesothorium 2 was being undertaken in this department by J. Kyles, C.G. Campbell and W.J. Henderson (to be published), using a double β-ray spectrometer, and the present work was intended to be complementary to their investigation. In particular, the objectives were to study the spectrum in the region between 600 and about 2,000 gauss cm. with the intention of measuring the intensities of the internal conversion lines, and then to extend the observations below 600 gauss cm. to

cover the energy region of the L-Auger lines.

4.3. Chemical separation of mesothorium 2.

The MsTh2 was separated chemically from a stock solution in dilute HCl, containing mesothorium 1 and its decay products associated with an appreciable activity of radium and its products and 100 mg. of barium carrier. The method used was based on that of Haissinsky (1933). It was found that about 1 mC activity due to MsTh2 could be obtained from the solution 24 hours after each extraction.

By adding NH_4OH to the stock solution, the grown MsTh2 and other decay products were precipitated as hydroxides with cerium or iron carrier. The precipitate was filtered off under reduced pressure using a "porosity 3" sintered glass filter funnel, and the filtrate containing the MsTh1 and radium re-acidified with HCl and set aside to allow more MsTh2 to grow. The precipitate was dissolved off the filter in dilute HCl and about 1 mg. each of lead and bismuth carriers added. Hydrogen sulphide was bubbled through this solution to precipitate as sulphides the activities due to polonium, bismuth, lead and thallium isotopes. The precipitate was filtered using a second sintered glass funnel and, after washing, the filtrate was boiled to remove the excess H_2S. About 1 mg. of barium was

added as hold back carrier and the mesothorium 2 and carrier re-precipitated and filtered using a third filter funnel. This removed any MsThl or radium in the filtrate, which was retained and eventually returned to the stock solution. The precipitate was dissolved in 1 N nitric acid to give a solution from which a source could be prepared.

After about a dozen separations the stock solution became saturated with ammonium salts. This prevented the precipitation of the hydroxides of the MsTh2 and carrier. By this time, too, the volume of the stock solution was about 10 ml., which was inconveniently large. The ammonium salts were removed by first neutralizing the stock solution and then adding a saturated solution of ammonium carbonate, which precipitated as carbonates the barium, radium and MsThl. After thorough washing to remove the unwanted salts, the precipitate was dissolved in about 2 ml. of dilute HCl. The solution was then set aside for 24 hours to allow MsTh2 to grow before the next separation.

The earlier sources were separated using 1 mg. of cerium as carrier, and in this case a method of obtaining carrier-free MsTh2 has been outlined by Peterson (M.D.D.C. 1709). The method consists in oxidising the cerium to the Ce^{IV} state and precipitating it as iodate, when the mesothorium 2 is left in solution. Peterson

recommends the use of silver oxide to oxidise the cerium, but even when freshly prepared it was found to be less effective than ammonium persulphate solution with the addition of a speck of solid silver nitrate. The oxidised solution was diluted to about 5 ml. with 1 N HNO_3 and HIO_3 was added drop by drop to precipitate the cerium and silver. The supernatant liquid was evaporated to dryness and ignited in a crucible to decompose the iodic acid and excess persulphate, leaving the MsTh2 in the crucible.

The method, although workable, was found to be rather uncertain, both in the oxidation of the cerium and the subsequent precipitation of the iodates. Too little HIO_3 did not precipitate all the cerium and too much led to a reduced yield of activity. Moreover, after the ignition not all of the mesothorium 2 in the crucible could be dissolved off. The yield was thus further reduced. In practice it is doubtful whether any of the sources used were truly carrier free although the process probably removed 80 or 90% of the 1 mg. of cerium initially present.

It was later found that if, in place of cerium, iron was used, the mesothorium could be carried down with as little as 20 or 30 μgm. of carrier. In view of this small weight of carrier, and because of the appreciable saving in time - important when a 6 hour

activity is being studied - the use of cerium was eventually abandoned.

In the experiments to be described sources prepared by both methods were used. The radioactive purity of the mesothorium 2 was checked by observing its half-life, which was found to be within 1% of the accepted value.

4.4. Source Mounting.

In an effort to reduce scattering, the sources were mounted so as to be as far as possible from heavy metals. A sketch of one of the aluminium source holders is shown in Figure 4.1. The short rod AB fitted into a hole in the end of the source rod of the spectrometer, and the source itself was mounted on a thin foil stretched across the ring C. Each source holder was made in one piece from one inch diameter aluminium rod.

When radioactive sources are deposited by evaporation from solutions, the material tends to form a highly non-uniform layer. Langer, Motz and Price (1950) have shown that variations in thickness up to a factor of 100 can occur. However, if the area on which the source is to be deposited is previously wetted with a weak solution of insulin, a very great improvement in uniformity can be achieved. Langer et al. showed that this technique gave sources the thickness of which was constant to within a factor of four.

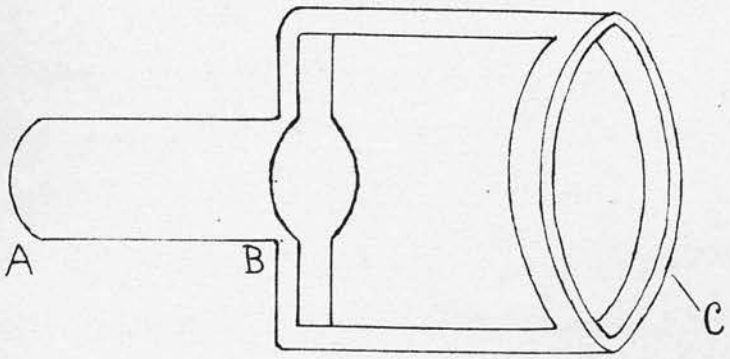

FIGURE 4.1

SOURCE HOLDER

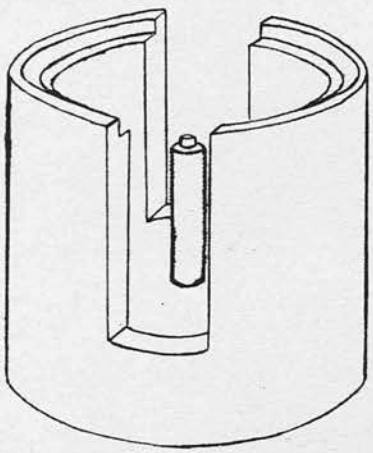

FIGURE 4.2

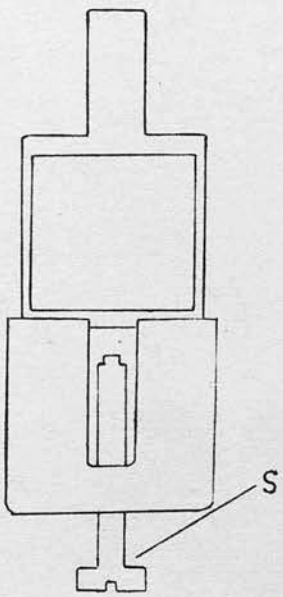

FIGURE 4.3

The method used in the present work was as follows. A drop of a 10% solution of insulin (40 units per ml.) was placed on the centre of a foil stretched over the ring of the source holder.

In order to locate the centre of the ring accurately, the device sketched in Figure 4.2 was used. It consisted of a cylindrical brass cup with a suitable step turned in its rim to fit the ring of the source holder. Through a tapped hole in the centre of its base passed a 0 B.A.screw. In use, the cup was mounted vertically, and the inverted source holder placed on top of it as shown in Figure 4.3. On the end of the screw S, which had been turned down to a diameter of 3 mm., a drop of insulin solution was placed, and the screw was then screwed up until the drop made contact with the foil on the source holder. The operation could be watched through slots cut in the side of the cup. After the surplus insulin had been removed with a very finely drawn pipette, the source holder was ready for the deposition of a radioactive source.

The chemically separated mesothorium 2 was contained in a few drops of dilute nitric acid solution, and one drop of this was deposited from a finely drawn pipette on the area of the foil previously wetted by the insulin. The drop spread over this area but no further. It was then evaporated to dryness under an infra-red

lamp, to produce a disc-shaped source about 3 mm. in diameter and having an estimated thickness of about 0.1 mg. per cm.^{2}.

It was found that the insulin was effective in producing a uniform deposit for only the first drop of radioactive solution. Accordingly all the sources used were prepared from one drop only of solution. They were about 1/10 mC. in strength and each was used for about 10 hours counting.

4.5. General Survey of the Spectrum.

A survey of the spectrum of MsTh2 was made over the range of $H\rho$ values from 500 to 2,500 gauss cm. Figures 4.4(a) and (b) show the graph obtained in a typical run, after correcting the counting rate for decay of the source and for absorption in the counter window. The latter correction was applicable only below 30 keV since an accelerating potential of 7 KV was used with a counter window which transmitted 37 keV electrons with 100% efficiency.

Table 4.1 shows the $H\rho$ values of the lines observed compared with the corrected* values of Black (1924).

* Black based his measurements on the $H\rho$ values for the lines of Ra(B + C) obtained by Ellis and Skinner (1924). In table 4.1 Black's values have been altered to agree with the later measurements on Ra(B + C) made by Ellis (1934).

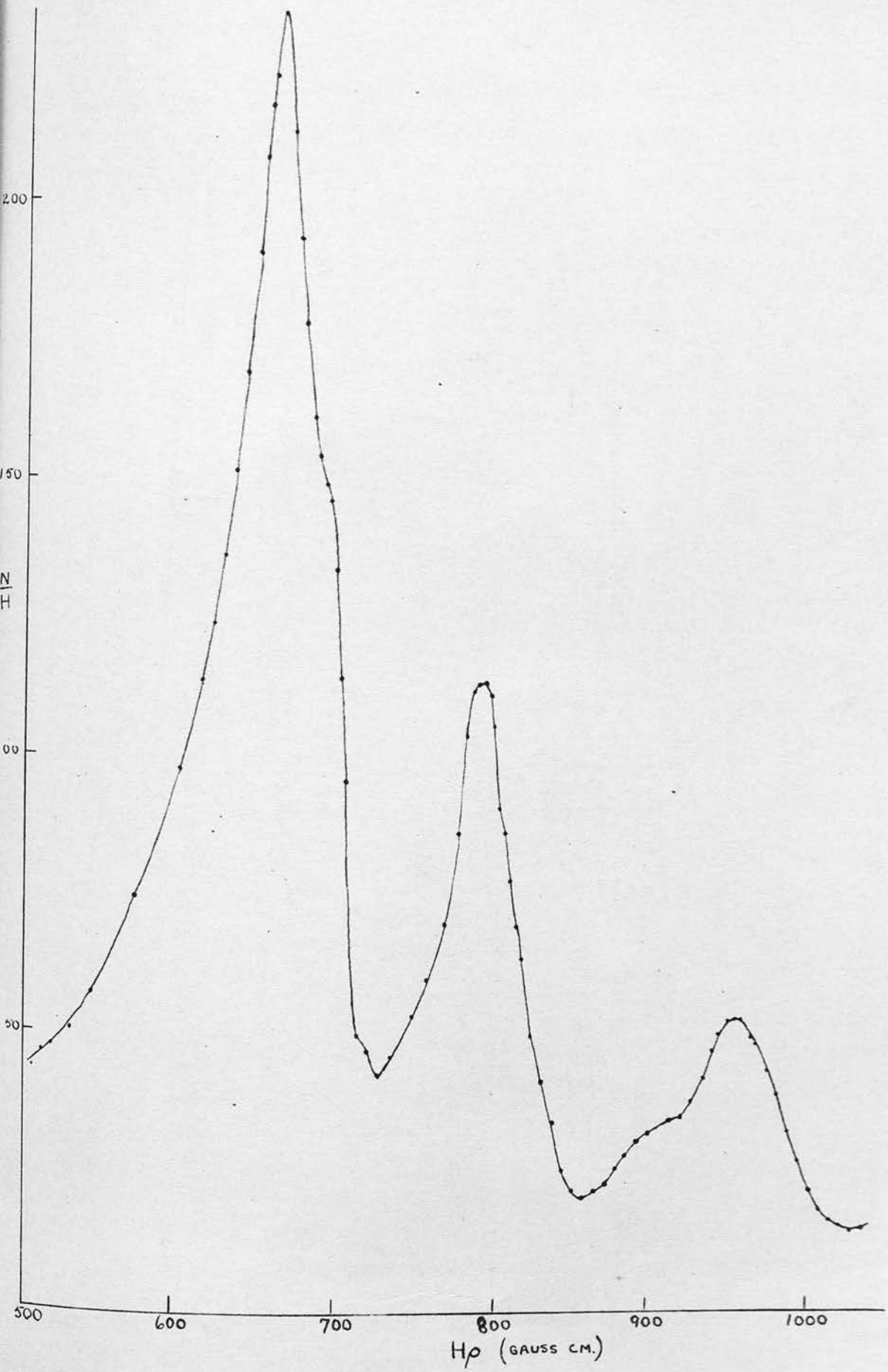

Figure 4.4(a). MsTh2 spectrum between 500 and 1000 gauss cm.

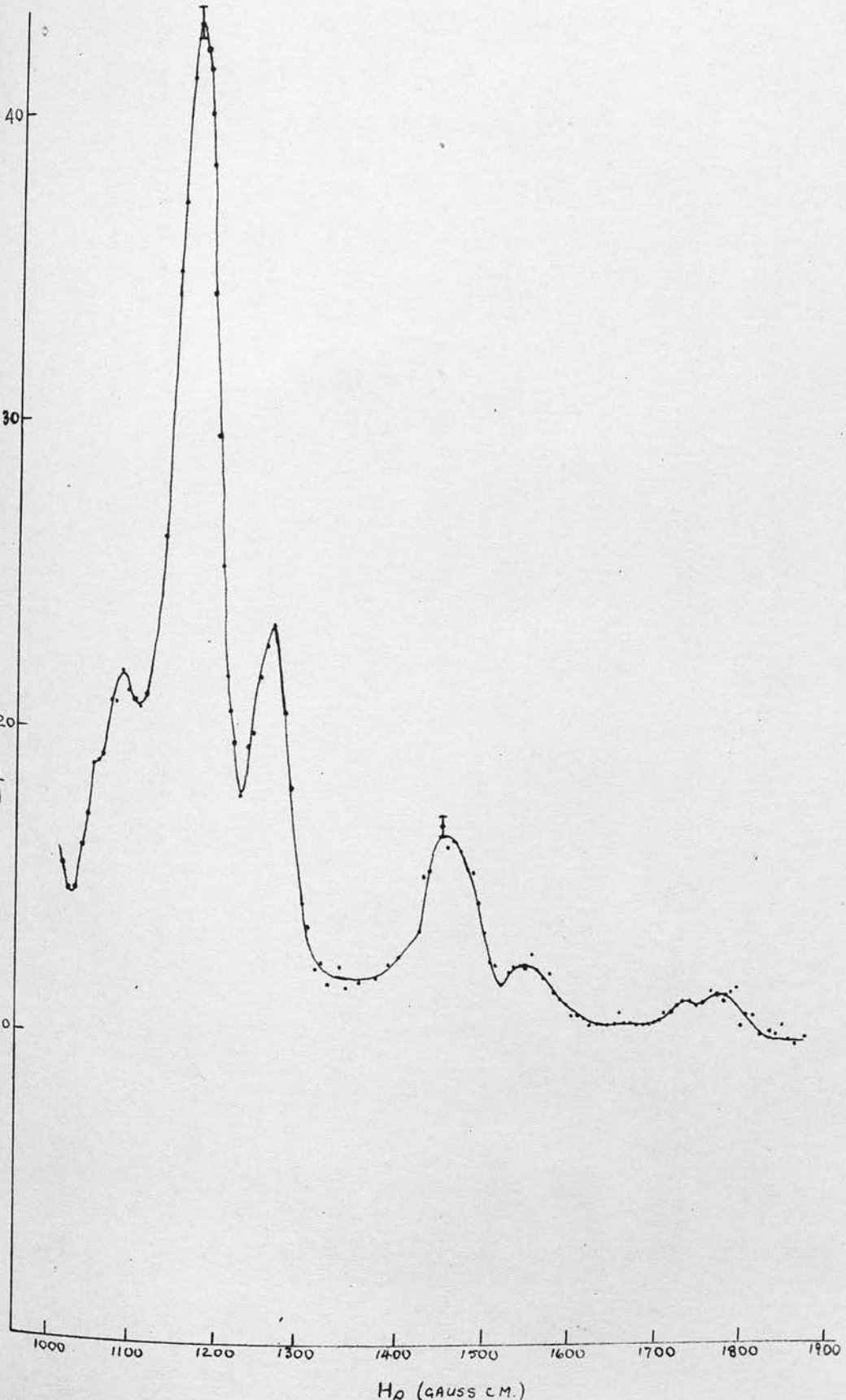

Figure 4.4(b). MsTh2 spectrum between 1000 and 1900 gauss cm.

Table 4.1.

Line No.	Author		Black	
	Hρ	Intensity	Hρ	Intensity
1	665	44	665	9.4
2	~693		696	8.0
3	789	15	790	6.1
4	~815		816	4.2
5	837	~0.1	836	0.56
6	-		864	0.38
7	900	~0.1	900	1.5
8	~950	8.0	946	4.7
9	~975		975	3.3
10	1070	1.3	1069	1.5
11	1099		-	
12	~1165	5.6	1162	3.3
13	~1185		1183	2.3
14	1260	1.8	1248	2.1
15			1267	0.56
16	-		1299	0.3
17	-		1336	
18	1460	1.3	1459	1.9
19	1550		1528	0.56
20	-		1681	
21	1725	~0.2	-	-
22	1770	~0.2	1770	0.7

In some cases the values obtained in the present work are indicated as being approximate. This was due to the fact that these lines were incompletely resolved.

The intensities of the lines were measured in the following way. The work of Kyles, Campbell and Henderson in this department showed that the β-continuum emitted by MsTh2 consists of six partial spectra having end points between 0.469 and 2.18 MeV. From the Fermi plots of these six partial spectra they were able to reconstruct the entire continuous spectrum from zero to the ultimate end point at 2.18 MeV. This reconstructed spectrum was shown to be in good agreement with experiment down to the lower limit of their observations on the continuum, namely about 2,000 gauss cm.

The present work extended up to about 2,500 gauss cm. and from about 1,600 gauss cm. up to this limit the spectrum is substantially free from lines, so the continuous spectrum of Kyles et al. could be fitted to the present observations with confidence. The area under the continuum was then taken to represent one electron per disintegration.

Since the areas under the profiles of the low energy lines were affected by back scattering from the source backing, two alternative methods of assessing their intensities were used. For the first measurement, the source was one from which the cerium carrier

had been almost completely removed by the method described in section 4.3. It was mounted on a thin aluminium leaf 0.2 mg. per cm.^{2} in thickness. The spectrum obtained is shown in Figure 4.5. The curve marked "C.S." in the figure is the continuous spectrum deduced by Kyles, Campbell and Henderson from the Fermi plots of the partial spectra. It has been fitted to the present observations in the range 1,600 - 2,500 gauss cm. In measuring the intensities, the region between the dotted line in Figure 4.5 and the continuous spectrum was assumed to be due to scattered electrons, and the line intensities were measured with a planimeter, using the dotted curve as a base. The results obtained are given in Table 4.2, in which the figures indicate the number of times each group of lines is emitted per 100 disintegrations.

Table 4.2.

Line No.	1 & 2	3 & 4	8 & 9	10 & 11	12 & 13	14 & 15
Intensity (%)	49.5	13.5	7.7	1.0	5.5	1.7

The second intensity measurement was made using a source mounted on gold leaf 0.22 mg. per cm.^{2} in thickness. In this case the area under each line was measured down to the extrapolated continuous spectrum, so that the measured intensity of each line included its own quota of back-scattered electrons. Corrections

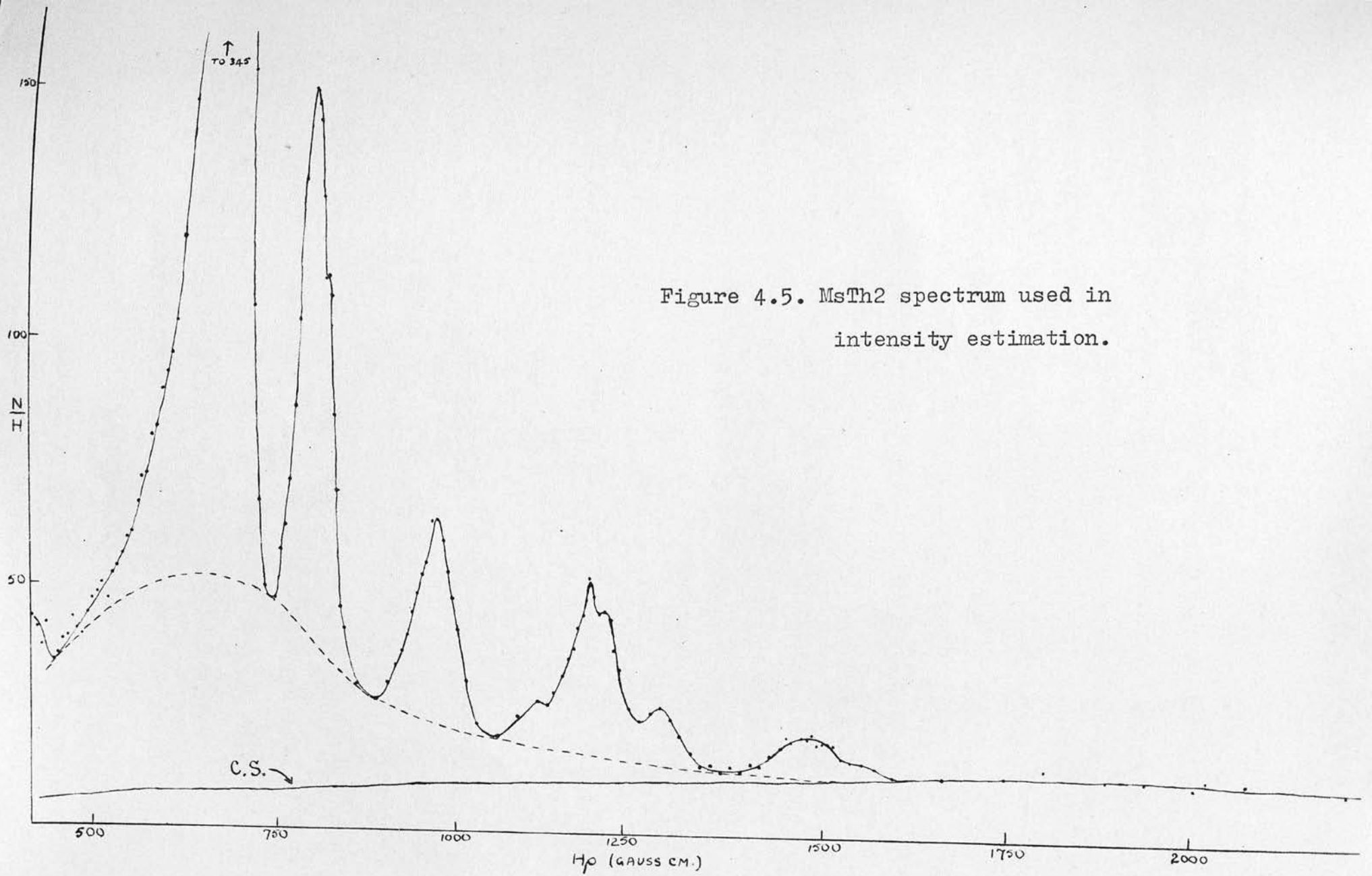

Figure 4.5. MsTh2 spectrum used in intensity estimation.

for back-scattering were made on the basis of the calculations and experiment described in Chapter III for a source mounted on 0.22 mg. per cm.^{2} gold leaf. There it was shown that there is an apparent increase of 55% in the intensity of a low energy line emitted from a source mounted on gold leaf, under the solid angle conditions obtaining in our spectrometer. This assumes that the energy of the line is sufficiently low for the back-scattering to have reached its constant saturation value. Hamilton and Gross (1950) have given two formulae showing the energy at which saturation back-scattering is reached, and the energy at which back-scattering begins. These formulae show that lines numbers 1 to 9 of Table 4.1 should suffer saturation back-scattering, while lines numbers 18 and above should suffer virtually no back-scattering. Accordingly, the measured intensities of the lines have been corrected by the factors shown in Table 4.3.

The two main sources of error in this method are in estimating the fraction of the scattered electrons to be allotted to each line, and in estimating the correction to be applied to the lines which are scattered less than the saturation amount. The first error is greatest in lines 1 to 4, and the second in lines 10 to 13.

Table 4.3.

Line No.	Measured Intensity (Arbitrary Units)	Estimated Scattering Factor	Corrected Intensity	
			(Arbitrary Units)	%
1 & 2	893	55%	576	39
3 & 4	364	55%	235	16
8 & 9	190	55%	122	8.3
10 & 11	33	40%	23.5	1.6
12 & 13	110	30%	85	5.7
14 & 15	34	15%	29.5	2.0
18	~20	0	~20	~1.3

The two sets of intensity measurements show reasonable agreement, and their mean values are those listed in Table 4.1. A comparison with the intensities of Black (also shown in Table 4.1), which were visual estimates of photographic blackening, shows Black's results for the four lines of lowest energy to be much too low. This is very probably due to a falling off in sensitivity of Black's photographic plate for low energy electrons.

4.6. Interpretation of the Internal Conversion Lines.

An analysis of the internal conversion lines of MsTh2 is given in Table 4.4, which shows that 28 lines can be interpreted in terms of 12 γ-rays. Line 7 is very probably a K-Auger line. The energies and inten-

sities quoted in Table 4.4 are those measured in the present work for lines 1 to 21. In the case of unresolved pairs of lines such as 1 and 2, the measured intensities have been divided in the ratio given by Black. For the higher energy lines the energies and intensities have been deduced from Black's results. His relative intensity scale was normalized to the present (absolute) scale at lines 12 and 13. The intensities of the higher energy lines are rather rough, since Black's figures were visual estimates of blackening.

Lines numbers 16, 17 and 20 were quoted by Black but were not observed. They have been omitted from Table 4.4. Two other lines which were observed are not included in Table 4.4 because their interpretation is not certain. The first of these is number 11 (1,099 gauss cm. or 97.0 keV), which may be due to conversion in the L_{III} shell of a γ-ray of 113.3 keV. The L_I and M conversion electrons of such a γ-ray would fall almost exactly on lines 10 and 12. The second is line number 21 (1,725 gauss cm. or 216.1 keV). This may be interpreted as the L_I conversion line of a fourteenth γ-ray of 236.6 keV. The K conversion line of this γ-ray would have an energy of 127.0 keV and would not be resolved from line 15, which is due to conversion of the 127.5 keV γ-ray in the N shell.

Table 4.4.

No. of Line	Hρ gauss cm.	E (keV)	Conv. shell and binding energy		Intensity %	γ-ray Energy (keV)	Mean γ-energy (keV)	Total conv. inty. %	No. of γ-ray
1	665	37.5	L_{II}	19.68	24	57.2			
2	693	40.6	L_{III}	16.30	20	56.9	57.0	59	γ1
3	789	52.16	M_{II}	4.81	15	57.0			
4	815	55.4	N_I	1.32		56.7			
5	837	58.3	L_{II}	19.68	~0.1	78.0	78.1		γ2
6	864	61.9	L_{III}	16.30		78.2			
7	900	66.9	K-Auger line						
9	975	77.7	$L_{I \text{ or } II}$	19.68	3.3	97.4	97.4	4	γ3
10	1069	92.2	M_I	5.18	-	97.4			
12	1165	108.0	L_{II}	19.68	3.3	127.7			
13	1185	111.5	L_{III}	16.30	2.3	127.8			
14	1248	122.4	M_I	5.18	1.8	127.6	127.5	7.4	γ4
15	1267	125.8	N_I	1.32		127.1			
8	950	74.04	K	109.6	4.7	183.6			
18	1460	161.9	L_I	20.5	1.3	182.4	183.7	6	γ5
19	1550	179.8	M_I	5.2		185.0			
22	1770	225.8	K	109.6	.75	335.4	335	0.9	γ6
24	2160	314.1	L	20.5	.19	334.6			
23	2081	295.5	K	109.6	.56	405.1	405	0.6	γ7
25	2303	348	K	109.6	.75	457.6			
26	2663	437	L	20.5	.38	457.5	457.5	1.3	γ8
27	2722	452	M	5.2	.19	457.2			
28	4012	796	K	109.6	.56	905.6	907	0.75	γ9
30	4347	889	L	20.5	.19	909.5			
29	4214	852	K	109.6	.28	961.6			
31	4530	940	L	20.5	.19	960.5	961	0.5	γ10
32	6430	1484	K	109.6	.1	1594	1594	0.1	γ11
33	6564	1523	K	109.6	.1	1633	1633	0.1	γ12

4.7. Further Intensity Considerations.

Lecoin, Perey and Teillac (1949) have studied the electron spectrum of MsTh2 in a Wilson cloud chamber. Although the resolving power of such a method is very low they were able to divide the observed electron tracks into two categories, viz. "soft" and "hard", containing 920 and 946 tracks respectively. The common limit of the two groups was found to be in the neighbourhood of 60 keV. Lecoin et al. also reported evidence for a time delay between the emission of a primary β-particle and a conversion electron of less than 60 keV. By using a source of MsTh1 and MsTh2 in equilibrium, in which the disintegration rate was known, Lecoin, Perey and Teillac deduced that MsTh2 emits roughly two electrons per disintegration, one in each of the "soft" and "hard" groups.

In a later experiment Lecoin, Perey and Riou (1949) used absorption methods to study the γ-rays and x-rays emitted by a source of MsTh2. Two electromagnetic radiations were observed, one having a mean energy of 460 keV and the other an energy of about 15.5 keV. The 460 keV radiation agrees with the mean energy of the known γ-rays, and the soft component was shown by selective absorption to consist of the L x-radiation of thorium. Since the absolute efficiency of their counter was known, Lecoin et al. deduced that the number of

L photons emitted per disintegration of MsTh2 was 0.30 ± 0.06.

It is important to see if these conclusions are in agreement with the present intensity measurements.

If the interpretation of the conversion line spectrum given in table 4.4 is accepted the numbers of K, L and (M + N) electrons emitted per hundred disintegrations of MsTh2 are found to be 7.8, 55.0 and 17.8 respectively, giving a total of 80.6 internal conversion electrons. In order to find the total number of electrons which would be counted in the cloud chamber experiments of Lecoin and his co-workers the number of L-Auger electrons emitted by MsTh2 must be estimated. The energies of these Auger electrons lie between about 6 and 15 keV, and so would be easily measured in the cloud chamber.

The direct measurement of the L-Auger line intensity made in the present work (which will be described in section 4.8) yielded a value of about 22 L-Auger electrons per hundred disintegrations, but this figure is probably too low because of the self absorption of some of these low energy electrons. On the other hand, a result deduced from one of the several estimates and measurements of the <u>average</u> L shell fluorescence yield might well be in error, since the mean fluorescence yield depends strongly on the relative numbers of

ionizations in the three L shells. However, Kinsey (1948a) has made a calculation of the fluorescence yield of each of the L shells based on the best available measurements of the total width of x-ray line and absorption edges for heavy elements and on the values of the expected contribution to the radiation width calculated relativistically by Massey and Burhop (1936). Kinsey's estimates may be used if the relative ionization in the three L shells is known. From table 4.4 we find that the internal conversion intensities are: L_I = 3.75, L_{II} = 28.9 and L_{III} = 22.3 per 100 disintegrations. In deducing these figures, the L conversion of the higher energy γ-rays has been assumed to take place entirely in the L_I shell. This approximation will introduce only a small error since the intensities of these lines are low.

The L_{II} and L_{III} ionizations are increased by the transfer of ionization from the K shell by K x-ray emission* and by the transfer of some of the L_I ionization to L_{III} by the Coster-Krönig effect. Taking Massey and Burhop's (1936) figures for the relative intensities of the K x-rays, and Kinsey's (1948a)

* The K-Auger effect has been ignored because the number of K ionizations is fairly small and because the K shell fluorescence yield is very high ($\sim$95%) for element 90.

estimate of 60% for the fraction of L_I ionization transferred to L_{III} by the Coster-Krönig effect, we finally get the ionization intensities: $L_I = 1.5$, $L_{II} = 30.8$, $L_{III} = 28.7$ per 100 disintegrations. Hence from Kinsey's values for the L_I, L_{II} and L_{III} fluorescence yields, viz. 15%, 56% and 39% respectively, we find that there are 1.3 + 13.5 + 17.5 = 32.3 L-Auger electrons per hundred disintegrations.

We conclude, therefore, that the total number of electrons emitted per disintegration of MsTh2, including the nuclear β-particle but excluding the very low energy M and N-Auger electrons, is 1.0 + 0.806 + 0.323 = 2.1. This is in good agreement with the cloud chamber results of Lecoin and his collaborators.

Also, since there are 32 Auger electrons from a total of 61 L shell ionizations, there must be 29 L x-ray photons per hundred disintegrations. This figure lies in the centre of the rather wide limits (30 ± 6) given by Lecoin, Perey and Riou for the L x-ray intensity from a source of MsTh2.

Finally, it is easy to check the numbers of electrons in the "soft" and "hard" groups as defined by Lecoin, Perey and Teillac. Dividing the continuous spectrum, the internal conversion electrons and the L-Auger electrons at 60 keV shows that there are 1.0 electrons in the low energy group and 1.1 in the high

energy group, in excellent agreement with the cloud chamber work of Lecoin and his co-workers.

The large measure of agreement which has been shown to exist among these three independent intensity measurements on the electronic and electromagnetic radiations from MsTh2 suggests that the absolute intensities listed in table 4.4 are fairly accurate. The measurements also serve as an experimental check on Kinsey's calculations of the L shell fluorescence yields, although the estimated error of Lecoin's x-ray intensity is rather large. It is interesting to notice that the <u>average</u> fluorescence yield quoted by Kinsey is quite inapplicable in the present case, as it was calculated on the assumption of initial ionization of the three L shells in the ratio 0.90: 0.09: 0.01, which is very different from the ratio 0.068: 0.526: 0.406 which exists in the case of MsTh2. Further, the correction which Kinsey suggests should be applied to his results (and which was used to obtain the value 0.47 used in the RaD work described in the previous chapter) is now completely negligible. The correction takes account of a transfer of ionization from the L_I to the L_{II} shell by a process similar to the Coster-Krönig transition, and is important only when the ionization in L_I greatly exceeds the excitation in the other levels.

4.8. The Low Energy Spectrum of Mesothorium 2.

Figure 4.6 shows the spectrum of MsTh2 between 250 and 500 gauss cm. The graph is the mean of four runs, using two thin sources, mounted on backings of 0.2 mg. per cm.^{2} gold leaf. Of the seven lines in Figure 4.6, six will be shown to be L-Auger lines, the seventh being an internal conversion line.

Taking the conversion line first, reference to table 4.4 shows that lines 12, 13, 14 and 15 were interpreted as the L, M and N conversion electrons of a γ-ray of 127.5 keV. As the binding energy of the K shell of radiothorium is 109.6 keV, an electron line due to internal conversion of this γ-ray in the K shell should be observed at about 18 keV. In Figure 4.6 a weak line (no. 7) appears at 460 gauss cm. (or 18.2 keV) which is very probably due to conversion of the 127 keV γ-ray in the K shell. The intensity of the conversion line on the scale of table 4.4 is about 0.13 so the K:L conversion ratio for the 127 keV γ-ray is $\frac{\alpha_K}{\alpha_L} \sim \frac{1}{40}$.

Lines 1 to 6 of Figure 4.6 are interpreted as L-Auger lines. In attempting to suggest the transitions which give rise to these lines we can be guided by the relative intensities of ionization in the three L shells of the residual radiothorium atom. This problem was discussed fully in section 4.7, where it was shown that the ratio of ionization intensity in

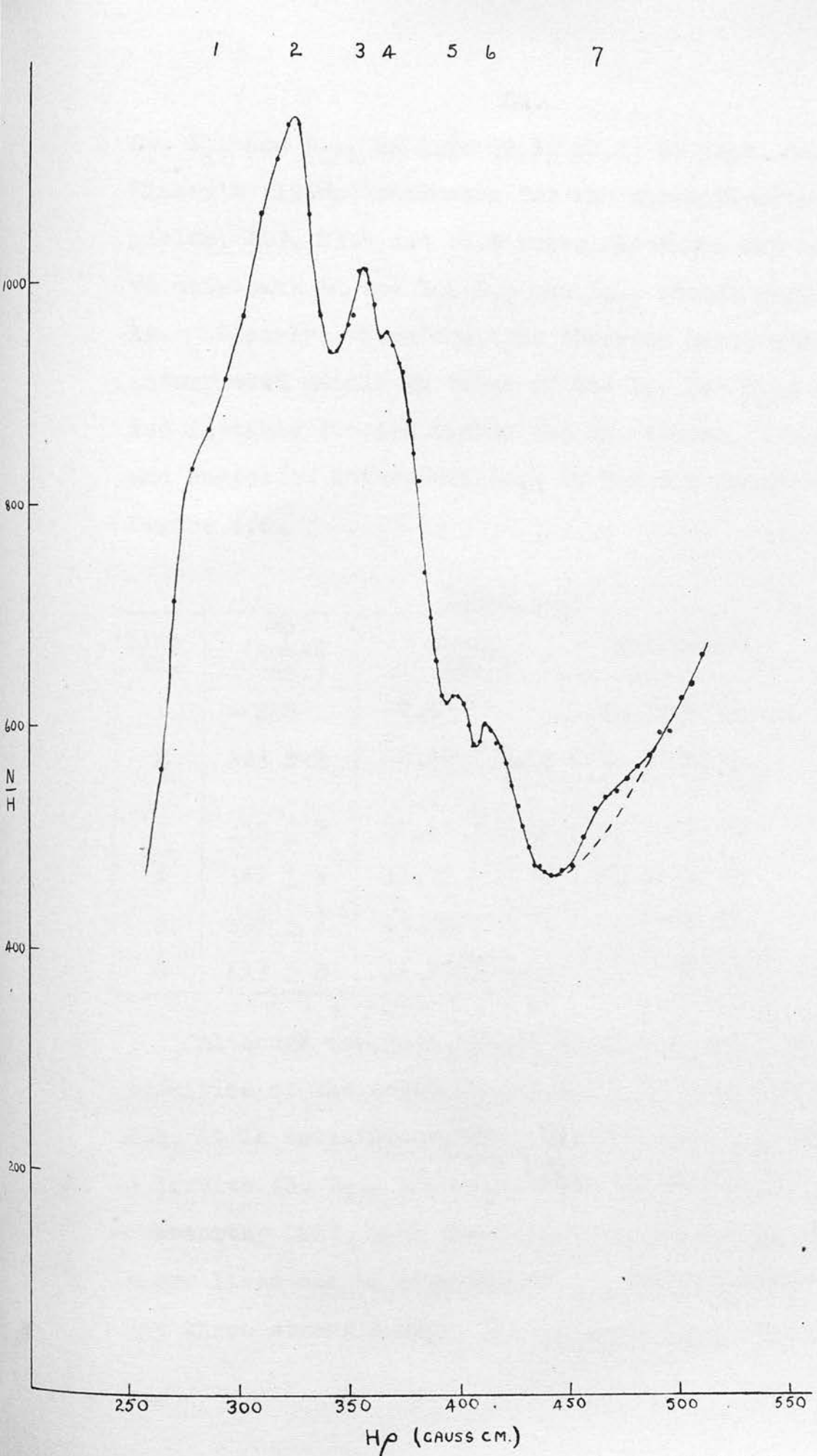

Figure 4.6. The low energy spectrum of MsTh2.

L_I, L_{II} and L_{III} is 1.5: 30.8: 28.7, so that, taking Kinsey's (1948a) estimates for the three fluorescence yields, 1.3, 13.5 and 17.5 Auger electrons are expected to originate in the L_I, L_{II} and L_{III} shells respectively. Clearly, therefore, the observed lines must be interpreted mainly in terms of the L_{II} and L_{III} shells, and in table 4.5 are listed the $H\rho$ values, energies and suggested interpretations of the six Auger lines of Figure 4.6.

Table 4.5.

Line No.	$H\rho$ (gauss cm.)	Energy (keV)	Assignment	Energy (keV)
1	~285	~7.1	$L_{III} \rightarrow M_{III}\, M_I$	7.09
2	323 ± 2	9.09 ± 0.10	$L_{III} \rightarrow M_V\, M_{III}$ $L_{III} \rightarrow M_V\, M_{IV}$	8.95 9.50
3	355 ± 2	10.97 ± 0.12	$L_{II} \rightarrow M_{IV}\, M_I$	11.04
4	367 ± 3	11.71 ± 0.19	$L_{III} \rightarrow M_V\, N_I$	11.67
5	398 ± 2	13.76 ± 0.14	$L_{II} \rightarrow N_{IV}\, M_I$	13.83
6	413 ± 2	14.79 ± 0.14	$L_{II} \rightarrow M_{IV}\, N_I$	14.91

Although accurate estimates of the relative intensities of the Auger lines cannot be made from Figure 4.6, it is satisfactory that the two strong lines 2 and 3 involve the L_{III} and L_{II} shells respectively. It is noteworthy that, with the exception of line 1, all the Auger lines can be regarded as due to "conversion" of the three strong x-rays, $L\alpha_1$ ($L_{III} \rightarrow M_V$), $L\beta_1$ ($L_{II} \rightarrow M_{IV}$)

and $L\gamma_1$ ($L_{II} \longrightarrow N_{IV}$), and even line 1 can be regarded as due to conversion in the M_{III} shell of the x-ray known as the ℓ line ($L_{III} \longrightarrow M_I$). Thus all of the transitions suggested in table 4.5 correspond to x-ray transitions which are allowed by the selection rules. In the case of the K-Auger lines, on the other hand, several workers, notably Ellis (1933), Arnoult (1939) and Flammersfeld (1939), have reported the presence of a fairly strong line corresponding to the transition $K \longrightarrow L_I L_I$. If such Auger electrons were to be considered as arising from an internal conversion process, the radiation converted would have to be that corresponding to the forbidden transition $K \longrightarrow L_I$. Although such "forbidden" Auger transitions have not been observed among the L-Auger lines of RdTh, it cannot be said that they do not exist. In the case of the L-Auger lines of RaE, reference to table 3.3 (Chapter III) shows that one of the lines may be explained either by the transitions $L_{II} \longrightarrow N_{IV}M_I$ and M_{II} or by the transition $L_I \longrightarrow M_I N_I$. The latter alternative would correspond to a transition forbidden by the x-ray selection rules. Because of the large number of possible transitions among the various L, M and N levels, a study of the L-Auger spectra using a very high resolution spectrometer would be required to decide whether such "forbidden" transitions occur in the L-Auger spectra as well

as among the K-Auger lines.

The only previous investigation of the low energy region of the MsTh2 spectrum was reported briefly by Yovanovitch and Proca (1926). The list of 16 lines given by these workers is reproduced in table 4.6.

Table 4.6.

No.	Intensity	Hρ	No.	Intensity	Hρ
1	Fairly strong	181	9	Average	606
2	Fairly strong	195	10	Weak	640
3	Very weak	299	11	Fairly strong	654
4	?	333	12	Very strong	668
5	?	417	13	Fairly strong	676
6	?	501	14	Very strong	700
7	?	529	15	Very weak	723
8	Average	597	16	Very weak	757

The authors identified lines 12 and 14 as the L conversion lines of the 57 keV γ-ray but made no attempt to interpret any of the other lines. However, lines 8, 9, 10 and 15 in the list of Yovanovitch and Proca agree quite closely with the strong lines in the spectrum of RaD, while line 7 (529 gauss cm.) is quite close to the A line in the spectrum of thorium C (533.6 gauss cm.). Moreover, the very low energy line at 195 gauss cm. (3.3 keV) might be identified with a peak in the spectrum of MsTh1 reported by Lecoin, Perey

and Teillac (1949). These facts suggest that the source used by Yovanovitch and Proca consisted of MsTh1 and its isotope radium, along with their decay products. Therefore, although some agreement can be traced between tables 4.5 and 4.6, the results of Yovanovitch and Proca have been disregarded.

In section 4.7 the expected total intensity of the L-Auger lines, on the basis of table 4.4 together with Kinsey's estimated fluorescence yields, was shown to be 32 per hundred disintegrations. An attempt was made to measure the Auger line intensity directly by a comparison with the internal conversion lines of the 57 keV γ-ray. All the lines should be affected to the same extent by back-scattering but, since the sources could not be made thinner than about 0.1 mg. per cm.^{2} for intensity reasons, the Auger lines would be reduced in intensity by source absorption. Figure 4.7 shows the result of a run covering the Auger region and the L and M conversion lines of the 57 keV γ-ray. Since the total intensity of the conversion lines was known from the work described in section 4.5, the total intensity of the Auger lines was found to be roughly 22 per hundred disintegrations. This result was obtained by direct measurement with a planimeter of the areas under the Auger lines and the internal conversion lines. The difference between this result and the estimated

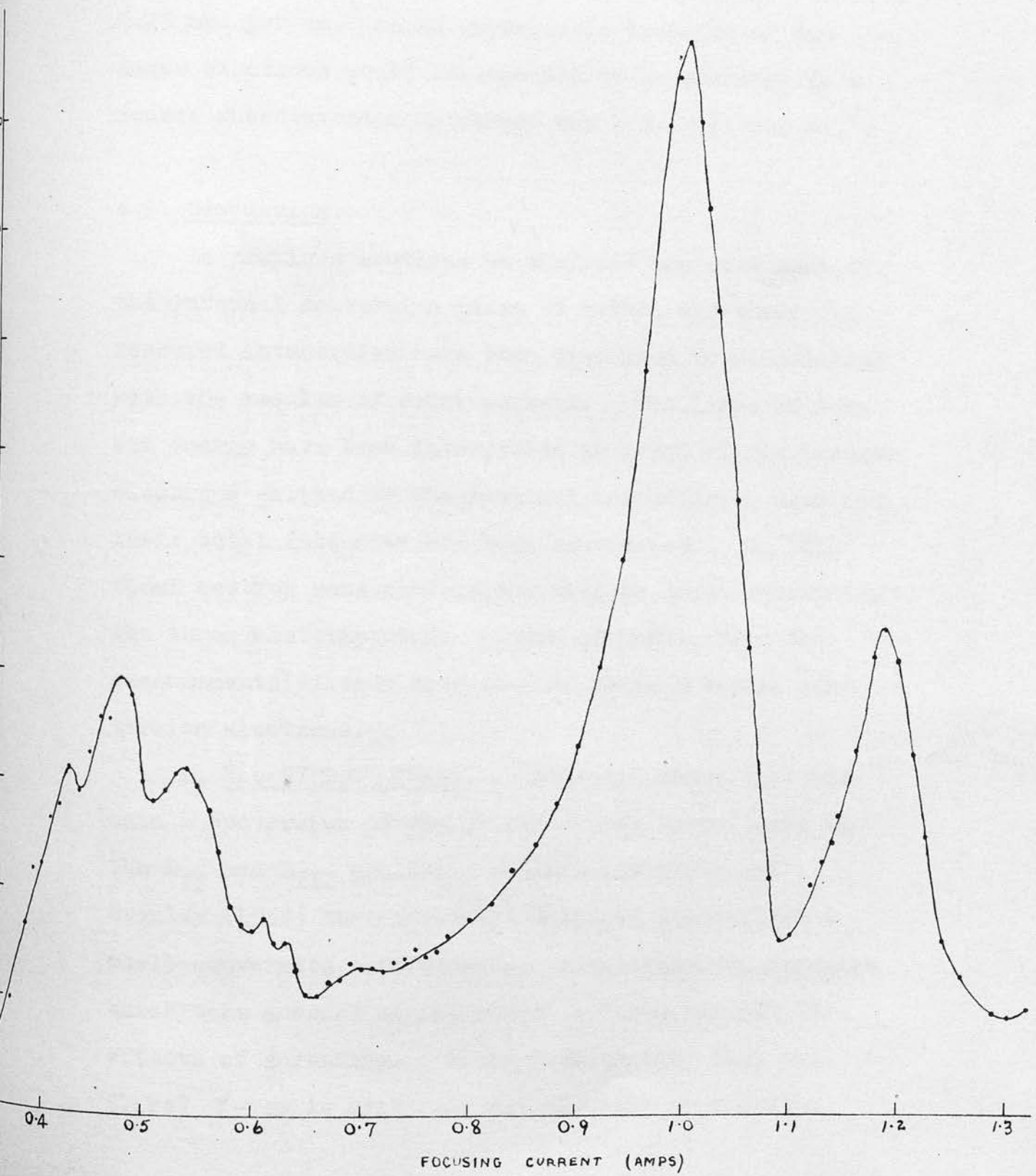

Figure 4.7. MsTh2 spectrum used in estimating intensity of the L-Auger electrons.

intensity of 32% for the Auger electrons is not too great to be attributed to self absorption in the source. The total range of 10 keV electrons is only about 0.25 mg. per cm.^{2} so an appreciable fraction of the Auger electrons would be expected to be absorbed in a source whose average thickness was $\sim$0.1 mg. per cm.^{2}.

4.9. Discussion.

In previous sections an analysis has been made of the internal conversion lines of MsTh2, and their measured intensities have been discussed in conjunction with the results of other workers. The lines of lowest energy have been interpreted in terms of the L-Auger electrons emitted by the residual radiothorium atom and their total intensity has been considered. In this final section some conclusions will be drawn concerning the three most important γ-rays of MsTh2, from the measurements already described on their internal conversion electrons.

1. The 57 keV γ-ray. Table 4.4 shows that the main L conversion of the 57 keV γ-ray takes place in the L_{II} and L_{III} shells. Gellman, Griffith and Stanley (1952) have recently published theoretical L shell conversion coefficients, calculated from formulae which take account of relativistic terms but not the effects of screening. Their results show that the 57 keV γ-ray is certainly not electric or magnetic

dipole, and suggest that it may be electric quadrupole. The conversion electrons of this γ-ray are emitted in about 60% of the disintegrations (table 4.4) and, in agreement with Lecoin, Perey and Teillac (1949), Kyles, Campbell and Henderson (private communication) have shown that its lifetime is greater than 10 m.sec. From these facts, it is very unlikely that there is another competing γ emission of higher energy, so that the 57 keV γ-ray must come from the first excited state of the radiothorium nucleus. To account for the half-life of the state, the radiation must be electric or magnetic quadrupole or of still higher order (Goldhaber and Sunyar, 1951). If it is assumed to be electric quadrupole, the first excited state of radiothorium will have spin 2 and even parity, in common with the majority of even-even nuclei so far studied (Goldhaber and Sunyar, 1951).

2. The 127 keV γ-ray. The available information about this γ-ray is that the L shell conversion is mainly in the L_{II} and L_{III} shells, and that the very low energy K conversion line is roughly 1/40 of the intensity of the L lines. For comparison with theory we may use the "threshold" K conversion coefficients of Spinrod and Keller (1951), and the L shell calculations of Gellman and his co-workers (1952). The results of these authors show that for electric quadrupole

γ-radiation of about this energy the L conversion coefficient is very much greater than the K coefficient. Since the L shell conversion coefficient changes very rapidly with energy in this energy region, and since Gellman, Griffith and Stanley give results for only three energies a more precise comparison of the experimental K:L ratio with theory is not possible. However, a comparison of the relative intensities of the L shell conversion lines as given in table 4.4 with the theoretical conversion coefficients of Gellman, Griffith and Stanley suggests that electric quadrupole is the correct assignment in this case.

3. The 184 keV γ-ray. The K:L ratio for this γ-ray is about 4.7 and the L shell conversion seems to be mainly in L_I. The L shell data of Gellman et al. show that the radiation is not electric quadrupole, but that it may be either electric or magnetic dipole. The empirical data of Goldhaber and Sunyar suggest that the K:L ratio is rather low for magnetic dipole radiation and rather high for electric dipole radiation. In the absence of any L shell data, magnetic quadrupole radiation cannot be ruled out.

If the 184 keV γ-ray is regarded as a cross-over for the cascade of the 127 keV and 57 keV radiations, the spins and parities attributed to the levels must be consistent with the above conclusions about the

individual γ-rays. Assuming that the 57 keV γ-ray comes from the first excited state of the even-even radiothorium nucleus, the choice of spins and parities for the 57 and 184 keV levels seems to be between (a) and (c) of Figure 4.8. Although (b) gives suitable polarities for the 57 and 184 keV radiations it would require the 127 keV γ-ray to be electric dipole, which is ruled out by the observed K:L ratio. Both (a) and (c) are open to slight objection, the first since it suggests that the 127 keV γ-ray should be a mixture of magnetic dipole and electric quadrupole radiations with the former predominating, whereas the experimental results suggest that this γ-ray is mainly electric quadrupole, and the second since the lifetime of a 3 + state of 57 keV energy would be several hours, which would be detectable by ordinary decay measurements.

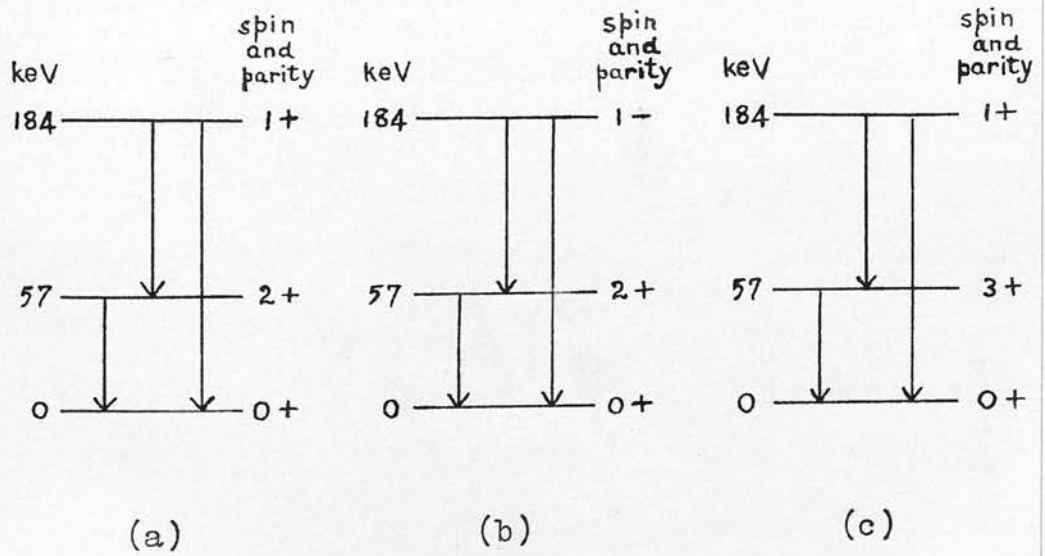

Figure 4.8.

The work of Kyles, Campbell and Henderson in this department favours (a) since it gives the better agreement with their conclusions on the partial β-spectra of MsTh2. The level scheme which they have suggested on the basis of coincidence experiments, together with the conclusions of the above paragraphs, is shown in Figure 4.9. All of the γ-rays of table 4.4 are included, together with the somewhat doubtful 113 keV and 236 keV radiations whose presence was suggested to explain two lines not included in table 4.4. The level scheme is not necessarily unique and, in particular, the spins and parities suggested might have to be modified in the light of future theoretical information.

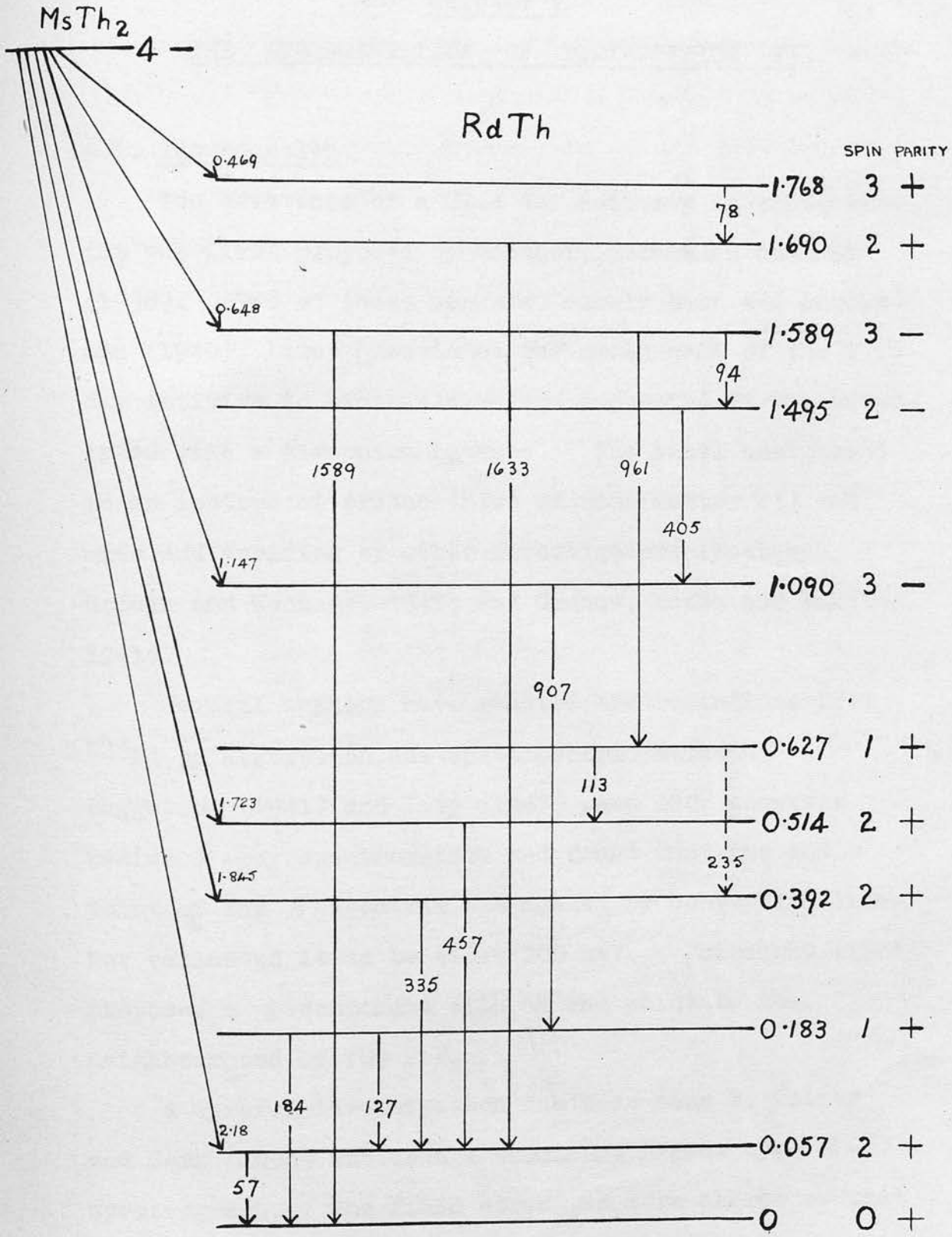

Figure 4.9. Suggested level scheme for the RdTh nucleus following β-decay of MsTh2.

Chapter V.

THE DISINTEGRATION OF PROTACTINIUM 233.

5.1. Introduction.

The existence of a 27.4 day activity in protactinium was first proposed by Meitner, Strassman and Hahn (1938). Two of these workers, namely Hahn and Strassman (1940), later questioned the assignment of the 27.4 day activity to protactinium and suggested it was associated with a zirconium isotope. The final assignment to an isotope of protactinium of mass number 233 was made and verified by other investigators (Seaborg, Gofman and Kennedy, 1941; and Grosse, Booth and Dunning, 1941).

Several workers have studied the radiations from ^{233}Pa by absorption and spectroscopic methods. Haggstrom (1941) and Levy (1947) used 180° constant radius β-ray spectrometers and found that the end point of the β-spectrum was masked by conversion lines but estimated it to be about 200 keV. Fulbright (1944) proposed a β-component with an end point in the neighbourhood of 700 keV.

A careful investigation has been made by Keller and Cork (1950) who used a permanent magnet type β-spectrograph. The field strengths were chosen so that the range from 19 keV to 1.5 MeV could be covered.

Keller and Cork observed 46 internal conversion lines and three weak K-Auger lines, all having energies below 411 keV. They also carried out an absorption experiment using lead absorbers which revealed no γ-ray harder than about 400 keV. They concluded that the β-ray end point was in the 200 keV region from absorption experiments using beryllium and aluminium and found no trace of a harder β-ray component as reported by Fulbright. The spectrometer used by Keller and Cork was a high resolution instrument and, in the lower energy region, was capable of resolving the L shell fine structure. They found lines due to internal conversion in the L_I and L_{II} shells, but detected no conversion in the L_{III} shell. A list of the γ-rays found by these workers, showing the internal conversions observed, is shown in table 5.1, and the nuclear level scheme which they suggested is shown in Figure 5.1. A 17.4 keV γ-ray (not observed) is postulated to make the scheme self-consistent.

After much of the experimental work to be described in the following sections had been carried out, a report on ^{233}Pa by Elliott and Underhill (1952) became available. These workers used a magnetic lens spectrometer and studied the spectrum above about 37 keV. They found that the main part of the β-continuum ends at about 260 keV and that about 8% extends to 570 keV. They

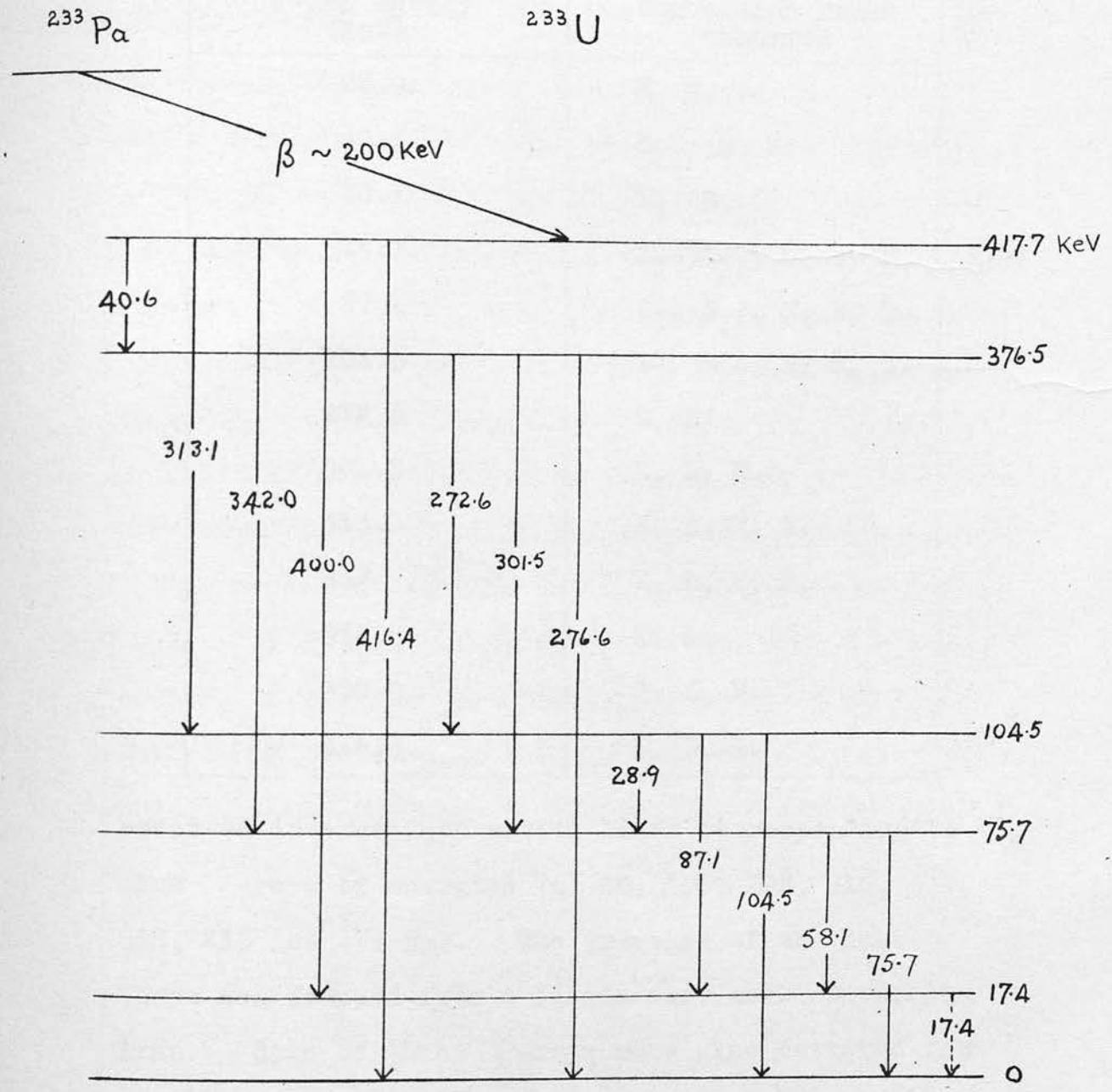

Figure 5.1. Nuclear level scheme for ^{233}U suggested by Keller and Cork (1950).

Table 5.1.

γ-ray energy (keV)	Conversion lines observed
28.9	M, N, O.
40.6	L_{II}, M, N.
58.1	L_I, L_{II}.
75.7	L_I, L_{II}, M, N, O.
87.1	L_I, L_{II}, M, N, O.
104.5	L_I, L_{II}, M, N, O.
272.6	K, L.
301.5	K, L, M.
313.1	K, L, M, N.
342	K, L, M, N.
376.5	K, L.
399.9	K, L, M.
416.4	K, L, M.

observed internal conversion lines corresponding to nine γ-rays of energies 76, 88, 105, 298, 310, 339, 398, 415 and 474 keV. The presence of the last of these was deduced from a single very weak conversion line. Some of these γ-rays were also detected from the photoelectrons which they ejected from silver and gold radiators. Elliott and Underhill also carried out a coincidence experiment using two lens spectrometers arranged end to end. One was focused on the intense K internal conversion line of the 310 keV

γ-ray, while the other was set on selected points in the spectrum. The 76, 88 and 105 keV transitions, as well as a large fraction (estimated at 75%) of the continuum, were found to be correlated with the 310 keV transition. This fact, together with the intensities of the γ-rays, both emitted and internally converted, led them to suggest the disintegration scheme shown in Figure 5.2. It will be noticed that the main part of the β-spectrum (i.e. below 260 keV) has been divided into six β-transitions.

The objects of the present work were to re-examine the spectrum of ^{233}Pa, particularly in the very low energy region, extending the observations below the limit of Keller and Cork's apparatus. Since there are many K and L conversion lines in the ^{233}Pa spectrum, an L-Auger spectrum will be present in the region between 7 and 17 keV. Also, if the interpretation of Keller and Cork is correct, some very low energy internal conversion lines are to be expected. In particular, L conversion electrons of the 28.9 keV γ-ray should appear at about 7 keV, and of the 40.6 keV γ-ray at about 19 keV. If the 17.4 keV γ-ray exists, M, N and O conversion electrons are to be expected.

5.2. Experiments with Source No. 1.

5.2.1. Source Preparation.

The ^{233}Pa was produced at A.E.R.E., Harwell, by

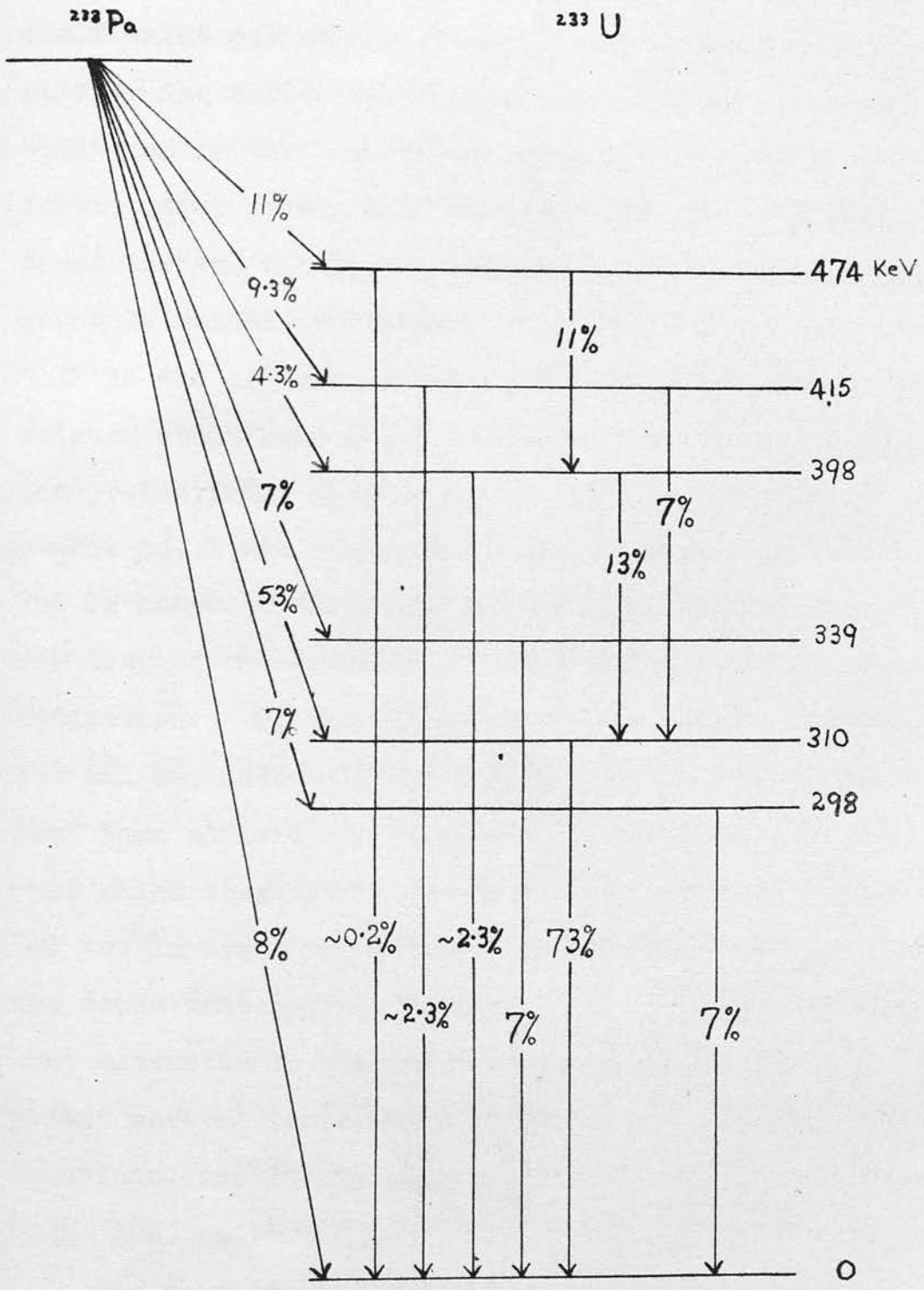

Figure 5.2. Disintegration scheme for $^{233}Pa \longrightarrow {}^{233}U$ suggested by Elliott and Underhill (1952).

slow neutron bombardment of ^{232}Th followed by β^--decay (half-value period = 23.5 min.), and purified chemically by the Radiochemical Centre, Amersham. It was delivered in the form of an organic compound, the protactinium having been combined with the complexing agent thenoyl tri-fluoro acetone. The resulting compound is soluble in benzene.

As the organic material containing the ^{233}Pa weighed about half a gram, it was essential to separate the protactinium chemically before making a source. Source no. 1 was prepared by the following method. The Pa compound was dissolved in 2 ml. benzene and one drop of the solution diluted to 2 ml. for a test separation. To the diluted solution about 0.5 ml. of 1 N HCl was added and thoroughly mixed. The liquids were then allowed to separate into two layers, a process which took only a few minutes. After separating the two layers they were tested for activity, when it was found that only a small fraction of the ^{233}Pa had been extracted by the HCl. The experiment was repeated several times using progressively stronger HCl solutions, and it was finally found that "conc. HCl" (i.e. 12N) extracted about 25% of the activity.

The main benzene solution was therefore treated in the same way using 12 N HCl, and the acid fraction evaporated down to about 0.5 ml. One drop of the

solution was evaporated under an infra-red lamp on to a piece of 0.2 mg./cm.^{2} gold leaf backed for extra strength by a 20 μgm./cm.^{2} nylon film, and mounted on an aluminium source holder of the type described in the previous chapter. The centre of the gold foil had been wetted with insulin solution.

A gold foil was used to prevent source charging, which can be serious at low energies if the source is mounted on a good insulator. Gold was used in preference to aluminium since the latter is readily soluble in HCl.

When dry, the source was a disc about 0.4 cm. in diameter and was a brownish deposit on the gold. This was thought to be due to the presence of some organic material from the complexing agent, as the protactinium was reported to be virtually free from inorganic contamination, but later work on source no. 2 showed that the residue was inorganic. The source was not so thick, however, as to blur the detail of the low energy spectrum, as will be shown in section 5.2.3.

5.2.2. The β-ray and electron spectrum above 16 keV.

Figure 5.3 shows the spectrum obtained using source no. 1, in the region above 16 keV. The statistical error was not constant throughout the spectrum, and is indicated on the graph. An accelerating potential of 7.0 KV was used in investigating the

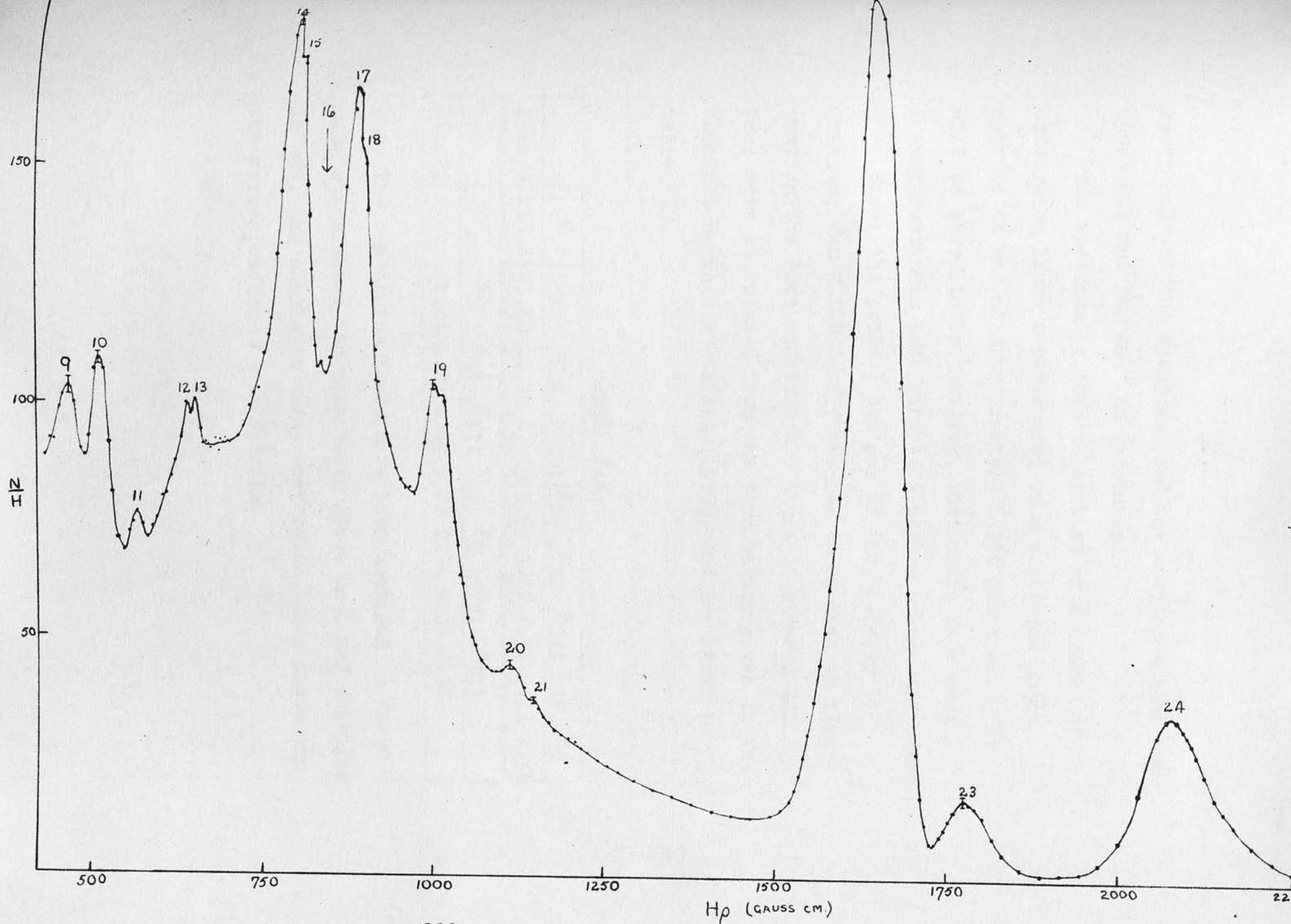

Figure 5.3. ^{233}Pa spectrum above 16 keV - source no. 1.

lower half of the spectrum, and the counter window was about 0.1 mg. per cm.^{2} in thickness.

The spectrum is seen to consist of a number of conversion lines superimposed on a continuum which appears to end at approximately 1,900 gauss cm. It will be shown later, however, that there is a weak β-ray continuum extending to a higher energy end point.

Since the product nucleus of the β-decay is uranium, the K-L-M--- differences to be used in interpreting the line spectrum are those of element 92. They were calculated from the term values given in the "Landolt-Bornstein" tables (1950), and are shown in table 5.2.

Table 5.2.

	K	L_I	L_{II}	L_{III}	M_I	M_{II}	M_{III}	M_{IV}	M_V
E(keV)	115.8	21.80	20.99	17.20	5.56	5.19	4.31	3.73	3.56

	N_I	N_{II}	N_{III}	N_{IV}	N_V	N_{VI}	N_{VII}
E(keV)	1.44	1.27	1.04	0.78	0.74	0.39	0.38

The conversion lines have been analysed in table 5.3, which shows the momenta in gauss cm., and energies in keV, the shells in which conversion takes place and the corresponding γ-ray energies.

Table 5.3.

No. of line	$H\rho$ (gauss cm.)	E (keV)	Level of Conversion	Energy of γ-ray (keV)
9	422	19.3	L_I and L_{II}	40.7
10	518	23.1	M	28.7
11	571	27.9	N	29.3
12	641.5	35.0	M	40.6
13	656	36.5	L_I	58.3
14	804	54.0	L_I	75.8
15	811	54.9	L_{II}	75.9
16	839	58.6	L_{III}	75.8
17	888	65.3	L_I	87.1
18	895	66.2	L_{II}	87.2
19	1010	83	L_I and L_{II}	104.4
20	1112	99.2	M	104.8
21	1142	104	N	105.4
22	1640	198	K	313.8
23	1777	227	K	342.8
24	2073	293	L	314
25	~2185	~320	L	342

The information is conveniently summarized in table 5.4, which shows more clearly the 8 γ-rays detected and the shells in which conversion was observed. The γ-rays reported by Keller and Cork are also shown for comparison. The agreement is good, on the whole, although the weak 272 keV γ-ray of

Keller and Cork was not found, and the conversion lines of the 301 and 313 keV γ-rays were not resolved. A further discussion will be given later.

Table 5.4.

γ-ray	Energy (keV)	Conversions observed	γ-ray energy of Keller & Cork (keV)
(1)			(17.4)
2	29	M, N	28.9
3	40.7	$L_I + L_{II}$, M	40.6
4	58.3	L_I	58.1
5	75.8	L_I, L_{II}, L_{III}	75.7
6	87.2	L_I, L_{II}	87.1
7	104.5	$L_I + L_{II}$, M, N	104.5
8			272.6
9			301.5
10	313	K, L	313.1
11	342	K, L	342
12			376
13			400
14			416

5.2.3. The Very Low Energy Region of the Spectrum.

A careful examination of the very low energy region of the spectrum was then undertaken. The accelerating potential was maintained at 7.0 KV and four runs were taken between $H\rho$ = 240 and $H\rho$ = 550 gauss cm.

The first and third runs were started at the upper momentum limit and the second and fourth at the lower momentum limit. A plot of the raw counts was made for each run, and these four plots were found to be closely similar, peaks appearing at very nearly identical positions in the four cases. In view of this consistency it is very unlikely that any of the peaks is due to a chance statistical fluctuation. The averaged, corrected low energy spectrum is shown in Figure 5.4.

The interpretation of the low energy lines is rendered uncertain by the fact that both Auger and internal conversion lines are present. Moreover, since the relative intensities of the ionization in the three L shells are not known, it is difficult to make an estimate of the relative intensities of the Auger lines originating in L_I, L_{II} and L_{III}. However, an examination of Figure 5.3. and table 5.3. indicates that internal conversion in the L_{III} shell is low, while that in L_{II}, although smaller than in L_I, is certainly not negligible. Anticipating the results of table 5.7. (section 5.3.3.) it can be shown that the relative intensities of the internal conversion in the K, L and (M + N) shells are approximately 113: 85: 14.5. In whatever ratio the 85 units in the L shells are divided among L_I, L_{II} and L_{III} (always remembering that $L_I \geqslant L_{II} \gg L_{III}$) it turns out that ultimately the

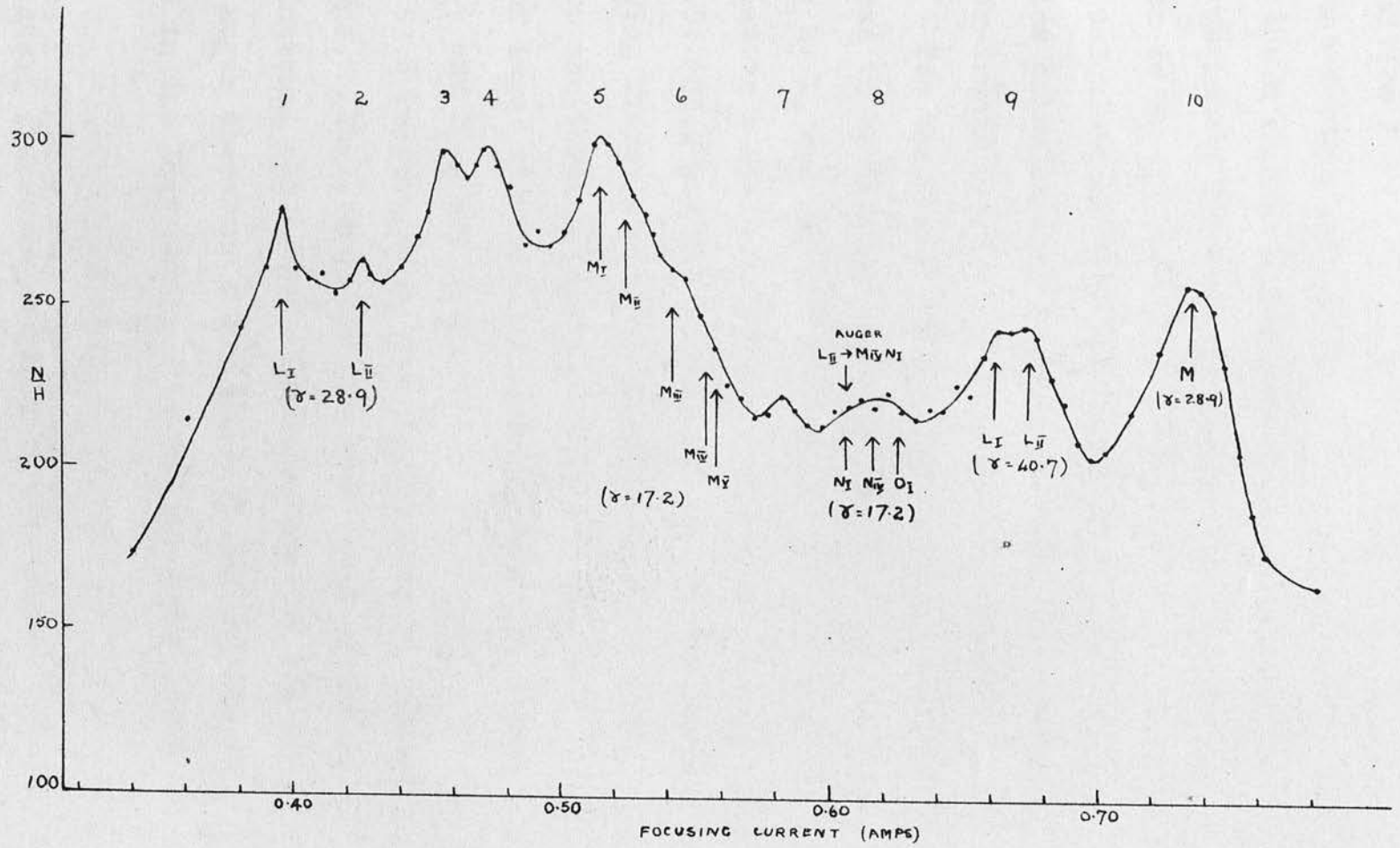

Figure 5.4. The low energy electron spectrum of ^{233}Pa.

ionization in L_{III} considerably exceeds that in L_I and L_{II}. The reasons for this are, firstly, that the x-ray transition $K \longrightarrow L_I$ is forbidden so that virtually all* of the K shell ionization is transferred to L_{II}, L_{III} and the M shells, and secondly that the Coster-Krönig transitions transfer a large fraction of the L_I ionization to L_{III}.

Two calculations have been made using the K x-ray intensities calculated by Massey and Burhop (1936) and the Coster-Krönig coefficient calculated by Kinsey (1948a). For the first, the initial L shell ionization was assumed to be divided among L_I, L_{II} and L_{III} in the ratio 76: 8: 1, and for the second, 45: 35: 5. The final relative L shell ionization intensities are 30.4: 35.8: 105.8 and 18: 62.8: 91.2 for the two cases. Hence, using Kinsey's (1948a) calculated fluorescence yields for the three separate shells, the relative numbers of Auger electrons originating from ionization in L_I, L_{II} and L_{III} are 25.6: 14.7: 62.4 and 15: 25.8: 53.8 respectively, for the two sets of initial assumptions. Thus, whatever the true ratio of the L_I and L_{II} internal conversion electrons, most of the observed L Auger electrons must be due to the filling of vacancies in the L_{III} shell. L_I and L_{II} Auger lines

* The K Auger effect can be ignored since the K shell fluorescence yield is very high.

should also be observed, but with smaller intensity.

With this conclusion in mind, the ten lines of Figure 5.4 have been interpreted as in table 5.5.

Table 5.5.

No. of line	Hρ (gauss cm.)	E (keV)	Interpretation
1	282	7.0	L_I (γ = 28.8 keV)
2	302	7.9	L_{II} (γ = 28.9 keV)
3	324	9.2	Auger $L_{III} \rightarrow M_V M_{III}$ (9.3 keV)
4	335	9.8	Auger $L_{III} \rightarrow M_V M_{IV}$ (9.9 keV)
5	365	11.6	M_I (γ = 17.2 keV)
			+ Auger $L_{II} \rightarrow M_{IV} M_I$ (11.7 keV)
6	~387	~12.9	M_{III} (γ = 17.2 keV)
7	413	14.8	Auger $L_I \rightarrow M_I N_I$ (14.8 keV)
			or Auger $L_{II} \rightarrow N_{IV} M_I$ (14.65 keV)
			$L_{II} \rightarrow N_{IV} M_{II}$ (15.4 keV)
8	~438	16 - 17	N and O (γ = 17.2 keV)
			+ Auger $L_{II} \rightarrow M_{IV} N_I$ (15.8 keV)
9	469	19.0	L_I (γ = 40.8 keV)
	478	19.7	L_{II} (γ = 40.7 keV)
10	522	23.4	M_I (γ = 28.9 keV)

Lines 1 and 2 are due to conversion in the L_I and L_{II} shells of a 28.9 keV γ-ray, already known from its M and N conversion electrons (see section 5.2.2.). Lines 3 and 4 are interpreted as Auger lines corres-

ponding to the transitions $L_{III} \longrightarrow M_V M_{III}$ and $L_{III} \longrightarrow M_V M_{IV}$. The same transitions appeared in the L-Auger spectra of RaE and RdTh, although in neither case were the two lines resolved. Lines 9 and 10 are also easily interpreted. The former is due to conversion of the 40.6 keV γ-ray in the L_I and L_{II} shells, the two lines being incompletely resolved, and the latter to the M shell conversion of the 28.9 keV γ-ray. These results are in agreement with the work of Keller and Cork.

Regarding the remaining four lines, if numbers 5 and 6 are due to Auger electrons, the most likely transitions appear to be $L_{II} \longrightarrow M_{IV} M_I$ and $L_{II} \longrightarrow M_{IV} M_{III}$, and, in view of the conclusions reached above about the relative intensities of the L_{II} and L_{III} Auger electrons, the observed intensity of lines 5 and 6 seems rather high. Further, the shape of the high energy side of the group of lines 5 and 6 suggests that the main contribution to the observed distribution is from the conversion of a single γ-ray in the five M shells. The arrows in Figure 5.4 show the calculated positions of M conversion electrons of a 17.2 keV γ-ray and it is clear that this interpretation fits the observations. It is assumed that the Auger lines - for example, those due to the transitions $L_{II} \longrightarrow M_{IV} M_I$ and $L_{III} \longrightarrow M_V N_I$ which are expected on the basis of the

results for MsTh2 $\longrightarrow$ RdTh - are submerged in the internal conversion lines.

If lines 5 and 6 are indeed due to internal conversion of a 17.2 keV γ-ray, it is to be expected that the γ-ray will also be converted in the N and O shells. The broad line number 8 in Figure 5.4 is very probably due to these conversions, together with an Auger line due to the transition $L_{II} \longrightarrow M_{IV}N_{I}$. The calculated positions of these lines are shown in the graph.

Finally, in Figure 5.4, line 7 may be due to the Auger transition $L_{I} \longrightarrow M_{I}N_{I}$, or to a combination of two lines resulting from the transitions $L_{II} \longrightarrow N_{IV}M_{I}$ and $L_{II} \longrightarrow N_{IV}M_{II}$.

The conclusions to be drawn from this study of the low energy region of the ^{233}Pa spectrum are therefore as follows:

1. The 28.9 keV γ-ray reported by Keller and Cork has been confirmed by the detection of its conversion electrons in the L_{I} and L_{II} shells at 7.0 and 7.9 keV respectively. As far as can be deduced from Figure 5.4, in which the lines are standing upon a background due to the β-spectrum and to back-scattered electrons, the M lines are rather more intense than the L lines.

2. L_{I} and L_{II} conversion lines of the 40.6 keV γ-ray have been found. Previously L_{II} was the only

L shell conversion reported, since the apparatus of Keller and Cork cut off at just over 19 keV.

3. While the existence of the "hypothetical" 17 keV γ-ray of Keller and Cork cannot be said to have been proved beyond all doubt, some evidence for its existence has been obtained.

4. In the case of the lines which have been interpreted as due to Auger electrons, the transitions agree with those suggested to explain similar lines in the spectra of RaE and RdTh.

5.2.4. The continuous β-spectrum.

Because of the large number of internal conversion lines it is difficult to deduce the shape of the continuous spectrum with any certainty. Further, as the source was supported on a gold foil, back-scattering would appreciably distort the shape of the continuum. A discussion of the continuous spectrum will be given in section 5.3.3.

5.3. Experiments with Source No. 2.

5.3.1. Introduction.

As has been mentioned, it was not possible to get satisfactory information about the shape of the continuous β-spectrum from source no. 1 because of back-scattering from the gold leaf on which it was mounted. Scattering might also distort the relative intensities

of the internal conversion lines. Moreover, the resolving power obtainable with source no. 1 was not sufficiently good in the high energy region - in particular, the K conversion lines of the 301 and 313 keV γ-rays were not resolved. To try to remove these defects a new source was prepared with the following objectives in mind (i) backing to be as thin and light as possible to reduce scattering (ii) source to be as thin as possible, despite loss of intensity, to reduce scattering and absorption in the source (iii) area of source to be smaller than before to improve resolution.

5.3.2. Source Preparation.

To ensure that no organic matter was left in the source, it was prepared by the following method. The protactinium compound was dissolved in benzene, evaporated to dryness in a platinum crucible and ignited. The residue was dissolved in 12N HCl, evaporated down to a small volume and one drop of the solution placed on a collodion film, previously wetted with insulin solution in the usual way. The collodion film was about 20 μgm. per cm.^{2} in thickness and was mounted on the standard source holder. The drop of solution was evaporated under an infra-red lamp, using gentle heat, the remainder of the film being protected by a piece of aluminium foil. When dry, the source was a thin deposit, spread evenly over the 0.3 cm. diameter disc previously wetted by the insulin. In colour, the

source was similar to no. 1, and since in the present case all organic matter had been removed in the ignition process, the residue on both sources must have been an inorganic impurity. The source was about one tenth as strong as no. 1 and was too weak to be used in the very low energy region. No attempt was made to "earth" this source to the spectrometer. As it was relatively weak, the rate of removal of charge would be correspondingly small, and the conductivity of the collodion was relied on to prevent the source from charging up to such an extent that the energies of the lines would be affected. In fact, no evidence of source charging was found - the energies of the observed lines agreed closely with the values found with source no. 1 over the energy range covered (i.e. above 23 keV).

5.3.3. Results.

The spectrum obtained with source no. 2 is shown in Figure 5.5. The resolving power at the higher energies is improved since it was possible to use a smaller exit aperture (3 mm. in diameter) with the smaller source. The 186 keV line (K conversion of the 301 keV γ-ray) now shows up. At the lower energies the statistical error was too large to show up the L shell fine structure. The interpretation of the lines is given in table 5.6, and agreement with the previous spectrum is seen to be good even at the lower

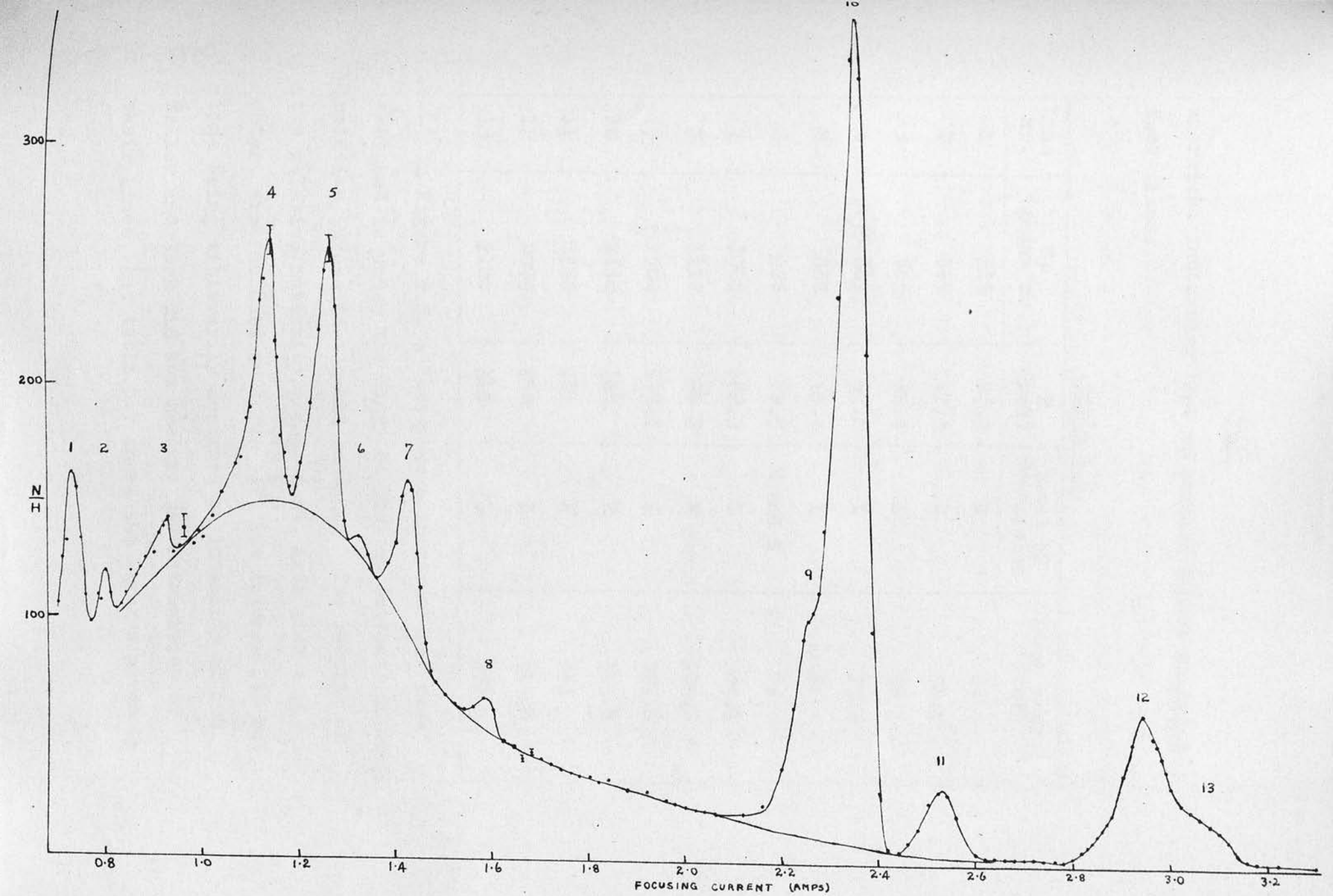

Figure 5.5. The spectrum of ^{233}Pa above 25 keV - source no. 2.

energies, indicating that no serious source charging took place.

Table 5.6.

Line no.	Hρ (gauss cm.)	E (keV)	Level of conversion	γ-ray energy (keV)
1	515	22.9	M	28.6
2	565	27.3	N	28.7
3	655	36.4	L	58
4	803	53.8	L	75.6
5	888	65.2	L	87
6	926	70.5	M and N	76
7	1005	82.3	L	104.1
8	1112	99.2	M	104.7
9	1580	185.8	K	301.6
10	1640	198	K	313.8
11	1780	228	K	343
12	2070	292	L	313.8
13	2180	319	L	340

In Figure 5.5, a "continuous spectrum" has been sketched in under the lines so that an estimate of their relative intensities could be made. The results of the relative intensity measurement, made with a planimeter, are included in table 5.7, the intense 198 keV line being arbitrarily assigned an intensity of 100. Keller and Cork did not measure the intensities of their lines, but table 5.7 shows the figures given by

Elliott and Underhill. Agreement between their results and the present ones is good, with the exception of line 9 (which was not completely resolved) and the weak line 6.

Table 5.7.

Line no.	Energy (keV)	Level of conversion	γ-ray energy	Conversion line intensity	Elliott's conversion line intensity
0*	19-19.7	L	40.7	5	-
1	22.9	M	28.6	10	-
2	27.3	N	28.7	1.5	-
3	36.4	L	58	4	-
4	53.8	L	75.6	21	20
5	65.2	L	87	17.4	24
6	70.5	M, N	76	1	5
7	82.3	L	104.1	10.4	11
8	99.2	M	104.7	2	3
9	158.8	K	301.6	4	10
10	198	K	313.8	100	100
11	228	K	343	8	10
12	292	L	313.8	25	25
13	319	L	340	4**	2.5

* The data for this line were obtained from Figure 5.4. It intensity was estimated by comparison with the M conversion of the 28.7 keV γ-ray.

** Includes the K conversion of 415 keV γ-ray - not resolved.

The continuous β-spectrum.

A Fermi plot of the continuous β-spectrum, as far as it can be deduced in the presence of the internal conversion lines, is shown in Figure 5.6. Six of the points, corresponding to energies between 140 and 210 keV, lie on a straight line which, on extrapolation, cuts the energy axis at about 252 keV. This agrees well with the value of 260 keV given by Elliott and Underhill for the end point of the main component of the β-spectrum. Below 140 keV the Fermi plot curves upwards, and while this could be caused by scattered electrons, it may be due, at least in part, to the presence of one or more partial β-spectra with end points lower than 250 keV. The two points at the high energy end of the plot (taken from the region between the conversion lines nos. 11 and 12 in Figure 5.5) lie well above the straight line. The points are subject to considerable error, but it seems probable that the β-continuum does, in fact, have a low intensity component with an end point considerably higher than 250 keV.

5.4. Preliminary discussion of results.

On the whole, the γ-rays detected from their internal conversion electrons agree well with the results of Keller and Cork, and some evidence has been

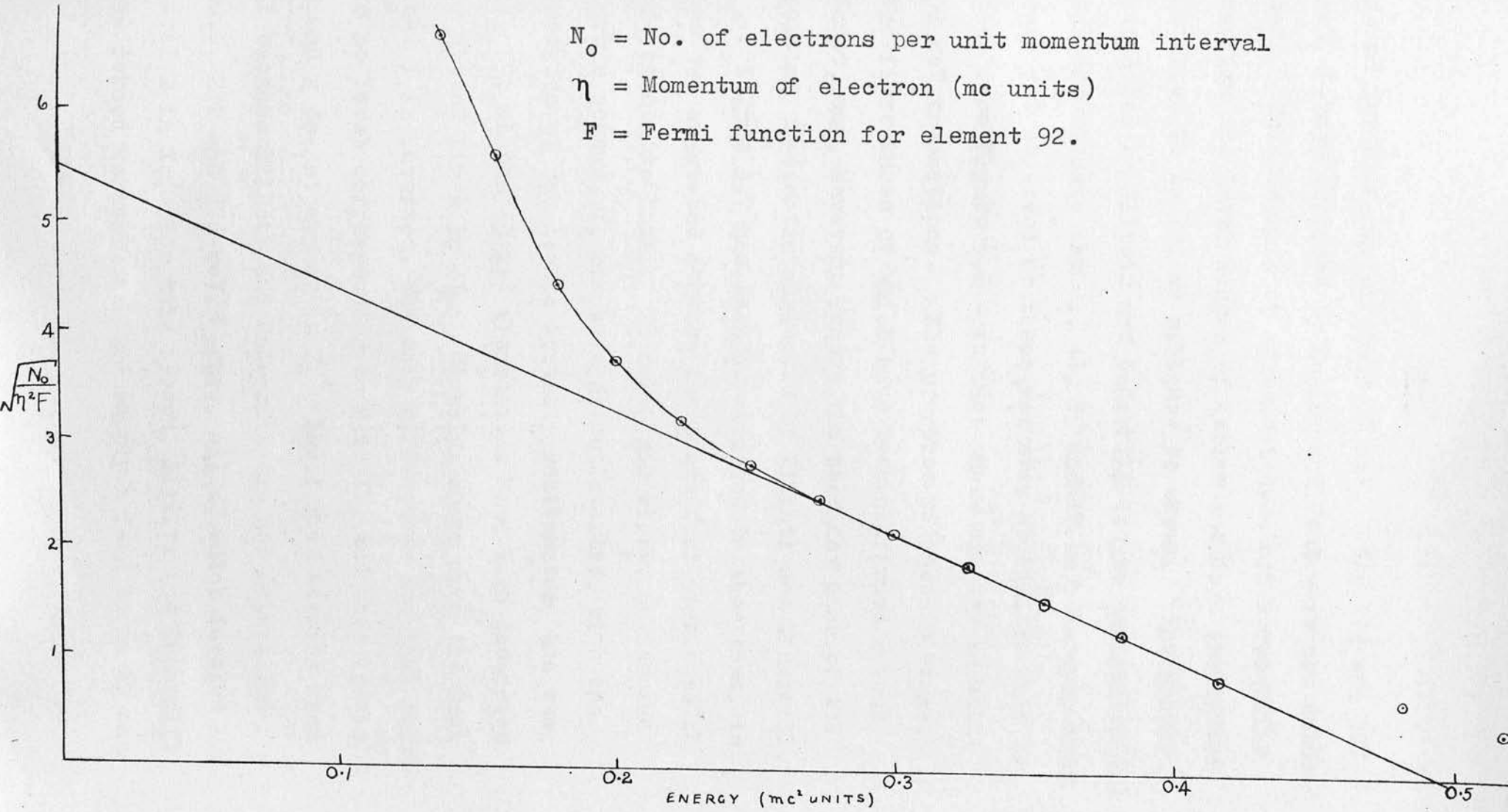

Figure 5.6. Fermi plot obtained from the spectrum of Figure 5.5.

found for a γ-ray of about 17 keV. The 272 and 377 keV γ-rays proposed by Keller and Cork were not detected. This measure of agreement does not necessarily confirm the level scheme of Keller and Cork (hereafter referred to as I), as will now be shown. The scheme suggested by Elliott and Underhill (to be designated II) can accommodate the 29, 41, 59 and 17 keV γ-rays, which were not observed by these workers, as will readily be seen from Figure 5.2 - in fact there are two possible 59 keV transitions. The presence of these γ-rays, the first three of which have been confirmed beyond doubt, may, however, remove the need for some of the partial β-spectra suggested by Elliott and Underhill.

Figure 5.7 has been constructed to show that, in the two suggested schemes there are four levels which are common to both. To make this clear, Keller and Cork's scheme, I, has been drawn inverted, with the energies of the levels suitably reallocated, and the 17, 29, 41 and 59 keV transitions have been indicated by dotted lines in II. Clearly, apart from the fact that I is inverted, the only differences are that there is no level corresponding to B in II, and that levels b and g do not appear in I. Level B is missing from II because Elliott and Underhill did not detect the 40.6, 272 and 376 keV γ-rays, all of which involve level B in I. For this reason, Elliott and Underhill are forced to include b and supply a feed to it by one

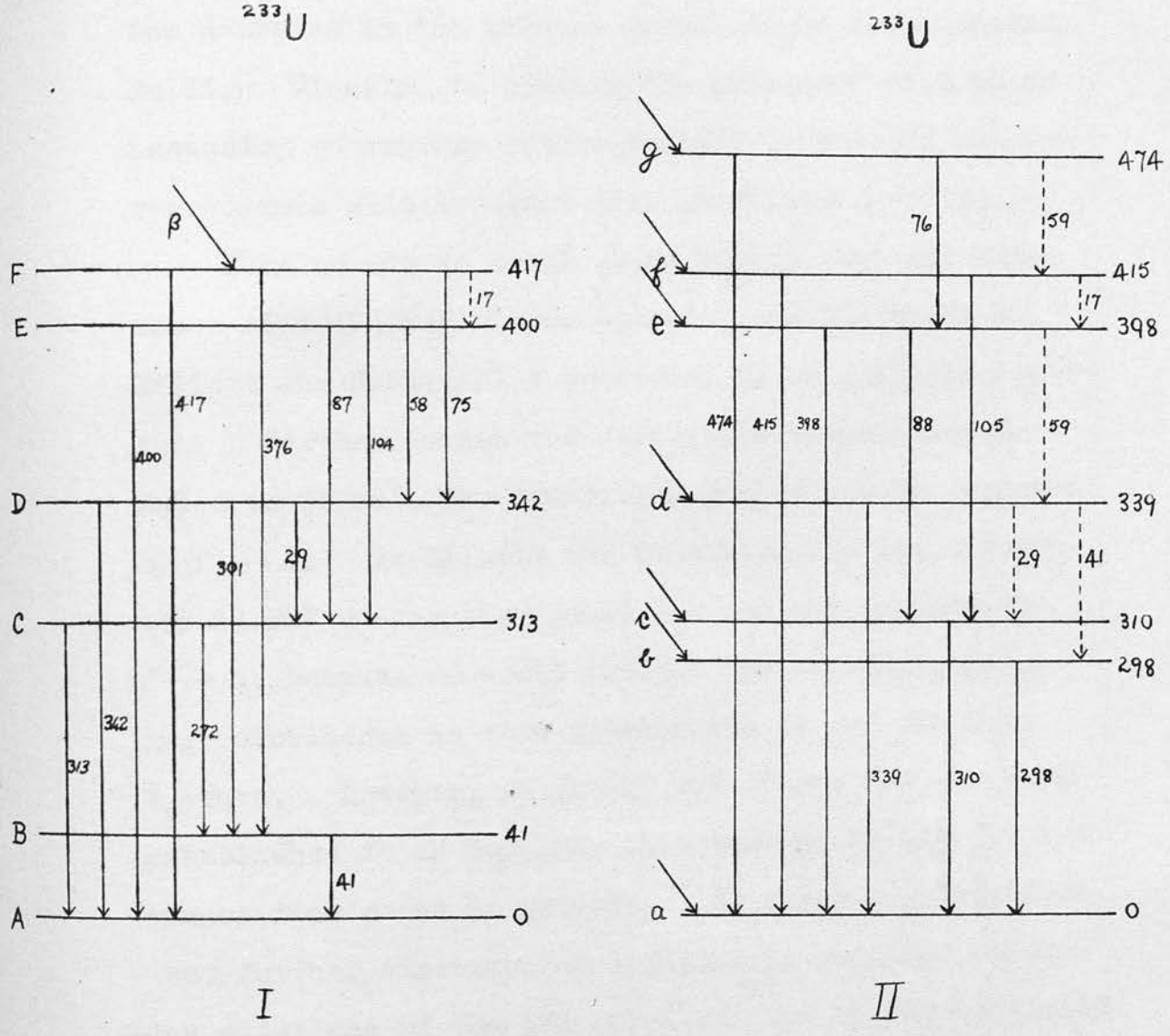

Figure 5.7. A comparison of the level schemes of Keller and Cork and of Elliott and Underhill.

of the partial β-spectra. It is noteworthy, however, that the energy difference between b and d is 41 keV, so that one of the "missing" γ-rays (the only one so far detected in the present work) can be accommodated in II. Clearly, to confirm the existence of B it is necessary to confirm either the 272 or the 376 keV γ-ray. This will be dealt with in a later section.

Turning now to level g, we recall that the existence of a 474 keV γ-ray appeared, on the basis of Elliott and Underhill's spectrum, to be a little doubtful. Further, since the difference between levels f and d is 76 keV, the transition $g \longrightarrow e$ can be replaced by $f \longrightarrow d$. As Elliott and Underhill did not observe the 29 keV γ-ray they could not use the transition $f \longrightarrow d$, because it would violate their experiment showing coincidence in time between the 76 and 310 keV γ-rays. However, as the 29 keV γ-ray has now been established it is possible that the 76, 29 and 310 keV transitions occur in cascade. We conclude, therefore, that further experimental evidence is required before the existence of the 474 keV level can be substantiated.

The remaining point of disagreement in the ^{233}Pa disintegration is the possibility that the continuous β-spectrum extends to an energy considerably greater than 260 keV. The work of Elliott and Underhill suggests an end point of 570 keV, which fits satisfactorily

into their decay scheme, but the only other report of a high energy end point places it at ~ 700 keV (Fulbright, 1944). The present work, as described so far, shows some indication of a β-component with an end point higher than 250 keV, but from the results so far presented it is not possible to arrive at any conclusion as to its possible end point, or even to state with certainty whether it exists at all.

This preliminary discussion has revealed three points which require further investigation. These are (i) an examination of the continuous spectrum at higher energies to find the end point of the high energy component, if it exists, (ii) a search for conversion electrons of a 272 keV γ-ray, and (iii) a search for conversion electrons of a 474 keV γ-ray.

The experiments which were carried out in an attempt to answer these questions are discussed in the next section.

5.5. Experiments with Source No. 3.

5.5.1. Source Preparation.

A search for weak conversion lines and a weak high energy β-spectrum required a fairly strong source - considerably stronger than those previously used in this work. Fortunately, some measurements on the γ-rays of ^{233}Pa were being carried out in the laboratory, using a strong source. When this had

become too weak for use in the curved crystal γ-ray spectrometer, it was dissolved off the platinum on which it was deposited, using hydrofluoric acid. About one third of the activity was removed by this process. The solution was evaporated to dryness in a platinum crucible and taken up again in concentrated HCl. One drop of this solution was deposited on gold backing 0.2 mg. per cm.^{2} in thickness and evaporated to dryness under the infra-red lamp. The resulting source was very much stronger than either of the previous sources and was thin enough to allow an examination of the higher energy half of the spectrum to be made. The experiments will be described in the order in which they were carried out.

5.5.2. Search for conversion electrons of a 272 keV γ-ray.

The 272 keV γ-ray was reported by Keller and Cork on the basis of its internal conversion electrons in the K and L shells. According to these workers the K conversion line had an energy of 156.6 keV corresponding to a momentum of 1,430 gauss cm. The ^{233}Pa spectrum between 1,270 and 1,525 gauss cm. was therefore examined carefully. In all, ten runs were made over this region giving about 50,000 counts on each point. The curve obtained is shown in Figure 5.8, in which the statistical error corresponds to about $\pm$ 0.4 mm. for

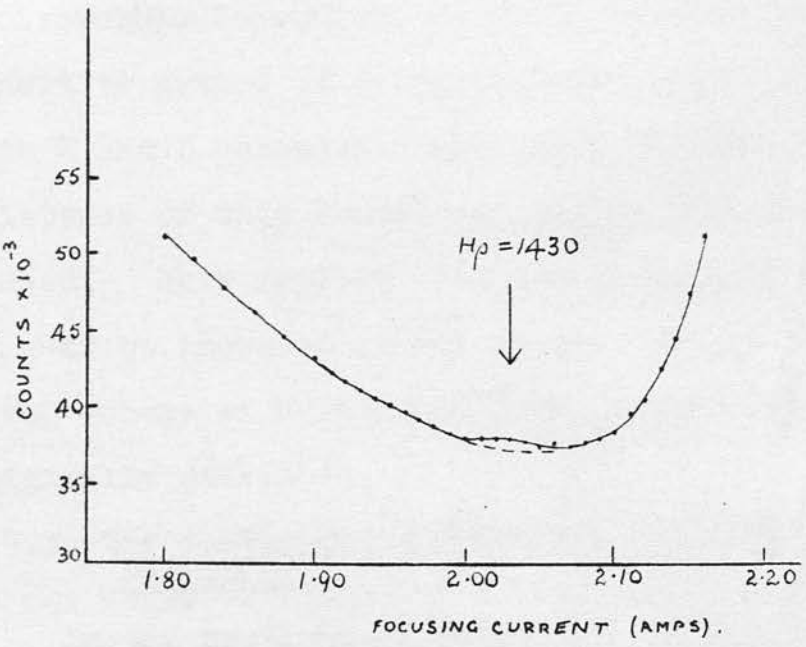

Figure 5.8. Result of a search for K conversion electrons of a 272 keV γ-ray in ^{233}Pa.

each point. The only departure from an otherwise smooth curve occurs at about 1,430 gauss cm., where there seems to be a very weak line. It has about the expected width for a line of this momentum, and its energy (156 keV) suggests that it is, in fact, the K conversion line of a γ-ray of 272.6 keV. On the basis of this evidence, together with the fact that Keller and Cork, using a semicircular spectrometer with photographic detection, which is possibly the most sensitive method of detecting weak lines, have reported both K and L conversion electrons of this γ-ray, the existence of this transition can be said to be established. This implies that the level B in Figure 5.7, I, must be included in the scheme, and so favours the level scheme of Keller and Cork, either inverted or as originally published.

5.5.3. The continuous β-spectrum of ^{233}Pa at high energies.

In the previous experiments, the spectrometer had been set for high collecting power, with a source--counter distance of about 50 cm. Under these conditions the maximum momentum which could be focused was about 2,500 gauss cm. Now, as a strong source was available it was possible to increase the source - counter distance to 80 cm., allowing the coil to focus electrons having momenta up to about 3,400 gauss cm. To check the new adjustment, the ^{233}Pa spectrum in the

neighbourhood of the intense conversion lines was examined, and the result is shown in Figure 5.9. The conversion lines are as expected, and the arrows on the diagram show the K, L and M lines of the 313 keV γ-ray, the K and L lines of the 342 keV γ-ray, and the K line of the 301 keV γ-ray. Figure 5.9 also shows evidence of a high energy continuous spectrum extending to over 3,000 gauss cm.

After this preliminary run, the high energy tail of the β-spectrum was examined carefully from about 235 keV upwards, and the spectrum obtained is shown in Figure 5.10. The vertical scale is expanded by about eight times compared with Figure 5.9. The group of lines marked 1 consists of the L and M conversion electrons of the 313 keV transition, and the L line of the 342 keV γ-ray. All of these have already appeared in Figure 5.9. The weak lines 2 and 3 at 2,430 and 2,500 gauss cm. respectively have not previously been detected in this work, and are interpreted as the L conversion lines of γ-rays of 400 and 417 keV respectively. The K conversion lines of these transitions are in the group of lines 1 and are not resolved from the other lines present. This interpretation is in agreement with both Keller and Cork and Elliott and Underhill.

A Fermi plot of the continuum was made from Figure 5.10, the points being selected between the

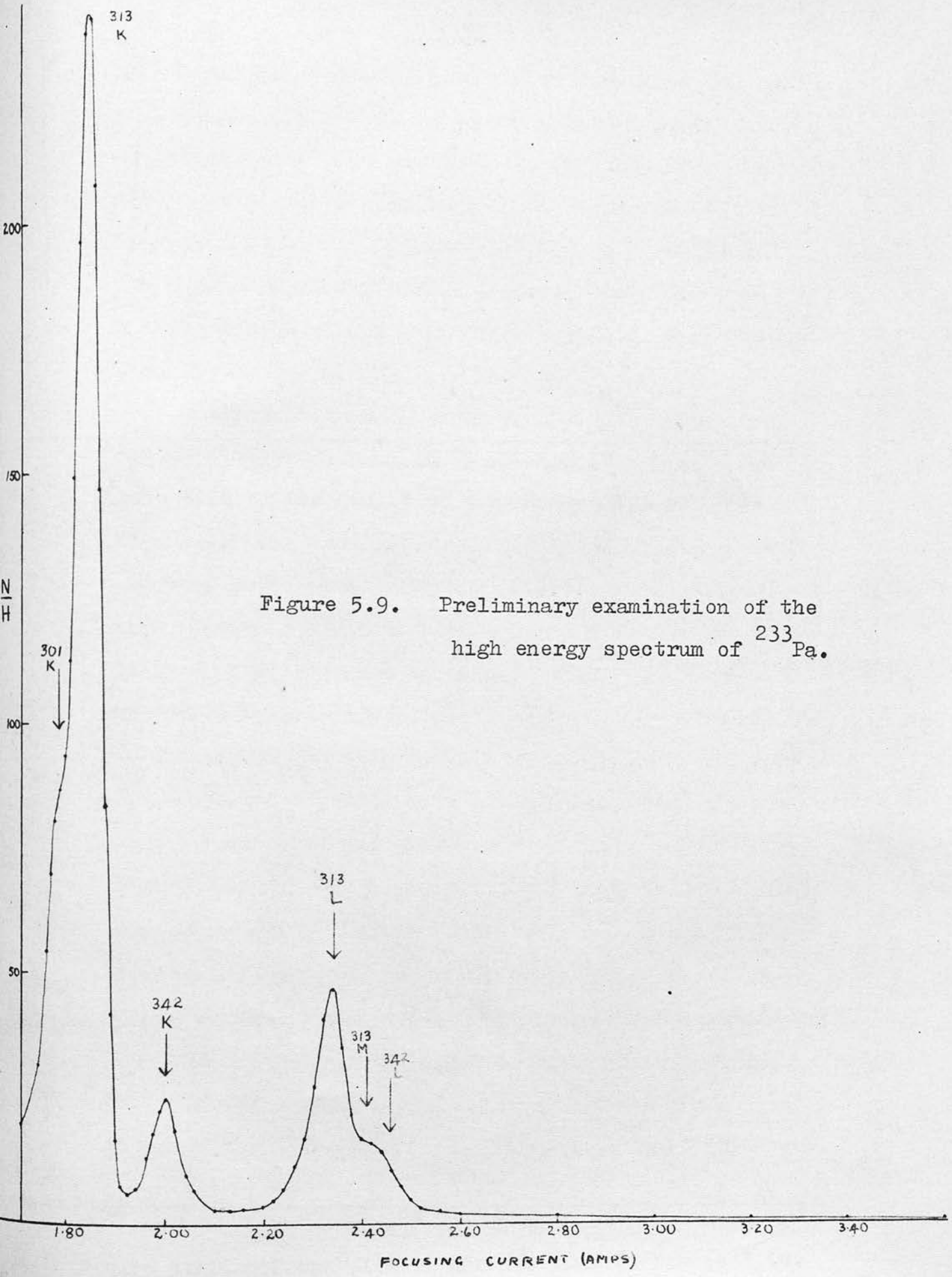

Figure 5.9. Preliminary examination of the high energy spectrum of ^{233}Pa.

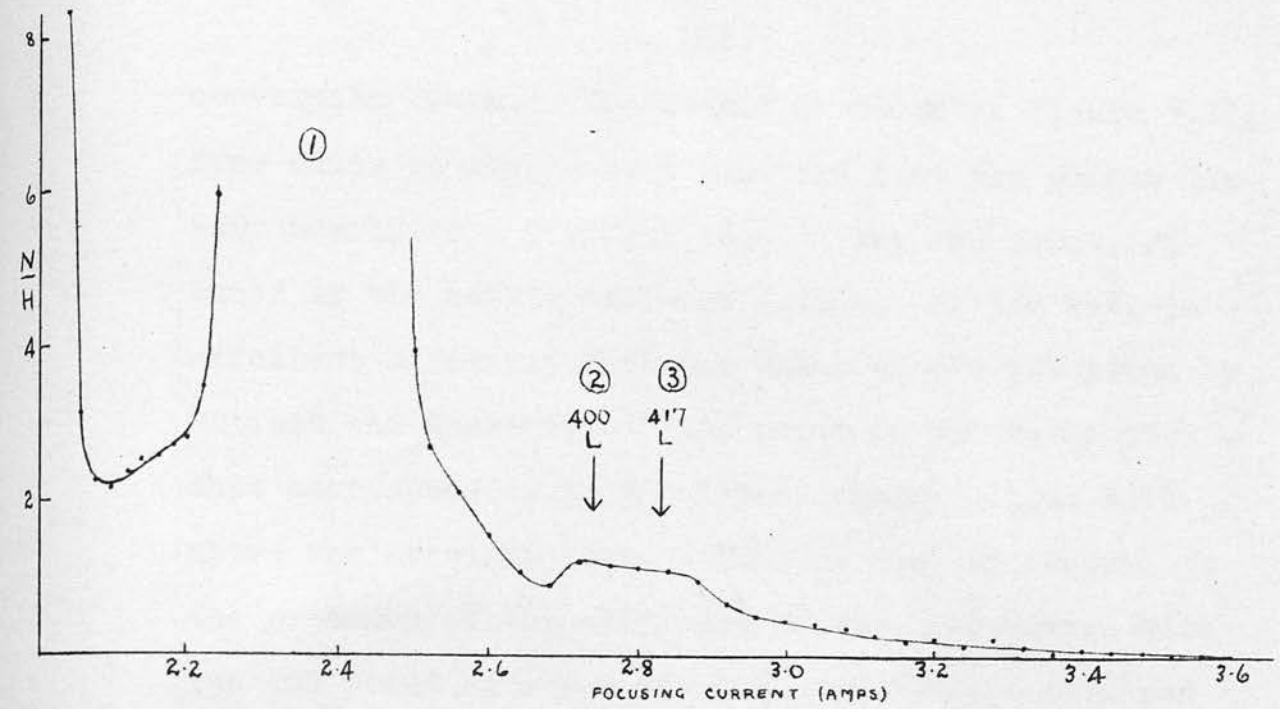

Figure 5.10. The "tail" of the β-spectrum of ^{233}Pa.

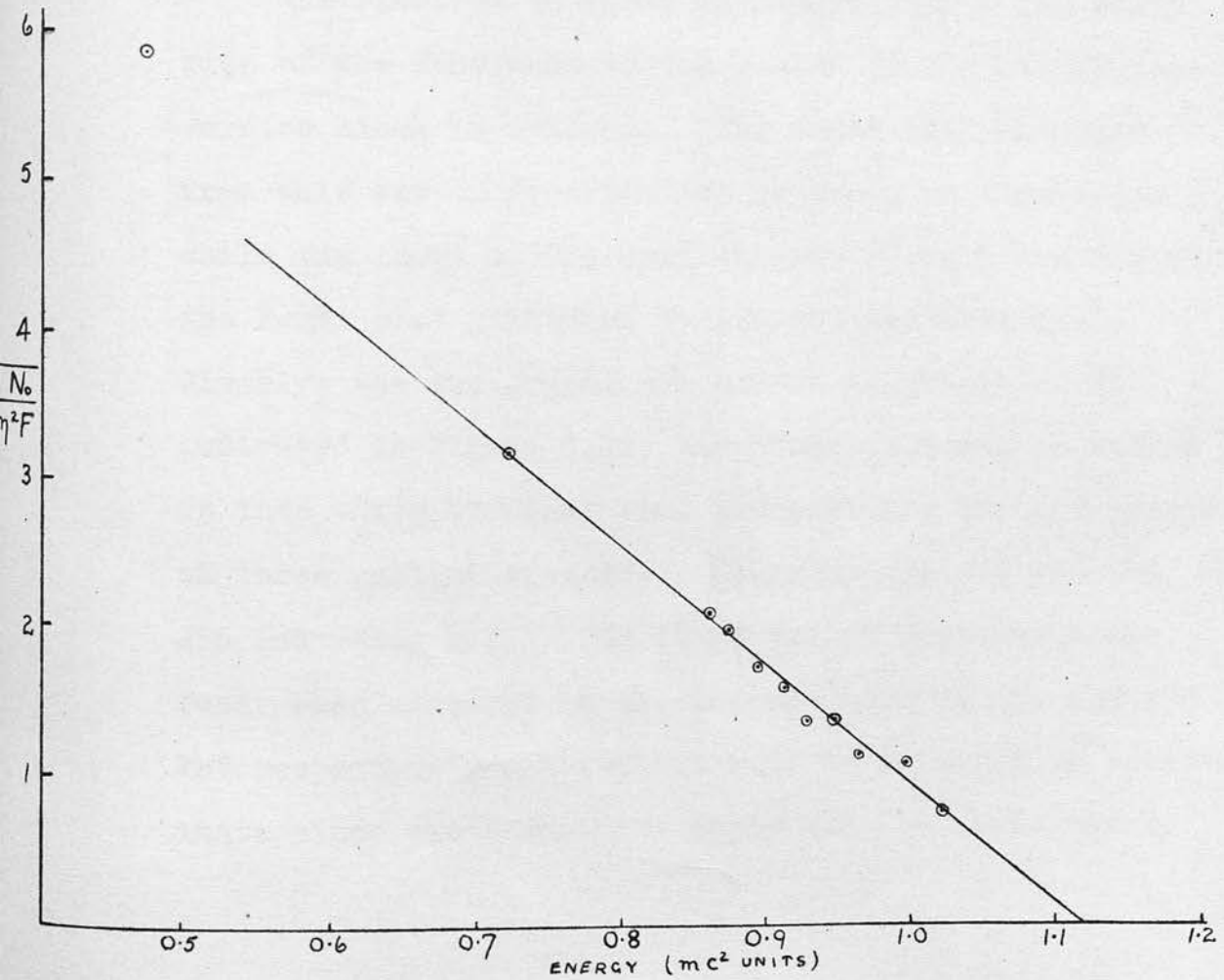

Figure 5.11. Fermi plot of the spectrum of Figure 5.10.

conversion lines. The result is shown in Figure 5.11, from which it can be seen that the last ten points lie very nearly on a straight line. The end point, deduced by the method of least squares, is 568 keV, in excellent agreement with the value of 570 keV given by Elliott and Underhill. One point on the Fermi plot - that corresponding to the lowest energy - lies well above the straight line. This is due, of course, to the presence of the main part of the β-spectrum with its end point at about 260 keV. To locate this end point, the observations were extended downwards in energy to about 90 keV.

The spectrum is shown in Figure 5.12 - the sharp rise of the continuum in the region of the strong conversion lines is evident. The Fermi plot obtained from this set of observations is shown in Figure 5.13, while the inset on the same diagram shows a tracing of the Fermi plot published by Elliott and Underhill. Clearly, the two graphs are almost identical. As indicated in Figure 5.13, the Fermi plot can be broken up into three straight line plots giving the end points of three partial spectra. These end points are 565, 256 and ~140 keV. The first two of these have already been measured in the present work as 568 and 252 keV respectively - the third must be regarded as approximate since the Fermi plot might well be distorted by

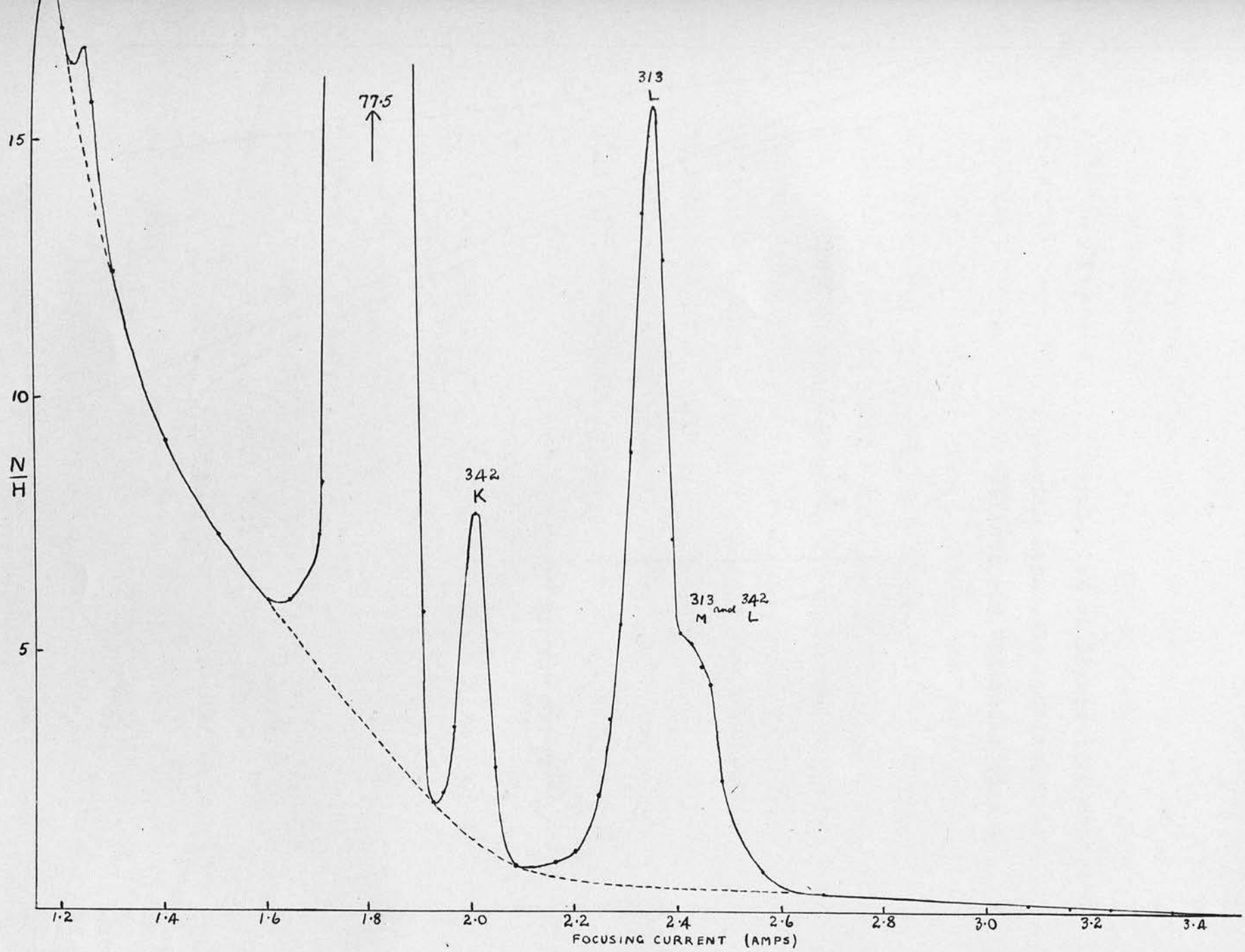

Figure 5.12. The β-spectrum of ^{233}Pa above 100 keV.

Figure 5.13. Fermi plot of Figure 5.12 compared with Fermi plot published by Elliott and Underhill (inset).

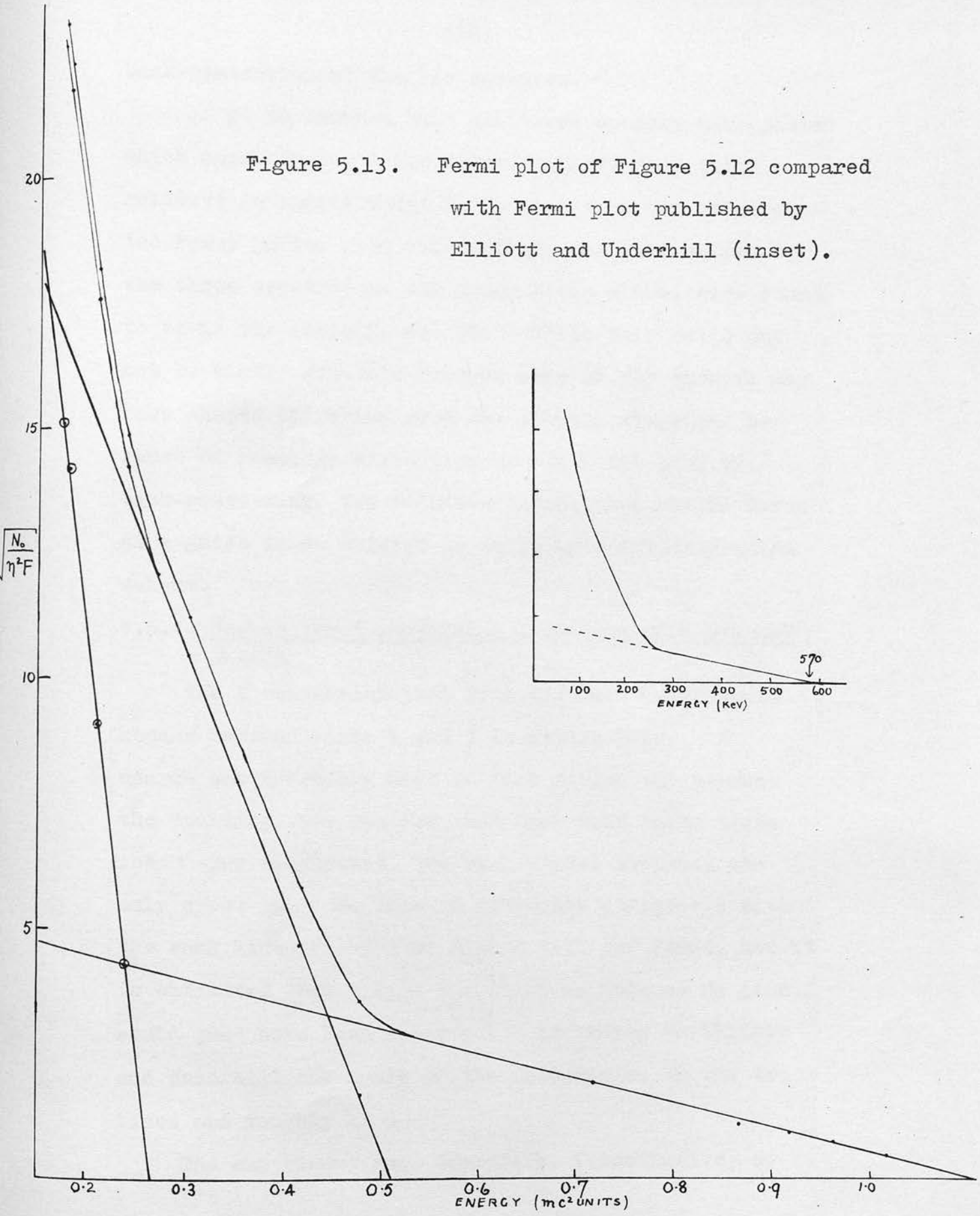

back-scattering at the low energies.

If it is assumed that all three spectra have shapes which approximate to the allowed shape, then their relative intensities may be deduced from the extrapolated Fermi plots. By this method, the intensities of the three spectra, in the order given above, were found to be in the ratio 5: 45: 50. While this ratio may not be highly accurate because some of the spectra may have shapes differing from the allowed shape and because of possible distortion of the Fermi plot by back-scattering, the relative intensities can be taken as a guide in an attempt to build up a disintegration scheme.

5.5.4. Search for K conversion electrons of a 474 keV γ-ray.

The K conversion line of a 474 keV γ-ray would appear between lines 1 and 2 in Figure 5.10. A search was therefore made in this region but because the counting rate was low, and less than three times the γ-ray background, the statistical accuracy was only about 3%. No line of intensity comparable with the weak lines 2 and 3 of Figure 5.10 was found, and it is estimated that a line one third as intense as line 2 would just have been observed. According to Elliott and Underhill the ratio of the intensities of the two lines was roughly 1: 3.

The experiment was, therefore, inconclusive, so

that the existence of a 474 keV level in the ^{233}U nucleus is still in doubt. It will be shown later that conclusive evidence might be obtained by the use of coincidence techniques.

5.6. Suggested Decay Scheme for $^{233}Pa \longrightarrow ^{233}U$.

The data which have been used in building up a disintegration scheme are as follows:

1. The energies of the transitions occurring in the ^{233}U nucleus, as given in earlier sections.

2. The relative intensities of the internal conversion electrons, as listed in table 5.7.

3. The end-points of the partial β-spectra.

4. The relative intensities of the partial β-spectra.

5. The internal conversion coefficients of the γ-rays.

6. The absolute intensity of the 313 keV transition.

Items 5 and 6 were taken from the results of Elliott and Underhill. The intensity of 75% which they gave for the 313 keV transition had to be increased to 80% to make the scheme self-consistent.

The data on the transitions in the daughter nucleus, ^{233}U, are summarized in table 5.8, the absolute intensities having been deduced from the measured

relative intensities of the internal conversion lines and the internal conversion coefficients, assuming a total intensity of 80% for the 313 keV transition.

Table 5.8.

No. of γ-ray	Transition Energy (keV)	Intensity of internal conversion electrons Relative	Absolute	Remarks	Absolute intensity of transition
1	17.2	?			?
2	28.7	M & N only 12	4%	Allow 2% for L conversion and unconverted γ-ray - based on Fig. 5.4	6%
3	40.7	5	2%	Relative intensity got from Fig. 5.4	3%
4	58	4	2%		3%
5	76	22	7.5%	Using Elliott's conversion coefficients	11%
6	87	17	6%	ditto	11%
7	104	12	4%	ditto	7%
8	272	-	-	Very weak	-
9	301	5	2%	Using Elliott's conversion coefficients	3%
10	313	125	43%	ditto	80%
11	342	10	3%	ditto	7%
12	400	-	-	Elliott's intensity	2.3%
13	417	-	-	ditto	2.3%

The end points of the partial β-spectra are 568 ± 5, 256 ± 4 and ~ 140 keV. The accuracy of

the third figure is probably no better than 10%. The intensities of the three β-spectra are roughly 5%, 45% and 50% respectively.

On the basis of these data, the disintegration scheme of Figure 5.14 is suggested. The levels in the ^{233}U nucleus correspond to an inversion of the scheme of Keller and Cork - the presence of the partial β-spectra and the relative intensities of table 5.8 forbid its use in the original form. The intensities of the transitions in the ^{233}U nucleus which are shown in Figure 5.14 are those listed in table 5.8, and it can be seen that the scheme adequately meets the requirement that the total intensity arriving at any level is equal to that leaving the level. It has been necessary to assume that the least energetic of the partial β-spectra is split into two having end points differing by 17 keV. If this is not done, an intensity of 18% must be assumed for the 17 keV transition. This was not found, and in the scheme a value of 5% has been suggested as the probable maximum intensity for this transition. The intensities suggested in the scheme for the partial β-spectra show reasonable agreement with the observations, which were accurate enough only to serve as a guide - 5%, 57% and (13 + 25)% compared with the observed values 5%, 45% and 50%.

While Figure 5.14 fits the observations satisfactorily it is not claimed to be unique. In

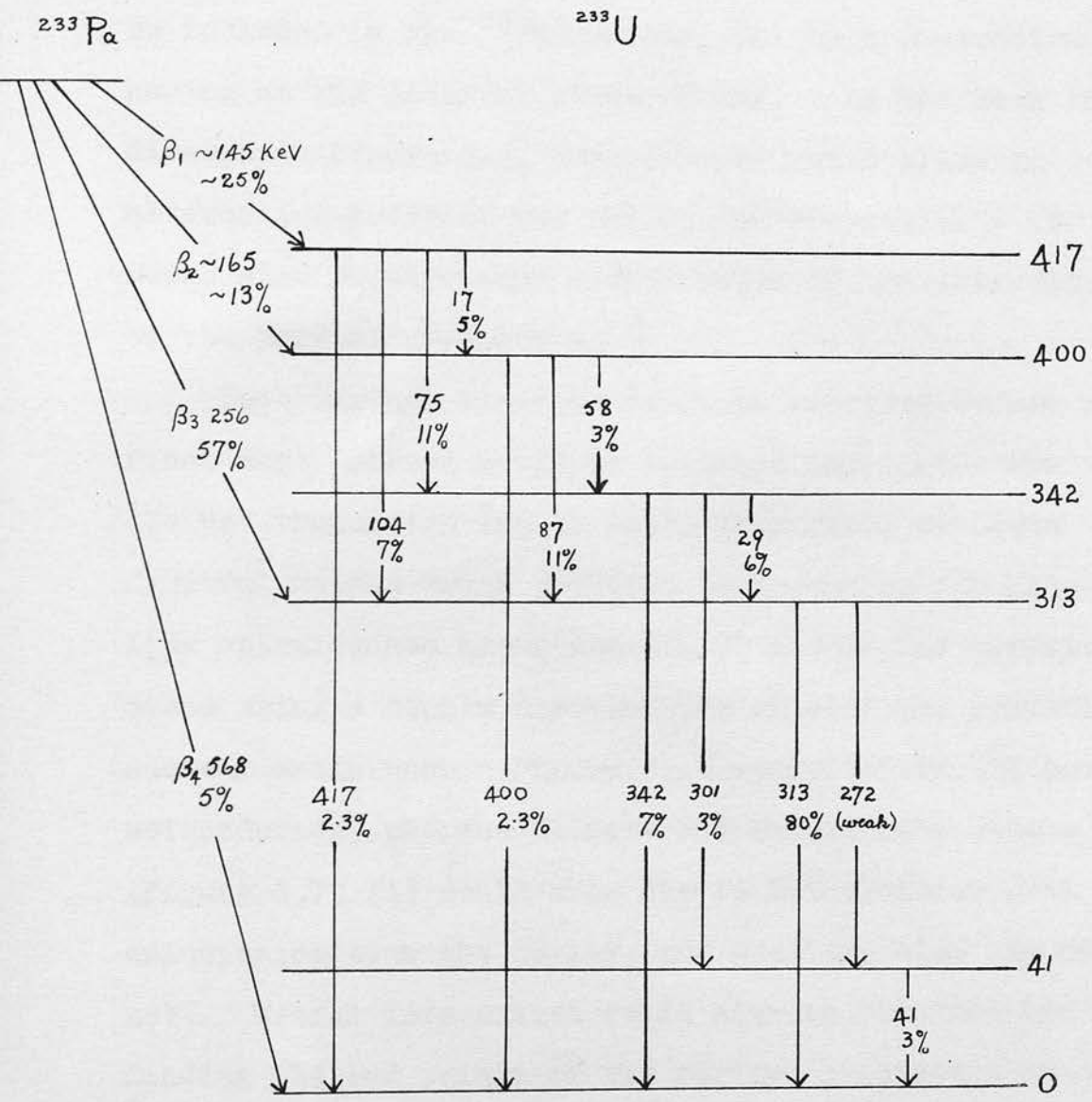

Figure 5.14. Suggested disintegration scheme for $^{233}Pa \rightarrow ^{233}U$.

particular, the weak 474 keV transition suggested by Elliott and Underhill has not been conclusively proved to be absent. If it is present, a 474 keV level must be included in the ^{233}U nucleus, fed by a β-spectrum having an end point at about 95 keV. As has been indicated in Figure 5.7, such a level would allow an alternative position for the 75 keV transition - it would also require some modification of the intensities of the partial β-spectra.

Some further research would be required before a final decay scheme could be proposed and, since the 474 keV transition is, at best, very weak, the most fruitful method would probably be to search for line to line coincidences among the 87, 75 and 58 keV transitions using a double spectrometer or electron sensitive nuclear emulsions. Figure 5.14 would forbid all such coincidences, whereas Elliott and Underhill's scheme (Figure 5.7, II) would show the 76 keV transition in coincidence with the 88 keV, and possibly also the 59 keV. Useful information could also be obtained by finding the end points of the partial β-spectra in coincidence with the various γ-rays.

No attempt has been made to assign spins and parities to the levels in the ^{233}U because of the lack of reliable information about the ground states of the two nuclei concerned in the disintegration, and

uncertainty concerning the internal conversion coefficients of some of the γ-rays.

5.7. The Counting Efficiency of ^{233}Pa.

Counting efficiency has been defined (see, for example, Karraker, 1951) as "the ratio of observed counts to the actual disintegrations under specified counting conditions". If a counter insensitive to electromagnetic radiations is used under suitable solid angle conditions the counting efficiency gives a measure of the total number of electrons per disintegration. This quantity has been measured by Karraker (1951) using a direct counting method, and by Seaborg et al. (1942), the respective results being 2.7 and 2.3 electrons per disintegration. Since the probable error quoted by Karraker is 10% he claims substantial agreement with Seaborg.

An estimate of the number of electrons per disintegration can be made from the results of the present work with an accuracy of the same order as that claimed by Karraker, provided the number of Auger electrons can be assessed. As has been explained in section 5.2.3, there is not enough information available concerning the relative intensities of the L_I, L_{II} and L_{III} conversion electrons to enable an accurate estimate of the intensity of the L Auger electrons to be made.

However, a rough value can be obtained by assuming a value for the total fluorescence yield of all three L shells.

From table 5.8 the total number of internal conversion electrons is 0.73 per disintegration. This result is unlikely to be greatly in error in view of the satisfactory way in which the intensities fit into the decay scheme. Further, it agrees well with the value of 0.72 deduced from the results of Elliott and Underhill, although the latter figure ought perhaps to be increased slightly to take account of the low energy transitions which they did not detect. The value 0.73 ± 0.08 has been assumed. This figure was divided among the K, L, M and N shells according to the measured relative intensities of the internal conversion electrons. After taking account of the transfer of ionization from the K to the L and M shells by K x-ray emission, the number of L Auger electrons was found to be 0.26 ± 0.08. This assumes a total L shell fluorescence yield of 0.52, a value based upon the calculations of Kinsey (1948a). The total number of electrons emitted per disintegration of ^{233}Pa is thus 2.0 ± 0.15.

In making this estimate, no account was taken of the K-Auger electrons since the K shell fluorescence yield for uranium is very high, and no account has been taken of the M or N-Auger electrons. The M-Auger electrons would have energies of about 2 keV and, since

Karraker used a windowless counter in determining the absorption curve of ^{233}Pa, it is possible that 2 keV electrons would be counted. Moreover, the sensitivity of the counter to the soft M x-rays might be appreciable. These considerations may account for at least some of the difference between Karracker's result and the present one.

5.8. Conclusions.

As the results obtained from the study of ^{233}Pa have been discussed at some length in earlier sections of this chapter, this section will consist simply of a recapitulation of the main conclusions.

1. γ-rays and internal conversion electrons. In the region above 19 keV, 12 γ-rays have been identified from a study of their internal conversion electrons. The energies of the γ-rays agree well with those given by Keller and Cork (1950) who, however, list one additional weak γ-ray of 377 keV. The relative intensities of the internal conversion electrons have been measured and the results agree well with the values given by Elliott and Underhill (1952).

2. The spectrum at low energies. Interpretation of the L-Auger spectrum is complicated by the presence of internal conversion electrons, but the transitions suggested to explain those lines definitely identified

as Auger lines are in agreement with transitions occurring in the spectra of RaE or RdTh or both. L conversion electrons of the 28.7 keV γ-ray have been identified in the 7 keV region, and some evidence has been obtained for a 17.2 keV γ-ray.

3. The continuous β-spectra. The main part of the β-spectrum of ^{233}Pa ends at 256 keV but there is a low intensity partial spectrum extending to 568 keV. These results agree very well with those of Elliott and Underhill. The main part of the continuum has been shown to consist of three partial β-spectra, the intensities of which have been roughly estimated.

4. Disintegration Scheme. The energies and intensities of the β-spectra and of the γ-rays and internal conversion electrons fit satisfactorily into the decay scheme given in Figure 5.14.

5. The number of electrons emitted per disintegration of ^{233}Pa. The number of electrons emitted per disintegration of ^{233}Pa, excluding M and N-Auger electrons, was found to be 2.0 ± 0.15. This is lower than the figures published by Karraker (1951) and by Seaborg (1942), but it is suggested that their values may include the M-Auger electrons and possibly an appreciable fraction of the M x-rays.

References.

Allen (1947) Rev. Sci. Instrum. 18, 739.

Amaldi and Rasetti (1939) Ricerca sci 10, 111.

Arnoult (1939) Ann. Phys., Paris 12, 240.

Bannerman and Curran (1952) Phys. Rev. 85, 134.

Black (1924) Proc. Roy. Soc. 106, 632.

Black (1925) Proc. Camb. Phil. Soc. 22, 838.

Bramson (1930) Z. Phys. 66, 721.

Broda and Feather (1947) Proc. Roy. Soc. A 190, 20.

Busch (1926) Ann. Phys., Lpz. 81, 976.

Butt (1949a) Thesis, Edinburgh.

Butt (1949b) Proc. Phys. Soc. B 62, 551.

Butt (1950) Proc. Phys. Soc. A 63, 986.

Cohen and Jaffe (1952) Phys. Rev. 86, 800.

Cork, Branyan, Stoddard, Keller, Le Blanc and Childs (1951) Phys. Rev. 83, 681.

Coster and Kronig (1935) Physica 2, 13.

Craig (1952) Phys. Rev. 85, 688.

Cranberg (1950) Phys. Rev. 77, 155.

Curran, Angus and Cockcroft (1949) Phil. Mag. 40, 36.

Curtiss (1926) Phys. Rev. 27, 257.

Deutsch, Elliott and Evans (1944) Rev. Sci. Instrum. 15, 179.

von Droste (1933) Z. Phys. 84, 17.

Elliott and Underhill (1952) A.E.R.E. Library, HAR 761.

Ellis (1933) Proc. Roy. Soc. A 139, 336.

Ellis (1934) Proc. Roy. Soc. A 143, 350.

Ellis and Skinner (1924) Proc. Roy. Soc. A 105, 165.

Evans (1934) Rev. Sci, Instrum. 5, 371.

Ewan (1952) Private communication.

Feather (1930) Phys. Rev. 35, 1559.

Feather (1938) Proc. Camb. Phil. Soc. 1, 34, 115.

Feather (1949) Nucleonics, July, p. 22.

Feather and Richardson (1948) Proc. Phys. Soc. 61, 452.

Flammersfeld (1939) Z. Phys. 114, 227.

Frilley, Gokhale and Valadares (1951) C.R. Acad. Sci., Paris 232, 157.

Fulbright (1944) P.P.R. CP - 1954.

Gellman, Griffith and Stanley (1952) Phys. Rev. 85, 944.

Goldhaber and Sunyar (1951) Phys. Rev. 83, 906.

Gray (1932) Nature, London 130, 738.

Grosse, Booth and Dunning (1941) Phys. Rev. 59, 322.

Haggstrom (1941) Phys. Rev. 59, 322.

Hahn and Strassman (1940) Naturwiss 28, 543.

Haissinsky (1933) C.R. Acad. Sci., Paris 196, 1778.

Hamilton and Gross (1950) Rev. Sci. Instrum. 21, 912.

Insch, Balfour and Curran (1952) Phys. Rev. 85, 805.

Jones and de la Perelle (1951) Nature, London 168, 160.

Karraker (1951) U.C.R.L. Report AECD 3154.

Keller and Cork (1950) Phys. Rev. 79, 1030.

Kinsey (1948a) Canad. J. Res. A 26, 404.

Kinsey (1948b) Canad. J. Res. A 26, 421.

Konopinski (1943) Rev. Mod. Phys. 15, 209.

Landolt-Bornstein (1950) 6 Auflage, Zahlenwerte und Funktionen.

Langer, Motz and Price (1950) Phys. Rev. 77, 798.

Lecoin (1935) C.R. Acad. Sci., Paris 200, 1931.

Lecoin (1938) J. Phys. Rad. 9, 81.

Lecoin, Perey and Riou (1949) J. Phys. Rad. 10, 390.

Lecoin, Perey and Teillac (1949) J. Phys. Rad. 10, 33.

Lee and Libby (1939) Phys. Rev. 55, 252.

Levy (1947) Phys. Rev. 72, 352.

Libby and Lee (1939) Phys. Rev. 55, 245.

Malter (1936) Phys. Rev. 50, 48.

Massey and Burhop (1936) Proc. Camb. Phil. Soc. 32, 461.

Meitner, Strassman and Hahn (1938) Z. Phys. 109, 538.

Mühelpfordt (1938) Z. Phys. 108, 698.

Neary (1940) Proc. Roy. Soc. A 175, 71.

Ouang, Surugue and Tsien (1943) C.R. Acad. Sci., Paris 217, 535.

Pestchek and Marshak (1952) Phys. Rev. 85, 698.

Peterson M.D.D.C. 1709.

Ramler and Freedman (1950) Rev. Sci. Instrum. 21, 784.

Richardson and Leigh-Smith (1937) Proc. Roy. Soc. A 160, 454.

Seaborg, Gofman and Kennedy (1941) Phys. Rev. 59, 321.

Seaborg, Gofman and Stoughton (1942) U.C.R.L. Report A 192.

Slack (1952) Naval Research Lab., Washington Report dated 23rd January, 1952.

Spinrod and Keller (1951) Phys. Rev. 84, 1056.

Stahel (1931) Z. Phys. 68, 1.

Stahel (1935) Helv. Phys. Acta 8, 651.

Teillac, Falk-Vairant and Victor (1952) J. Phys. Rad. 13, 143.

Thibaud (1926) Ann. Phys., Paris 5, 73.

Tsien (1946) Phys. Rev. 69, 38.

West, Meyerhof and Hofstadter (1951) Phys. Rev. 81, 141.

White and Millington (1928) Proc. Roy. Soc. 120, 701.

Yovanovitch and d'Espine (1927) J. Phys. Rad. 8, 276.

Yovanovitch and Proca (1926) C.R. Acad. Sci., Paris 183, 878.

Acknowledgments.

It is a pleasure to acknowledge my indebtedness to Professor N. Feather, F.R.S., who suggested the problems discussed in this thesis and under whose direction the work was carried out.

I also wish to thank Dr. N. Miller for his advice on the chemical separation of the sources and particularly for his guidance in the development of the method for separating MsTh2.

Many other members of the Department of Natural Philosophy assisted with helpful suggestions and I am especially indebted to Dr. R.D. Connor for comments on the investigation of the spurious counts in the electron accelerator, to Dr. M.A.S. Ross and Dr. H.O.W. Richardson for discussions on the disintegration of RaD and to Mr. J. Kyles for some stimulating conversations concerning MsTh2 and for permission to use some of the results (as yet unpublished) of the experiments carried out by him and his co-workers.

Thanks are also due to Mr. A. Headridge and his staff in the workshop and to the other technicians in the Department of Natural Philosophy, who have been helpful and co-operative at all times.